NEACRP-L-320

OECD/NEA COMMITTEE ON REACTOR PHYSICS

ANALYSIS OF THE OECD/NEACRP PROBLEM N°20 ON INTERNATIONAL CRITICALITY CODES FOR FUEL PELLETS IN FISSILE SOLUTION

A. SANTAMARINA - H.J. SMITH
CEA - DRN/DER/SPRC - Cadarache

Criticality Calculations Working Group

December 1990

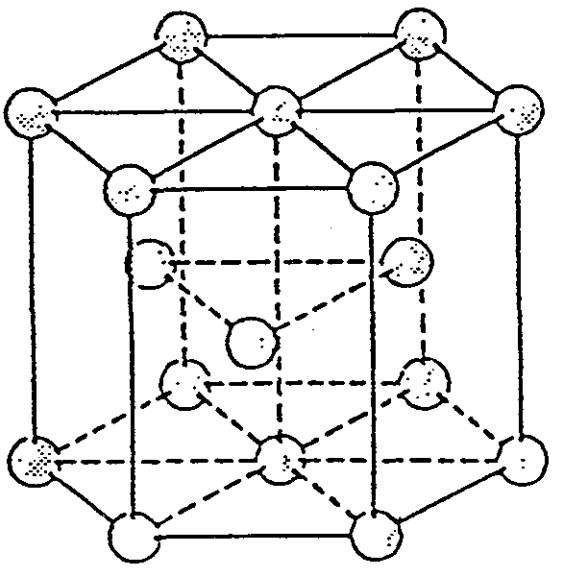

OECD/NEA

NEACRP-L-320 Criticality Codes for Fuel Pellets in Fissile Solution. Problem 20. OECD 1990

NEACRP-L-320

OECD/NEA COMMITTEE ON REACTOR PHYSICS

ANALYSIS OF THE OECD/NEACRP PROBLEM N°20 ON INTERNATIONAL CRITICALITY CODES FOR FUEL PELLETS IN FISSILE SOLUTION

A. SANTAMARINA - H.J. SMITH
CEA - DRN/DER/SPRC - Cadarache

Criticality Calculations Working Group

December 1990

A - A REFERENCE METHOD FOR TREATING THE FUEL DOUBLE HETEROGENEITY. STUDY OF DISCREPANCIES INTRODUCED BY DIFFERENT SELF-SHIELDING FORMALISMS.

B - AN ANALYSIS OF THE RESULTS OF THE OECD CRITICALITY WORKING GROUP BY NEUTRON BALANCE METHOD.

ANALYSIS OF THE OECD/NEACRP PROBLEM N° 20

ON INTERNATIONAL CRITICALITY CODES

FOR FUEL PELLETS IN FISSILE SOLUTION

A. SANTAMARINA - H.J. SMITH

ABSTRACT

The reference calculations, based on the APOLLO-Pic method implemented in the framework of this study, demonstrated that the actual reactivity variation (benchmark n° 20) is a monotonic decrease with pellet "dissolution".
At the opposite of the contributor's results, based on the international criticality code SCALE, the reactivity loss with dissolution is weak :
$\Delta\rho^{ref}$ = - 3000 pcm compared to $\Delta\rho^{scale}$ = - 25 000 pcm (50 % ; P.F = 0.6)

The discrepancy is mainly due to ^{238}U resonant absorption which can induce, in this fuel double heterogenity problem n° 20, as much as - 30 000 pcm K_∞ underestimation.

It was pointed out that design-oriented transport codes must be improved by accurate deterministic formalisms : PIC equivalence method, subgroup theory (WIMSE), ultrafine slowing-down calculation (ROLAIDS).

Ultimate confirmation of the reference results presented in this paper should be provided by a set of critical experiments which mock-up hypothetical dissolver geometries.

Finally it should be noted that thanks to the interest and the efforts of the OECD/NEA Criticality Working Group in performing the international benchmark exercise and in pursuing the explanation of the discrepancies, a potentially dangerous inadequacy in criticality calculation methods was exposed and resolved.

OECD/NEACRP CRITICALITY WORKING GROUP

Chairman: G.E. Whitesides, ORNL

Country	Organisation	Program(s) Used	Members
France	CEA/DRN/Cadarache	APOLLO-PIC	A. Santamarina H.J. Smith
	CEA/IPSN/Fontenay aux Roses	APOLLO	L. Maubert G. Poullot
	CEA/DMT/Saclay	TRIPOLI	J.C. Nimal C.M. Diop
Germany	GRS/Garching	SCALE	W. Weber
Italy	ENEA/Casaccia	XSDRNPM, MCNP	P.A. Landeyro
	ENEA/Trisaia	XSDRNPM, MCNP	F. Siciliano
Japan	JAERI/NSRC	ANISN, VIM	Y. Naito
	PNC/RTDD-PDS	SCALE	T. Matsumoto
Sweden	EMS	SCALE	D. Mennerdahl
U.K.	UKAEA/SRD/Culcheth	MONK-6.3	G. Walker
	BNFL/Risley	WIMSE	P.R. Thorne
U.S.A.	ORNL	SCALE, ROLAIDS	L.M. Petrie G.E. Whitesides
OECD	NEA Secretariat		E. Sartori

LIST OF CONTENTS

A - A REFERENCE METHOD FOR TREATING THE FUEL DOUBLE HETEROGENITY.

STUDY OF DISCREPANCIES INTRODUCED BY DIFFERENT SELF-SHIELDING FORMALISMS.

A. SANTAMARINA- H.J. SMITH

ABSTRACT

The loss of reactivity of a LWR fuel assembly undergoing dissolution may be poorly calculated as was shown by the wide spread of OECD benchmark results [1] on fuel dissolver calculations. The aim of this paper is to supply a reference calculation of k_∞ as a function of dissolution of the fuel pellets. This goal was achieved, first by a deterministic transport calculation based on the APOLLO code and second by a continuous energy Monte Carlo calculation using the TRIPOLI Code.

This paper presents the reference self-shielding formalism based on the effective cross-section concept. Standard approximations used in self-shielding computations for heterogeneous media are described.

A comparison of the results of design-oriented calculations and the reference calculations is given. The reference calculations show a monotonic loss of reactivity to a maximum value of 3000 pcm (10^{-5} in $\Delta k/k$) over the complete range of dissolution. On the other hand the standard approximations may overestimate reactivity losses by 5000 pcm in the pellet dissolution range 25 - 75 %.

1 - INTRODUCTION

The loss of reactivity of a LWR fuel assembly undergoing dissolution may be poorly calculated as was shown by the wide spread of OECD Benchmark results [1] on fuel dissolver calculations. At this June 1988 Critically Working Group Meeting, it became apparent that there was an unacceptably large, (20 % in $\Delta k/k$), dispersion in the results for thoretical Benchmark exercises 19, 20, 21, which represent problems with a double heterogeneity.

The international community emphasized the importance of the Benchmarks because they have a direct impact on the safety in a fuel dissolver and on optimizing the reprocessing operations and costs (transports and storage included). Therefore a specific study to resolve this problem was suggested, involving a reactor physics analysis of the "resonance interference of adjacent media".

To achieve this objective we focussed on problem 20 of the Benchmark exercices as being the more discrepant case. This problem corresponds to a 2.5 % enriched UO_2 spherical pellet in a borated water solution.

This paper aims first to investigate potential biases in k_{eff} linked to dissolver calculations. The next chapter is devoted to leakage rate calculation, sensitivity of k_∞ to nuclear data, and approximations in cell methods. In the third chapter, the P_{IC} self-shielding formalism used in our reference calculation and standard approximations used in design calculations are detailed. Then, the k_∞ results of these various calculation schemes are compared in the fourth section.

Secondly this study aims to supply a reference calculation of the k_∞ as a function of dissolution of the fuel pellets. This goal is achieved in the last section, first by a reference APOLLO deterministic transport calculation, and second by a continuous energy Monte-Carlo calculation using the TRIPOLI code.

2 - THE POTENTIAL SOURCES OF BIAS

Figures 1 and 2 present the variation of k_{eff} with dissolution of the pellet as calculated by the various contributors to benchmark problem 20, for packing fractions (P.F.) of 0.4 and 0.6 respectively ($PF = V_{fuel}/V_{tot}$). The loss of reactivity of the dissolver with pellet dissolution, computed from these data, appears to be completely different for each calculational tool. This disagreement is not linked to the initial value of the dissolver reactivity. At zero dissolution, when 100 % of the fuel is in the pellets and the pellets are distributed uniformly within the water/boron solution, the spread of computed k_{eff} values is 3000 pcm (1 pcm = $10^{-5} \frac{\Delta k}{k}$) in the PF = 0.4 geometry. This geometry is typical of the moderation ratio in PWR's and the spread in k_{eff} values is consistent with the uncertainties in basic nuclear data. In the undermoderated (PF = 0.6) lattice the spread in k_{eff} values increases to 4200 pcm and can be explained on the basis of uncertainties associated with fast and resonance region cross-sections. This has been demonstrated previously in a sensitivity study of a High Conversion Reactor [4] that showed a corresponding standard deviation of ± 2500 pcm which was also confirmed by the results of the OECD/NEA benchmark exercise on HCLWR cell calculations [5] that showed a spread of 4000 pcm in the calculated k_∞ values.

To remove the scatter due to basic nuclear data we shall use the variation of dissolver reactivity with pellet dissolution where :

$$\rho = \ln k$$

and $\Delta\rho = \rho(x\ \%) - \rho(100\ \%)$

The k_{eff} and $\Delta\rho$ values of the international contributors are summarized in Table 1. It can be seen that the reactivity loss at 50 % dissolution ranges between $\Delta\rho$ = - 1200 pcm in UK calculations and $\Delta\rho$ = - 21000 pcm in Japanese and American SCALE calculations.

TABLE 1

A SUMMARY OF K-EFFECTIVE AND DELTA RHO VALUES
FOR BENCHMARK EXERCISE 20 CALCULATIONS
(JUNE 1988)

		K-EFFECTIVE		DELTA RHO	
		PF=0.4	PF=0.6	PF=0.4	PF=0.6
USA/ORNL					
R-XSDRNPM	100	0.87695	0.84013	0	0
	75	0.84080	0.76543	- 4210	- 9312
	50	0.84296	0.77416	- 3953	- 8178
USA/ORNL					
XSDRNPM	100	0.88218	0.84707	0	0
	75	0.78003	0.71036	-12306	-17601
	50	0.76383	0.68869	-14405	-20699
FRANCE/CEA					
APOLLO	100	0.88380	0.86040	0	0
	75	0.83690	0.80350	- 5453	- 6842
	50	0.83440	0.80020	- 5752	- 7254
UK/SRD					
MONK 6.3	100	0.90190	0.87570	0	0
	75	0.90010	0.86660	- 200	- 1045
	50	0.88340	0.86570	- 2073	- 1149
UK/BNFL					
WIMSE	100	0.88820	0.84090	0	0
	75	0.86530	0.82610	- 2612	- 1776
	50	0.86200	0.82260	- 2994	- 2200
ITALY/ENEA-T*					
KENO-IV	100	0.87433	0.84534	0	0
	75	0.82662	0.80615	- 5611	- 4747
	50	0.82021	0.78308	- 6390	- 7650
ITALY/ENEA-C**					
XSDRNPM	100	0.87919	0.84273	0	0
	75	0.83009	0.78668	- 5747	- 6883
	50	0.82754	0.78317	- 6054	- 7330
ITALY/ENEA-C					
KENO-IV	100	0.87704	0.84177	0	0
	75	0.83981	0.78712	- 4338	- 6713
	50	0.82347	0.78384	- 6303	- 7130
JAPAN/PNC					
KENO-IV	100	0.88068	0.84826	0	0
	75	0.78011	0.70573	-12126	-18395
	50	0.76060	0.68583	-14659	-21256

* ENEA TRISAIA
** ENEA CASACCIA

To determine the origin of the discrepancy we decompose the dissolver k_{eff} value into two factors ; P^*, a non-leakage factor, and the k_∞ factor of the dissolver. The inaccuracy of the k_∞ calculation is also split into two components ; a contribution based on the uncertainty in nuclear data and a contribution based on the method of calculation.

2.1 - "Core" Calculation Biases and Neutron Leakage Rate

- Theoretical Considerations and the Decomposition of k_{eff}

The k_{eff} values reported in table 1, corresponding to a "core" calculation, can be factored as follows :

$$k_{eff} = k^* \cdot P^* \quad \text{where}$$

k^* = Production/A^{mixt}
P^* = $A^{mixt}/(A^{mixt} + A^{refl})$ and
A^{mixt} = Absorptions in the pellet + solution mixture
A^{refl} = Absorptions in the reflector

The non-leakage probability, P^*, can be expressed as :

$$P^* \simeq 1/(1 + M^2 \cdot B_g^2) \quad \text{where}$$

M^2 = the migration area which quantifies the "blackness" of the fissile mixture.

B_g^2 = the geometric buckling factor which characterizes the neutron leakage level, and

$$B_g^2 = [Jo/(R^{mixt} + \delta)]^2$$

δ is the reflector saving and corresponds here to $\delta_{H_2O} \simeq 7$ cm for pure water. R^{mixt} is the radius of the fissile solution ($R^{mixt} = 20$ cm).

The actual neutron multiplication factor of the fissile zone, k^*, can be expressed as :

$$k^* = k_\infty \cdot C^{spectrum}$$

where k_∞ is the neutron multiplication factor of the cell (pellet + solution) in an infinite lattice and $C^{spectrum}$ is the perturbation factor linked to the more thermalized neutron spectrum at the boundary between the fissile medium and the reflector.

- Comparison of the $P = k_{eff}/k_\infty$ Calculations of the International Contributors

To understand the spread of calculated k_{eff} values amongst the various participants it is necessary to uncouple or isolate the contribution of each factor in the equation for k_{eff}. The ratio :

$$P = \frac{k_{eff}}{k_\infty} = C^{spectrum} \cdot P^* = \frac{C^{spectrum}}{1 + M^2 \cdot B_g^2}$$

can be seen to include all potential sources of bias in the "core" calculations since it is a function of the non-leakage factor (hence the reflector saving and in-core reactions via the migration area) and the spectral perturbation effect at the dissolver/reflector boundary. Thus we can determine the contribution of each parameter to the value of k_{eff}. By comparing the values of P calculated by the international contributors, summarized in table 2, we can also determine the individual contributions to the spread in k_{eff} values from each source.

The data of table 2 are plotted in figure 3 for P.F = 0.6. We can see that there is satisfactory agreement before dissolution of the pellets. The value of P ranges between 0.771 and 0.787 which corresponds to an induced spread limited to 2000 pcm on the value of the dissolver k_{eff}.

TABLE 2

A SUMMARY OF LEAKAGE FRACTIONS

FOR BENCHMARK EXERCISE 20 CALCULATIONS

(JUNE 1988)

P=KEFF/KINF

	100%		75%		50%	
	PF=0.6	PF=0.4	PF=0.6	PF=0.4	PF=0.6	PF=0.4
USA/ORNL						
R-XSDRNPM	.78418	.79429	.73031	.78540	.74336	.79233
XSDRNPM	.78629	.79672	.81503	.80837	.82154	.81132
FRANCE/CEA						
APOLLO	.77978	.78595	.79202	.79192	.79330	.79316
UK/SRD						
MONK 6.3	.77073	.78440	.77785	.80942	.79233	.79087
UK/BNFL						
WIMSE	.75559	.78637	.75796	.78836	.75907	.78974
ITALY/ENEA-T*						
KENO-IV	.78169	.79774	.79888	.79077	.79473	.79709
ITALY/ENEA-C**						
XSDRNPM	.78294	.79486	.79562	.80110	.79814	.80327
KENO-IV	.78272	.79339	.79701	.80311	.79748	.79893
JAPAN/PNC						
XSDRNPM	.78907	.79651	.81130	.80958	.81962	.80897

* ENEA TRISAIA
** ENEA CASACCIA

- Variation of P with pellet dissolution

During dissolution of the pellets the value of the P factor increases as a result of a decrease in the migration area and modification of the spectral perturbation effect. The variation of P with dissolution expressed as [P(x %) - P(100 %)]/P(100 %) can be broken into three components as follows :

$$\frac{\Delta P}{P} = \frac{\Delta C^{spect}}{C^{spect}} - \frac{\Delta M^2}{M^2} \cdot \left(\frac{M^2 B_g^2}{1 + M^2 B_g^2}\right) - \frac{\Delta B_g^2}{B_g^2} \cdot \left(\frac{M^2 B_g^2}{1 + M^2 B_g^2}\right)$$

Table 3 summarizes the values of each term at various levels of dissolution determined in our reference calculations (see APOLLO P_{IC} in § 3). These components correspond to the reference curve in figure 3. The value of the weighting factor $M^2 B_g^2/(1 + M^2 B_g^2)$ is about 0.225.

% Pellet Remaining	ΔP/P (total) pcm	$C^{spectrum}$ component pcm	M^2 component pcm	δ_{refl} component pcm
100	0	0	0	0
75	+ 577	+ 566	+ 141	- 130
50	+ 815	+ 810	+ 195	- 190

TABLE 3

VARIATION OF THE DISSOLVER $P = k_{eff}/k_\infty$ FACTOR WITH PELLET DISSOLUTION

Table 3 indicates that the non-leakage probability, P^*, is constant during dissolution because the M^2 and reflector saving variations are of approximately the same magnitude but in opposite senses. In fact, variations in the value of P in "core" calculations are caused mostly by the overthermalization effect at the dissolver/reflector boundary.

As the pellets dissolve there is a decrease in the self-shielding effect. This results in increased resonance absorption and a corresponding decrease in the migration area ($M^2 = \bar{D}/\bar{\Sigma}_a$) of the fissile medium. On the other hand the increase in ^{238}U captures increases the sensitivity of the multiplying medium to the reflector thermalization effect. The $C^{spectrum}$ factor thus becomes larger as dissolution proceeds.

Figure 3 shows that the shape of the P vs pellet dissolution curves for the results of other contributors is consistent with our reference shape, however, the rate of increase is overestimated. In the NITAWL/SCALE calculations (see § 3, 4 and reference 2) this effect is due to overestimating the ^{238}U resonance capture rate with pellet dissolution. For example, the "NO DANCOFF pellet/solution" model (ND model) used in Italian calculations (XSDRNPM and KENO-IV, performed through the SCALE package) and in French non-P_{IC} APOLLO calculations, infers a 280 % overestimation of the $\Delta\bar{\Sigma}_a/\bar{\Sigma}_a$ at 50 % pellet dissolution. The variation of leakage fraction due to migration area is overestimated by a factor of 2.8. The spectral effect is overestimated by a factor of 2.2. These two components in the $\Delta P/P$ values of the ND model are the reason why the French and Italian values, [(P(50 %) - P(100 %)/P(100 %)], $\Delta P/P$ = + 1800 pcm compared to our reference value $\Delta P/P$ = + 800 pcm.

As shown in figure 3, the use of the new ROLAIDS routine in the SCALE system introduced a bias on the value of the leakage fraction as pellet dissolution proceeds. Although ROLAIDS improves the k_∞ calculation as a function of pellet dissolution (see next chapter) it causes another problem for fuel double-heterogeneity which is probably linked to migration area and scattering cross-sections in this routine.

2.2 - The sources of disagreement in k_∞ calculations

As indicated above, with the exception of ROLAIDS, "core" computations are generally satisfactory and cannot explain the observed spread in the international calculations of reactivity loss with pellet dissolution. We demonstrated that disagreement in the variation of P with pellet dissolution is due mainly to discrepancies in the k_∞ cell calculation such as the homogenized $\overline{\Sigma}_a$ cross-sections in double-heterogeneity cases. Furthermore disagreements in the shape of the P vs pellet dissolution curve are only the feedback effects of large biases in the k_∞ calculation, a feedback which tends to reduce the spread observed in the international k_∞ results.

Table 4 summarizes the k_∞ results and associated reactivity loss with dissolution of the contributors. Reactivity loss is defined as $\Delta\rho = \ln(k_\infty^{x\%} / k_\infty^{100\ \%})$. These data confirm the conclusion described above, showing that the reactivity loss at 50 % dissolution ranges from $\Delta\rho$ = - 2650 pcm to - 25000 pcm for the PF = 0.6 case. This large spread in calculated reactivity loss is shown graphically in figures 4 and 5 corresponding to PF = 0.4 and 0.6 respectively.

It remains to explain the discrepancies in the lattice k_∞ calculations and we present, below, sensitivity studies that permit us to show neutronics parameters that are capable of creating such large disagreements on reactivity loss.

TABLE 4

A SUMMARY OF K-INFINITY AND DELTA RHO VALUES
FOR BENCHMARK EXERCISE 20 CALCULATIONS (JUNE 1988)
AND REFERENCE VALUES (JUNE 1989)

		K-INFINITY		DELTA RHO	
		PF=0.4	PF=0.6	PF=0.4	PF=0.6
FRANCE/CEAREF					
APOLLOREF	100	1.12101	1.10081	0	0
	75	1.08936	1.07732	- 2864	- 2157
	50	1.08393	1.07042	- 3364	- 2800
	25	1.08042	1.06670	- 3688	- 3148
	0	1.07811	1.06512	- 3902	- 3296
USA/ORNL					
R-XSDRNPM	100	1.10407	1.07135	0	0
	75	1.07054	1.04809	- 3083	- 2194
	50	1.06390	1.04143	- 3707	- 2832
USA/ORNL					
XSDRNPM	100	1.10727	1.07730	0	0
	75	0.96494	0.87158	-13758	-21191
	50	0.94147	0.83829	-16222	-25084
FRANCE/CEA					
APOLLO	100	1.12450	1.10340	0	0
	75	1.05680	1.01450	- 6210	- 8400
	50	1.05200	1.00870	- 6664	- 8973
UK/SRD					
MONK 6.3	100	1.14980	1.13620	0	0
	75	1.11200	1.11410	- 3343	- 1964
	50	1.11700	1.09260	- 2894	- 3912
UK/BNFL					
WIMSE	100	1.12950	1.11290	0	0
	75	1.09760	1.08990	- 2864	- 2088
	50	1.09150	1.08370	- 3422	- 2650
ITALY/ENEA-T					
XSDRNPM	100	1.10195	1.08300	0	0
	75	1.04010	1.01100	- 5777	- 7688
	50	1.02826	0.98380	- 6921	- 9430
ITALY/ENEA-C					
KENO-IV	100	1.10070	1.07842	0	0
	75	1.04552	0.99835	- 5143	- 7715
	50	1.02986	0.98412	- 6652	- 9126
JAPAN/PNC					
XSDRNPM	100	1.10568	1.07501	0	0
	75	0.96359	0.86987	-13753	-21175
	50	0.94020	0.83677	-16213	-25054
FRG/GARCHING					
XSDRNPM	100	1.13000	1.12000	0	0
	75	1.06174	1.02003	- 6231	- 8417
	50	1.04329	1.00110	- 7984	-10290

2.2.1 - Spread due to nuclear data

The sensitivity studies, as does the neutron balance analysis of the benchmark calculations [2], show that different nuclear data sets account for the spread in k_∞ results at zero dissolution and that these spreads are 4100 pcm and 5900 pcm for PF = 0.4 and 0.6 respectively. On the other hand, the sensitivity studies demonstrated that the use of various different nuclear data files affected, only to a slight degree, the shape of the computed reactivity loss curve.

Figure 6 shows the effect of the nuclear data for fissile nuclei. The shape of the k_∞ vs pellet dissolution curve covering the complete dissolution range corresponds to the reference APOLLO calculations with the P_{IC} method.

The calculations were performed with the reference "CEA 86" 99-group cross-section library [6] based on the JEF library and internal CEA evaluations. The ^{235}U multigroup set was processed from our thermal cross-section evaluation [7] based on integral experiments in EOLE and MINERVE zero power reactors [8]. Another set of calculations was performed wherein the original ^{235}U cross-section data were replaced by the standard ENDF/BV data. Figure 6 shows that the k_∞ level is uniformly increased by Δk_∞ = + 500 pcm in the PF = 0.4 case and + 400 pcm in the PF = 0.6 (tight lattice) case. Figure 6 points out that the shape of the k_∞ vs pellet dissolution curve does not depend on the origin of the ^{235}U nuclear data.

2.2.2 - Errors introduced by cell methods

Since uncertainties in nuclear data cannot explain the discrepancies in reactivity loss calculations, the origin of the biases in the cases with pellet dissolution must be in formalisms and cell calculation methods. We note that cell calculations (pellet plus associated volume of solution in an infinite array) are carried out prior to "core" calculations to derive homogenized and energy-

collapsed cross-sections ; the homogenization and group-collapsing, performed using cell methods, require the following modelling considerations :

- A geometrical pattern is chosen for the cell calculation. For example in benchmark problem n = 20, the actual geometry of spherical pellets on a triangular or square pitch is replaced by a spherical cell pattern. This geometrical model is very accurate in well-moderated lattices such as the PF = 0.4 exercise. For the PF = 0.6 tight pitch case we calculated that the spherical cell pattern can introduce a maximum bias of $\Delta k_\infty/k_\infty$ = + 600 pcm at zero dissolution. Hence, geometrical modelling approximations contribute less than 500 pcm to the disagreement in calculated reactivity loss among the contributed results.

- Cell spatial processing is accurately treated since all contributors used transport calculations (S_n or first collision probability methods). Furthermore due to the low moderation ratios in the benchmark problem, the thermal disadvantage factor $\bar{\phi}_{mod}/\bar{\phi}_{fuel}$ is about 1.1 and cannot introduce significant errors in the homogenized cross-sections.

- Mutual shielding between ^{235}U and ^{238}U resonances modifies the k_∞ level but induces no change in the rate of reactivity loss with pellet dissolution. An accurate mutual shielding routine [9] was implemented in the 1986 version of APOLLO, specifically for High Conversion Reactor calculations. We verified that the mutual shielding in problem n = 20 amounts to a $\Delta\bar{\sigma}_c^{238}/\bar{\sigma}_c^{238}$ = 2 % decrease of the one-group self-shielded ^{238}U cross-section. This resonance interaction effect is quasi-independent of the dissolution level and represents a maximum k_∞ increase for PF = 0.6 of $\Delta k_\infty/k_\infty$ = + 600 pcm.

- The overall self-shielding effect, graphed on figure 7, amounts to a large $\Delta\rho$ = 60 000 pcm reactivity modification in our 99-group calculation. Owing to its magnitude, this phenomena is the only effect which can explain the benchmark calculation discrepancies. Hence, k_∞ biases are introduced by self-shielding formalisms, in the specific diluted cases, where resonant uranium isotopes stand in various media. This is due to the use of the standard Equivalence Theorem and the DANCOFF method which does not apply in such fuel double-heterogeneity problems, as shown in the next chapter.

3 - THE SELF-SHIELDING THEORY

The standard self-shielding formalism is presented first. The method is based on pretabulated homogeneous medium "effective" cross-sections and on the Equivalence Theorem. This formalism determines an homogeneous medium equivalent to the actual lumped fuel ; in many codes the array effect is accounted for by a transmission probability through the moderator, i.e. the DANCOFF factor.

In the specific case of fuel nuclei in the moderator, such as the solution in a dissolver, the standard model does not apply. We present below the P_{IC} method which is a generalization of the effective cross-section formalism.

3.1 - Standard self-shielding formalism

This formalism will be described as it is implemented in the APOLLO code. Self-shielded multigroup cross-sections are pretabulated in the APOLLO energy-mesh. The tabulation concept is based on a flux separation between the macroscopic slowing-down component and the fuel rapidly-varying fine structure.

a) The fine structure equation

In a heterogeneous cell with a single resonance isotope 0 in the fuel rod, the flux $\phi_f(u)$ in the fuel is derived from (assuming the flat flux approximation per medium) :

$$V_f \cdot \Sigma_o(u) \cdot \phi_f(u) = V_f.P(u).R_o\phi_f + V_{mod} \cdot P_{mf} \cdot R_m\phi_m \quad (1)$$

where R is the slowing-down operator and P is the first collision probability.

The macroscopic flux (spatially uniform) is defined as :

$$\psi(u) = R_m\phi_m(u)/\Sigma_m(u) \quad (2)$$

The flux $\phi_f(u)$ is factorized as the product of this macroscopic slowing down flux times a rapidly-varying fine-structure φ :

$$\phi_f(u) = \psi \cdot \varphi(u) \quad (3)$$

Assuming $R_o\phi_f(u) = \psi(u) \cdot R_o\varphi(u)$, the equation (1) yields the fine structure equation :

$$1/N_o \cdot R_o\varphi - (\sigma_o + \sigma_e)\varphi + \sigma_e = 0 \quad (4)$$

where σ_e is the equivalent cross-section :

$$\sigma_e(u) = \sigma_o(u) \frac{1 - P}{P} \quad (5)$$

$\sigma_o(u)$ is the total microscopic cross-section of the resonant nuclide.

σ_e^{238} versus σ_t^{238} (u) variation in zero dissolution cases is graphed on figure 8.

b) Tabulation of effective cross-sections

Since $\sigma_e(u)$ is weakly dependent on σ_o variations, the fine structure equation (4) is solved for constant values of σ_e (homogeneous medium) ; the corresponding refined "reaction rates" are then pretabulated in APOLLO for the discrete values σ_e^i (background cross-sections) and various temperatures T_j of the fuel :

$$\sigma^g_{eff_{ix}} = 1/\Delta u_g \cdot \int_g \sigma_x(u)\ \varphi(u)\ du \qquad (6)$$

where Δu_g stands for the lethargy width of the group g in the APOLLO mesh, and σ_{eff_x} is the effective cross-section for a reaction x (capture, fission, scattering).

c) Self-shielded multigroup cross-sections

The multigroup cross-sections must preserve the resonance reaction rates :

$$T^g_x = \int_g \sigma_x(u).\phi_f(u)\ du \ \# \ \psi^g \int_g \sigma_x(u).\varphi(u)du = \psi^g.\sigma^g_{eff}.\Delta u_g$$

then, the equivalence between reference refined reaction rates and APOLLO multigroup reaction rates yields :

$$\sigma^g_x \cdot \varphi^g = \sigma^g_{eff_x}\ (het) \qquad (7)$$

The self-shielded multigroup σ^g_x cross-sections are derived from this formula through solving iteratively the fine structure equation (4) on the multigroup APOLLO mesh :

$$\sum_{l=1}^{g} \sigma^l_{so} \cdot \varphi^l \cdot P_{l\to g} \cdot \Delta u_l - \sigma^g_o \varphi^g + \sigma^g_e (1 - \varphi^g) = 0 \qquad (8)$$

d) Equivalence Formalism (heterogeneous medium/homogeneous medium)

An intermediary step in the calculation of the σ_x^g is the computation of the geometry-dependent effective cross-sections $\sigma^g_{eff_x}$(het). This is done by performing an equivalence between the fine structure solutions of Eq. (4) in a homogeneous medium and in the actual geometry. The equivalence is obtained by equating the corresponding effective (absorption) resonance integrals over the entire resonance range :

$$I^{hom}(\sigma_{ev}) = I^{het}$$

The value of the geometry-dependent resonance integral is computed in the narrow-resonance approximation by pre-tabulated Lebesgue quadrature formula, and σ_{ev} is then obtained by interpolation on the infinite-medium pre-tabulated values $I(\sigma_e^i)$. Then the value of Bell's factor "a" is obtained from the definition :

$$a = \sigma_{ev}/\sigma_{e\infty} \qquad (10)$$

$$\text{where } \sigma_{e\infty} = \lim_{\sigma_{o}\to\infty} \frac{\sigma_o\,(1 - P)}{P}$$

Finally group-by-group geometry dependent effective cross-sections are calculated by interpolation on the σ_{eff} (σ_e^i, T_j) tables using the equivalent cross-section :

$$\sigma^g_{ev} = a.\sigma^g_{e\infty}\ (\Sigma^g_{mod})$$

e) Isotope mixture in the fuel rod

When various isotopes j are mixed in the fuel rod, the mutual-shielding effect is accounted for in APOLLO in the following way :

$$\sigma^{g}_{ev} = a^{o} \cdot \Sigma^{g}_{e\infty}/N_o + \sum_{j\neq o} \Sigma_{pj}/N_o \qquad (11)$$

where :

$$\Sigma^{g}_{e\infty} = \lim_{\Sigma_{fuel} \to \infty} \Sigma_f \, (1 - P)/P$$

Σ_p : potential scattering

This formulation of the mutual shielding effect accounts for dilution effects and corresponds to non-resonant and non-absorbing isotopes intermixed with the resonant isotope.

3.2 - The reference P_{IC} method

In the general situation where the resonant isotopes stand in j = 1, 2,..., N media of the calculation geometry, we have to generalize the previous formalism. Let k = 1, 2,..., M, indicate the numbering of the M non-fissile media. To simplify the presentation, we suppose that fuel media are constituted of ^{238}U nuclides only.

In every fissile medium i, the flux satisfies the equation :

$$V_i \, \Sigma_{ti} \, \phi i = \sum_{j=1}^{N} V_j \cdot P_{ji} \cdot R_8 \, \phi_j + \sum_{j=1}^{M} V_k \cdot P_{ki} \cdot R_k \, \phi_k \qquad (12)$$

The macroscopic flux is : $\psi = \dfrac{R_k \, \phi_k}{\Sigma_{tk}}$ (13)

The fine structure φ_j at the resonance energies is defined for each fuel region as follow :

$$\phi_j = \psi \cdot \varphi_j \qquad (14)$$

Accounting for reciprocity relations between collision probabilities, and the $R_8\ \phi_j = \psi . R_8\ \varphi_j$ slowing-down model, equation 12 becomes :

$$V_i\ \Sigma_{ti}\ \varphi_i = \sum_{j=1}^{N} V_i . P_{ij} . R_8\ \varphi_j \cdot \frac{\Sigma_{ti}}{\Sigma_{tj}} + V_i\ \Sigma_{ti} \sum_{k=1}^{M} P_{ik} \quad . \qquad (15)$$

Now we have to introduce the P_{IC} hypothesis :

$$\frac{R_8\ \varphi_1}{\Sigma_{t_1}} = \frac{R_8\ \varphi_2}{\Sigma_{t_2}} = \ldots = \frac{R_8\ \varphi_N}{\Sigma_{t_N}} \qquad (16)$$

Note that this approximation is justified in the Narrow Resonance model. Hence equation (15) becomes :

$$\Sigma_{ti}\ \varphi_i = R_8\ \varphi_i \cdot \sum_j P_{ij} + \Sigma_{ti}\ (1 - \sum_j P_{ij}) \qquad (17)$$

with the P_{IC} definition $P_{IC} = \sum_{j \in C} P_{ij}$ (18)

The equation (17) supplies the fine structure equation in the i^{th} fissile medium in the following manner :

$$R_8\ \varphi_i - (\Sigma_{ti} + \Sigma_e^i)\ \varphi_i + \Sigma_e^i = 0 \qquad (19a)$$

$$\Sigma_e^i = \Sigma_{ti} \cdot \frac{(1 - P_{IC})}{P_{IC}} \qquad (19b)$$

This fine structure equation is formally identical to equation (4) corresponding to fuel rods in an infinite array, but one must use a specific "P_{IC}" equivalent cross-section according to relations (18) and (19b).

Unlike the equivalent cross-sections in an infinite array (see figure 8), the $\sigma_e^{P_{IC}}$ is strongly dependent on the σ_t^{238} cross-section as shown in figure 9. Hence, at the peaks of the large resonances the geometrical component vanishes and the limiting value is equal to the "background" cross-section (potential scattering of fuel isotopes j intermixed with the resonant nuclide) :

$$\sigma_{e\infty}^{P_{IC}} = \frac{1}{N8} \sum_{j \neq U^{238}} N_j \cdot \sigma_p^j \qquad (20)$$

This limit must be compared to the standard formalism :

$$\sigma_{e\infty}^{238} = 1/N^{238} \left[\frac{1 - C}{\bar{l}} + \sum_{j \neq U^8} N_j \ \sigma_p^j\right] \qquad (21)$$

where $\bar{l}$ is the mean chord length in the pellet.

In fuel double-heterogeneity problems, the DANCOFF factor C no longest has significance because the resonant isotope also occurs outside the pellet. Consequently the "moderator transmission probability" concept is not adequate. Comparison of formulas (20) and (21) indicates that one should use, in the standard formalism, value of C = 0 for the DANCOFF factor when $\sigma_t^{238U} \rightarrow \infty$.

One should also note that the Bell factor, $a = \sigma_{ev}/\sigma_{e\infty}$, which accounted for the average variation of σ_e with the σ_t^{238} (u) variation is no longer useful.

3.3 - Models and approximations in criticality calculations

Dissolver design calculations use currently the standard self-shielding formalism (see § 3.1) corresponding to resonant isotopes located in a single medium.

3.3.1 - "No DANCOFF between pellet and solution" : ND model

In this model, uranium isotopes located in the fuel and in the solution are considered to be independant. The self-shielding effect is different in the various fuel media but the overshadowing effect, of the ^{238}U nuclei in the solution on the ^{238}U self-shielding of the pellet nuclei (and vice-versa), is neglected.

The ND model was used in APOLLO in the French contribution to the dissolver benchmarks ; due to the Nordheim Integral Method, the ND approximation is also implemented in the SCALE code system used by the several contributor countries. Although APOLLO does not utilize a DANCOFF approximation as do the SCALE modules, we deduced the DANCOFF factor from its exact collision probability calculations. These reference C values are compared in table 5 to the C values computed [10] by SUPERDAN and used in the NITAWL self-shielding routine of the SCALE system by the Italian contributors.

Benchmark case		Pellet		Solution	
		APOLLO	SCALE	APOLLO	SCALE
zero-dissolution 100 %	1b : PF = 0.6	0.5768	0.5594	-	-
	3b : PF = 0.4	0.3418	0.3255	-	-
mid-dissolution 50 %	1f : PF = 0.6	0.3930	0.3273	0.8384	0.0
	3f : PF = 0.4	0.2114	0.1868	0.8966	0.0

TABLE 5

DANCOFF FACTOR USED IN THE ND MODEL

Table 5 points out that the C factors are consistent in the pellet but the DANCOFF correction is systematicaly underestimated in the SCALE calculations. This is likely due to a DANCOFF correction which is limited to the nearest and second nearest neighbor lumped fuels. This underestimation of the pellet self-shielding is probably at the origin of the low k_∞ values obtained by users of the SCALE package (see in table 4 at zero-dissolution the comparison of French + British k_∞ values and the other k_∞ results based on SCALE use).

In diluted cases table 5 shows that DANCOFF correction is neglected by the SCALE system in the fissile solution. Consequently, inside the ND model used by SCALE, the overall self-shielding effect is underestimated. The SCALE self-shielding processing inside the solution is probably the explanation of the poor performances of the SCALE system in US and Japanese calculations.

3.3.2 - Average self-shielding model

In the APOLLO design calculations, one can use an averaged self-shielding effect among the various fissile media. Then in each group an independant-space equivalent cross-section is computed according to equation (5) :

$$\sigma_{e_i}^{av.} = \sigma_{t_i} \cdot (1 - \overline{P})/\overline{P} \qquad i = {}^{235}U,\ {}^{238}U, \ldots$$

A single shielded multigroup cross-sections set is derived and used in both pellet and solution medium.

For large σ_t values such as the peak of ^{238}U resonances, this model tends towards the homogeneous medium self-shielding.

3.3.3 - Homogeneous self-shielding approximation

Since resonant nuclides are located in the overall geometry for diluted cases, we tested the use of self-shielded factors corresponding to the homogeneous mixture of pellet and solution. The unique equivalent cross-sections is :

$$\sigma_{e_i}^{hom} = \sum_{j \neq i} \bar{N}_j \, \sigma_p^j \, / \, \bar{N}_i$$

4 - DISCREPANCIES LINKED TO VARIOUS SELF-SHIELDING MODELS

Discrepancies on the reactivity loss with pellet dissolution are introduced through self-shielded multigroup sets. The self-shielding effect is characterized by the σ_e equivalent cross-section value.

4.1 - The $\sigma_e(u)$ parameter

The actual σ_e^{238} variation versus σ_t^{238} (corresponding to reference P_{IC} calculation) is compared in tables 6 and 7 to the σ_e^{238} values obtained in the various models. This comparison is given at mid-dissolution.

The ND model supplies strongly overestimated $\sigma_e(u)$ values in both pellet and solution media. The equivalent cross-section overestimation increases strongly at the peak of the resonances : tables 6 and 7 point out that the corresponding capture reaction rates are overestimated by a factor 2 in the pellet because of the factor 4 on the σ_e pellet value.

For every σ_t^{238} level, the σ_e values of the Average and Homogeneous models are calculated as expected between the reference σ_e pellet and the σ_e solution values. It can be noted that this single value is overestimated : this spatial averaged equivalent cross-section is roughly comparable to $(\sigma_e^{pellet} + \sigma_e^{sol})/2$, hence the resonance integral varies as $\sqrt{\sigma_e}$.

σ_{tot}^{238U} (b)	Reference P_{IC}		σ_e^{ND} "No Dancoff"		$\sigma_e^{average}$	σ_e^{hom}
	Pellet	Solution	Pellet	Solution		
10.	67.54	106.1	103.80	212.2	82.99	101.67
50.	61.62	115.7	99.58	212.2	83.39	101.67
100.	55.19	126.5	95.24	212.2	84.17	101.67
250.	41.61	149.3	86.90	212.2	87.06	101.67
500.	30.13	167.5	80.93	212.1	90.92	101.67
1000.	20.97	180.4	77.15	212.0	94.88	101.67
5000.	10.98	192.3	73.99	211.9	100.01	101.67
∞	8.00	195.4	73.13	211.8	101.67	101.67

TABLE 6

σ_e^{238} (barns) versus σ_t^{238} in various models

BENCHMARK N° 20, 50 % PELLET DISSOLUTION, P.F = 0.4

σ_{tot}^{238U} (b)	σ_e P_{IC}		σ_e^{ND} "No Dancoff"		$\sigma_e^{average}$	σ_e^{hom}
	Pellet	Solution	Pellet	Solution		
10.	40.74	51.48	73.98	108.0	45.60	49.58
50.	37.48	55.57	72.03	108.0	45.68	49.58
100.	33.84	60.21	69.95	108.0	45.85	49.58
250.	25.93	70.32	65.75	108.0	46.48	49.58
500.	19.28	78.57	62.56	107.9	47.33	49.58
1000.	14.26	84.43	60.45	107.8	48.19	49.58
5000.	9.34	89.76	58.64	107.6	49.25	49.58
∞	8.00	91.13	58.13	107.5	49.58	49.58

TABLE 7

σ_e^{238} (b) versus σ_t^{238} - 50 % PELLET DISSOLUTION, P.F = 0.6

4.2 - The Interpolation equivalent cross-sections σ_{ev}

The σ_{ev} value deduced from eq. (10) corresponds to an $\bar{\sigma}_e(u)$ value averaged on the σ_t^{238} variations. This Interpolation equivalent cross-section is the constant value which preserves the overall I_{eff} resonance integral. This σ_{ev} value is used as the interpolation parameter in effective cross-section tabulations.

Tables 8 and 9 supply this Interpolation "background" value for the ^{238}U isotope in the various diluted cases. Tables 9 and 10 show the overestimation of σ_{ev} by the ND model, as soon as the pellet starts to dissolve and that the double heterogeneity effect increases.

Dissolution level	σ_{ev} P_{IC}		σ_{ev} ND		average σ_{ev}	hom σ_{ev}
	Pellet	Solution	Pellet	Solution		
1b : 100 % pellet	56	-	56	-	56.0	101.7
1d : 75 % pellet	39	305	66	430	84.4	101.7
1f : 50 % pellet	36	172	87	212	92.9	101.7
25 % pellet	36	125	113	139	98.28	101.7
Homogeneous : 0 %	-	101.7	-	101.7	101.7	101.7

TABLE 8 - "INTERPOLATION" EQUIVALENT CROSS-SECTION P.F = 0.4

Dissolution level	σ_{ev} P_{IC}		σ_{ev} ND		average σ_{ev}	hom σ_{ev}
	Pellet	Solution	Pellet	Solution		
3b : 100 % pellet	38	-	38	-	38.0	49.6
3d : 75 % pellet	27	127	48	224	45.3	49.6
3f : 50 % pellet	25	77	64	108	47.4	49.6
25 % pellet	25	59	96	69	48.8	49.6
Homogeneous : 0 %	-	49.6	-	49.6	49.6	49.6

TABLE 9 - INTERPOLATION EQUIVALENT CROSS-SECTION P.F = 0.6

4.3 - K-Infinity and $\Delta\rho$ loss with pellet dissolution

The main effect is linked to ^{238}U resonances, because of cancellation between fission and capture self-shielding in ^{235}U isotope.

Table 10 presents a summary of K_∞ variation and $\Delta\rho$ reactivity loss in the various calculational models.

Reactivity losses in the various calculation models are graphed on figures 10 and 11. The reference calculation shows a monotonic loss of reactivity to a maximum value of 3900 pcm and 3300 pcm (respectively P.F = 0.4 and 0.6) at complete dissolution. Standard approximations of design-oriented calculations may overestimate reactivity losses by 5000 pcm in the 75 % - 50 % dissolution range corresponding to Benchmark specifications.

Figures 10 and 11 indicate that the ND model used by Benchmark contributors is the most inaccurate model as soon as 10 % of the pellet is dissolved. Comparison of these curves with the $\Delta\rho$ computed by SCALE users and graphed on figures 4, 5 points out that Italian and German results are consistent with the APOLLO "ND" calculations. Large biases in automated SCALE calculations, shown in figures 4 and 5, are linked to an additional error in the solution self-shielding calculation as demonstrated in the companion paper.

TABLE 10

K-INFINITY AND REACTIVITY LOSS(DELTA RHO)
FOR APOLLO CALCULATIONS

		K-INFINITY		DELTA RHO	
		PF=0.4	PF=0.6	PF=0.4	PF=0.6
REFERENCE					
	100	1.12101	1.10081	0	0
	75	1.08936	1.07732	- 2864	- 2157
	50	1.08393	1.07042	- 3364	- 2800
	25	1.08042	1.06670	- 3688	- 3148
	0	1.07811	1.06512	- 3902	- 3296
NO DANCOFF					
	75	1.05943	1.02723	- 5650	- 6918
	50	1.05491	1.01955	- 6077	- 7668
	25	1.05868	1.02924	- 5721	- 6723
AVERAGE					
	75	1.06737	1.06398	- 4903	- 3403
	50	1.07156	1.06430	- 4511	- 3373
	25	1.07541	1.06484	- 4153	- 3322
HOMOGENEOUS					
	75	1.06504	1.06409	- 5122	- 3393
	50	1.06925	1.06433	- 4727	- 3370
	25	1.07287	1.06443	- 4389	- 3361

5 - REFERENCE CALCULATIONS

Our reference calculation is based on the APOLLO assembly code. Hence APOLLO is used by the CEA, the French utility Electricity de France and the constructor FRAMATOME for PWR and HCR calculations, it can be seen as a general purpose spectrum code based on the multigroup integral transport equation ; Refined collision probability modules allow the computation of 1D geometry with linearly anisotopic scattering and two term flux expansion. In 2D-geometries, modules based on the substructure method provide fast and accurate design calculations and a module based on a direct discretization is devoted to reference calculations. The SPH homogeneisation technique provides equivalent cross-sections between coarse and refined calculations. APOLLO can compute the depletion of any medium, accounting for any heavy isotope or fission product chain.

The new APOLLO version and its "CEA 86" multigroup library, based on the JEF1 file and on our own CEA evaluations, was used in this study. These multigroup cross-section set are in a 99-group energy mesh, with 52 fast groups down to the E = 2.77 eV thermal energy cut-off.

APOLLO-CEA 86 has been systematically checked against critical experiments and PWR measurements [6]. The multiplication factors of uranium and plutonium fueled lattices are calculated within 1000 pcm accuracy for every moderation ratio.

To check the consistency of the APOLLO deterministic transport calculation,it was carried out "reference" Monte-Carlo calculations with the French TRIPOLI system. The TRIPOLI code performs continuous energy calculations in 3D geometry. 45000 data points were used in the energy mesh of the resonance region. "Cell" calculations were carried out in a spherical pattern. The results are $\pm$ 200 pcm accuracy (one standard deviation) [12].

It was verified that the use of the optical reflection in the spherical cell pattern is not realistic and leads to erroneous $K\infty$ - values. This is demonstrated by the following test calculations performed in the P.F = 0.4 zero dissolution case :

Reflection model geometry	Optical spherical cell	Isotropic spherical cell	Optical square pitch
$k\infty$ TRIPOLI	1.164	1.121	1.118

It can be seen that the $k\infty$ = 1.121 TRIPOLI value in the cosine current reflection model is perfectly consistent with the value in the actual square pitch geometry. This $k\infty$ = 1.12 TRIPOLI value is consistent with the APOLLO value and corresponds to a reactivity loss $\Delta\rho$ = 4300 pcm with complete pellet dissolution.

The "reference" APOLLO-PIC and TRIPOLI $\Delta\rho$ reactivity loss calculations are graphed on figures 12 and 13. Previous 1988 MONK.6 results and up-dated 1989 MONK.6 calculations are also plotted.

At the PARIS - June 89 Meeting of OECD/NEACRP Criticality Calculation Working Group Meeting, complementary reference results were provided by other continuous-energy Monte-Carlo calculations : the italian criticality group performed MCNP calculations [10,11], and VIM calculations with ENDF/B IV library were carried out by the japanese representative [13].

The challenging fuel double heterogeneity calculation gave incentive to reactor physics teams to produce reliable calculation results on problem n°20, supplied to us at the PHYSOR'90 Conference [14] : the IKE german team provided CGM/ANISN calculations on an hyperfine slowing-down group structure [15] with the JEF1 data ; fine mesh slowing-down calculations were also performed [16] at JAERI with the PEACO code.

The $k\infty$ obtained with these rigorous methods are summarized here after in table 11.

PF = 0.4	APOLLO-PIC CEA-86	WIMSE 1989 calc.	MCNP[10] JEF-1	VIM[13] ENDF/BIV	CGM[15] JEF-1
100 %	1.1210	1.1269	1.1168	1.1075	1.1243
75 %	1.0894	-	-	-	1.0935
50 %	1.0839	1.0864	1.0761	1.0658	1.0875
25 %	1.0804	-	-	-	1.0838
0 %	1.0781	-	-	-	1.0815

P.F = 0.6	APOLLO CEA-86	WIMSE 1989 Calc.	MCNP[10] JEF-1	VIM[13] BIV	PEACO[16]	CGM JEF-1
100%	1.1008	1.1032	1.0902	1.0839	1.0865	1.1028
75 %	1.0773	-	-	-	1.0615	1.0777
50 %	1.704	1.0727	1.0586	1.0491	1.0546	1.0707
25 %	1.066/	-	-	-	1.0498	1.0674
0 %	1.0651	-	-	-	1.0470	1.0655

TABLE 11 : K∞ values in reference calculations

All these reference calculations indicate a monotonic reactivity loss with pellet dissolution as shown in figures 12,13. Deterministic and Monte-Carlo calculations are consistent. The results are in close agreement on the slight rate of the reactivity loss, -3700 pcm to -3000 pcm at mid-dissolution for P.F = 0.6 to P.F = 0.4. The spread of reference calculations is less than 1000 pcm.

REFERENCES

[1] E. SARTORI - WHITESIDES
OECD/NEA Criticality Calculations Working Group Meeting
PARIS, June 27-30 1988.

[2] H.J. SMITH - A. SANTAMARINA
"An analysis of the results of an international OECD/NEA criticality benchmark calculation on fuel dissolvers".
OECD Criticality Meeting.
PARIS, June 27-29 1989.

[3] A. KAVENOKY et al.
"The APOLLO assembly spectrum code".
Proc. International Topical Meeting on Advances in Reactor Physics, Mathematics and Computation" - Vol. 3.
PARIS - 27 - 30 April 1987.

[4] A. SANTAMARINA
CEA/DRE/SEN Report n° 83-161.
February 1983.

[5] H. AKIE - Y. ISHIGURO - H. TAKANO
"Summary Report on the International Comparison of NEACRP Burn-up Benchmark Calculations for HCLWR Lattices".
JAERI-M-88-200 Report - NEACRP-L-309.
October 1988.

[6] A. SANTAMARINA - H. TELLIER
"The French PWR multigroup cross-section library and its integral qualification".
Proceedings of the International Conference on Nuclear Data.
MITO - JAPAN - 30 May - 3 June, 1988.

[7] A. SANTAMARINA - C. GOLINELLI - L. ERRADI
Proceedings ANS Topical Meeting on Reactor Physics, 1, 48
CHICAGO (USA).
September 1984.

[8] A. SANTAMARINA et al.
"Nuclear Data qualification trough French LWR Integral Experiments".
International Conférence in Nuclear Data, 1, 509.
SANTA-FE (NM) 13-17 March 1985.

[9] A. SANTAMARINA et al.
"Development of French computer codes and methods for HCLWR design calculations".
OECD/NEACRP specialists meeting on HCLWR.
PARIS 19-22 April 1988.

[10] P. LANDEYRO.
Personal communication.

[11] F. SICILIANO.
Personal communication.

[12] J.C. NIMAL
"Criticality calculations by TRIPOLI-2 Monte-Carlo Code".
OECD-NEACRP Criticality Working Group Meeting.
PARIS June 27-29 1989.

[13] Y. NAITO
"Computed Results on exercise 20 with the computer Code VIM".
NEACRP Criticality Working Group Meeting.
PARIS June 1989.

[14] A. SANTAMARINA, H. SMITH, G.E. WHITESIDES
Proceeding of the international PHYSOR Conference, Vol 2, p. XI-95.
MARSEILLE - France, April 23-27 1990.

[15] W. BERNNAT, J. KEINERT
"Calculation of the benchmark 20 of the OECD-NEA Working Group"
Report KFK 4695 - IKE 6/180 - March 1990

[16] K. TSUCHIHASHI
Personal Communication at PHYSOR Conference - April 1990.

Figure 1 : Keff values

Benchmark n° 20

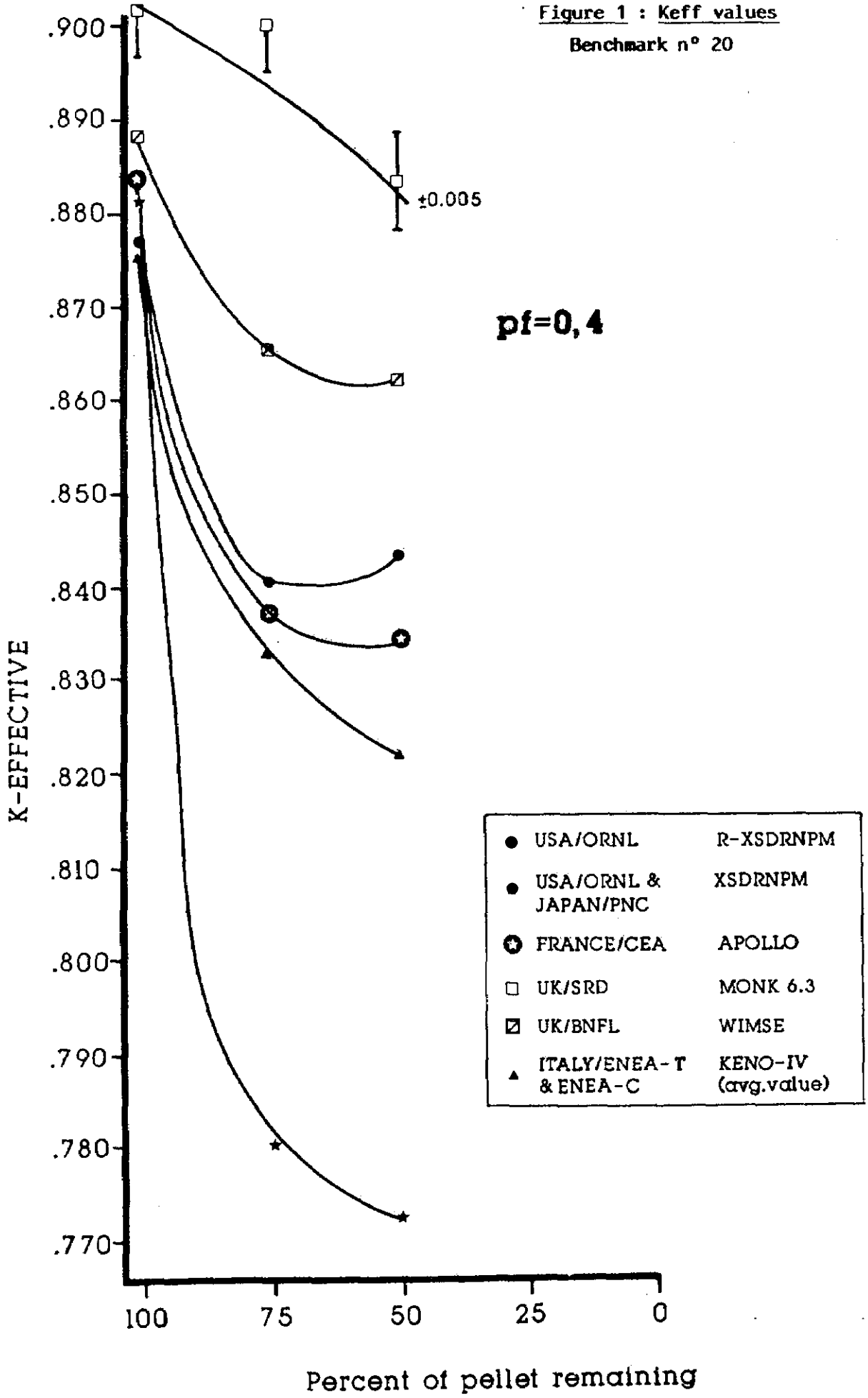

Figure 2 : Keff values

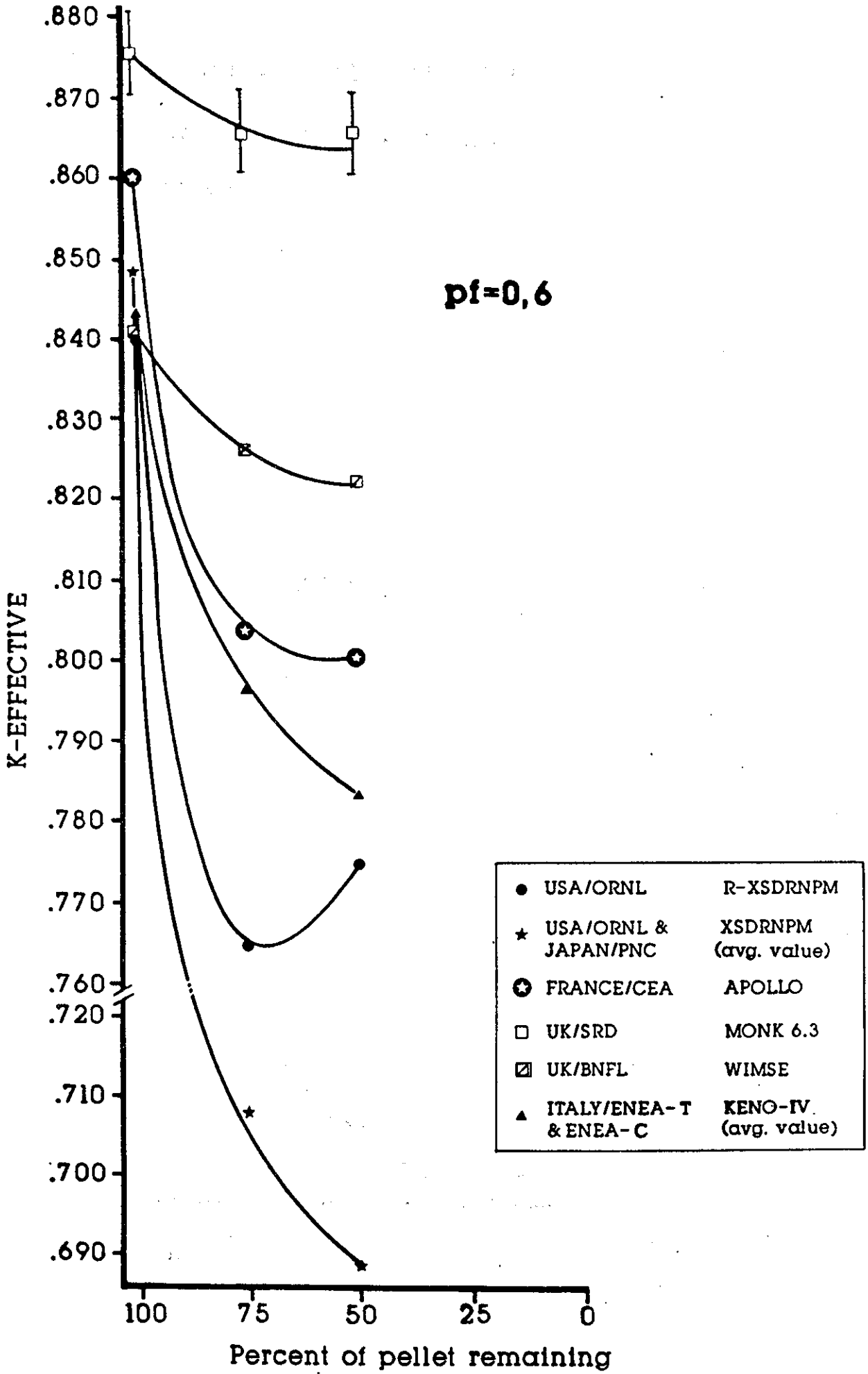

Fig.3 **Non-leakage factor** $P=\frac{Keff}{K\infty}$

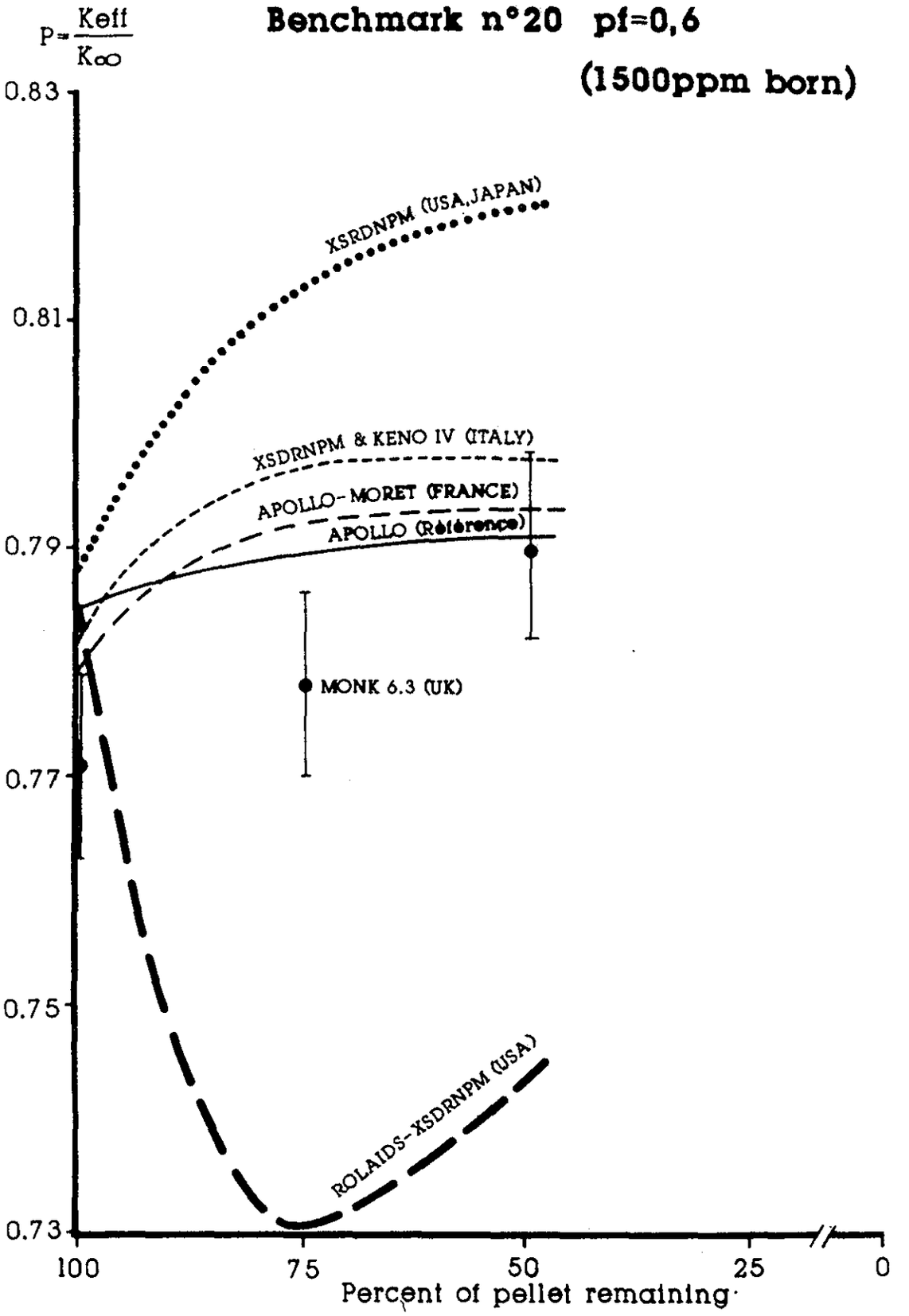

Figure 4 : Reactivity Loss in benchmark n° 20

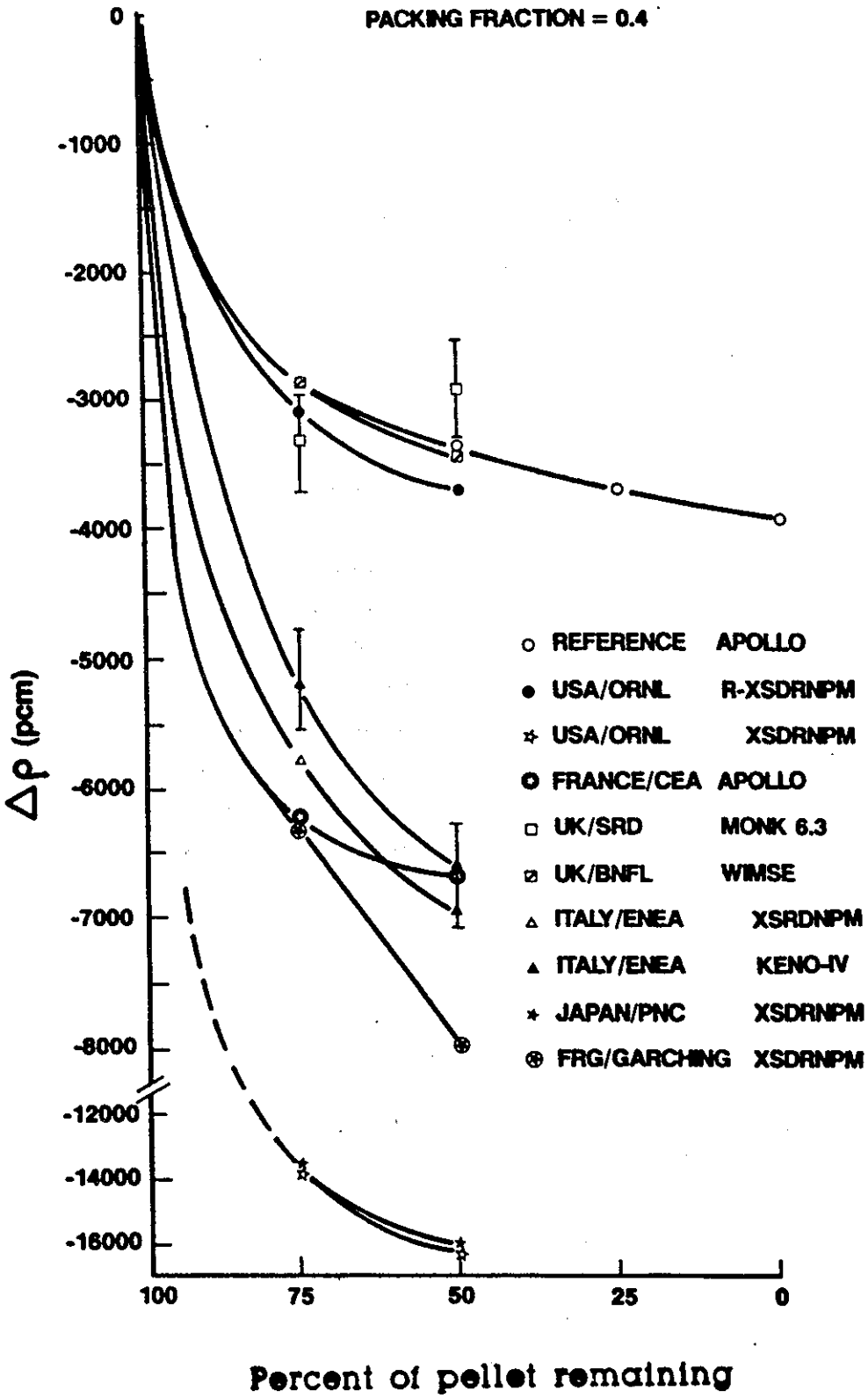

Figure 5 : Reactivity Loss

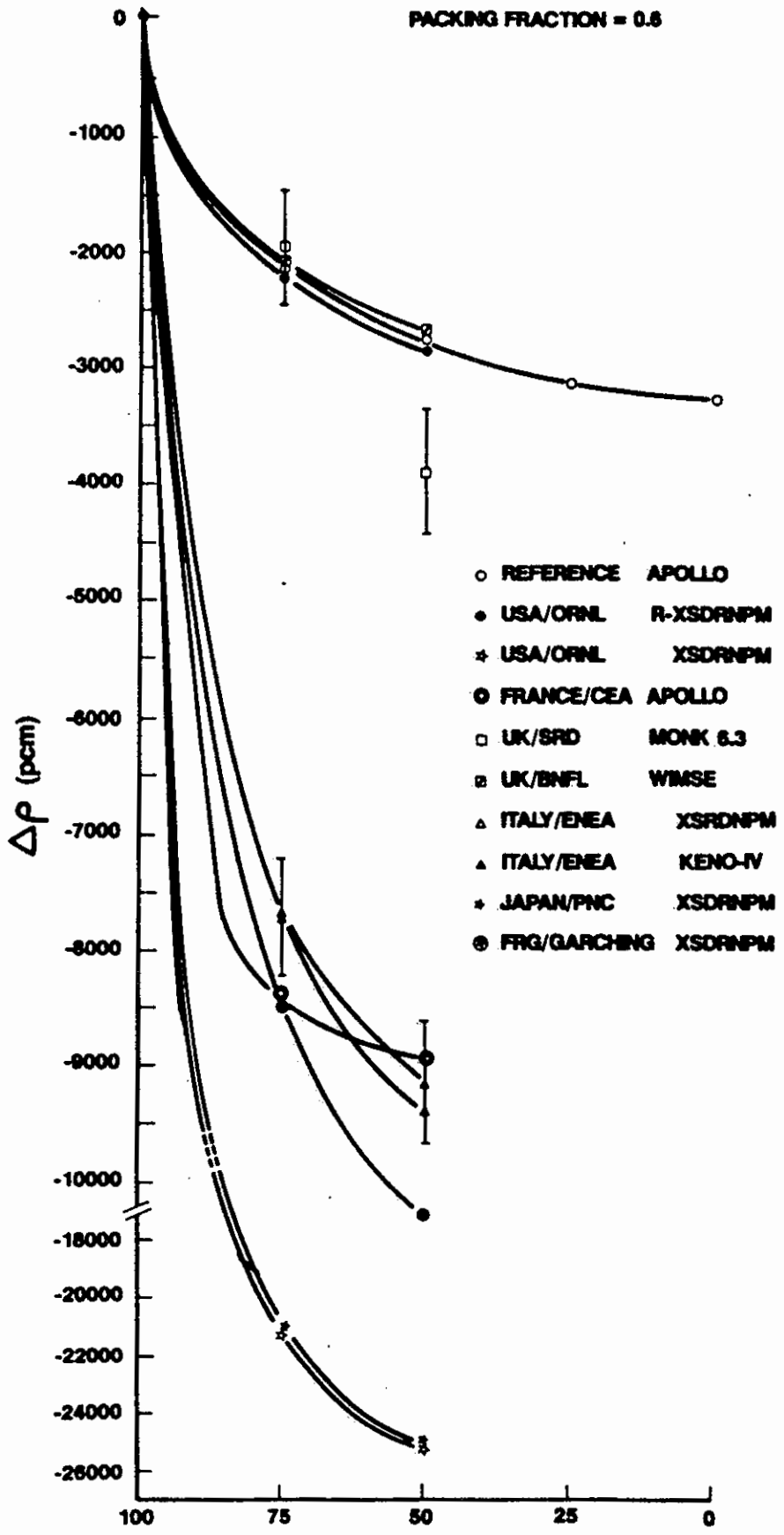

Fig.6 **K∞ shope with ^{235}U cross-section set**

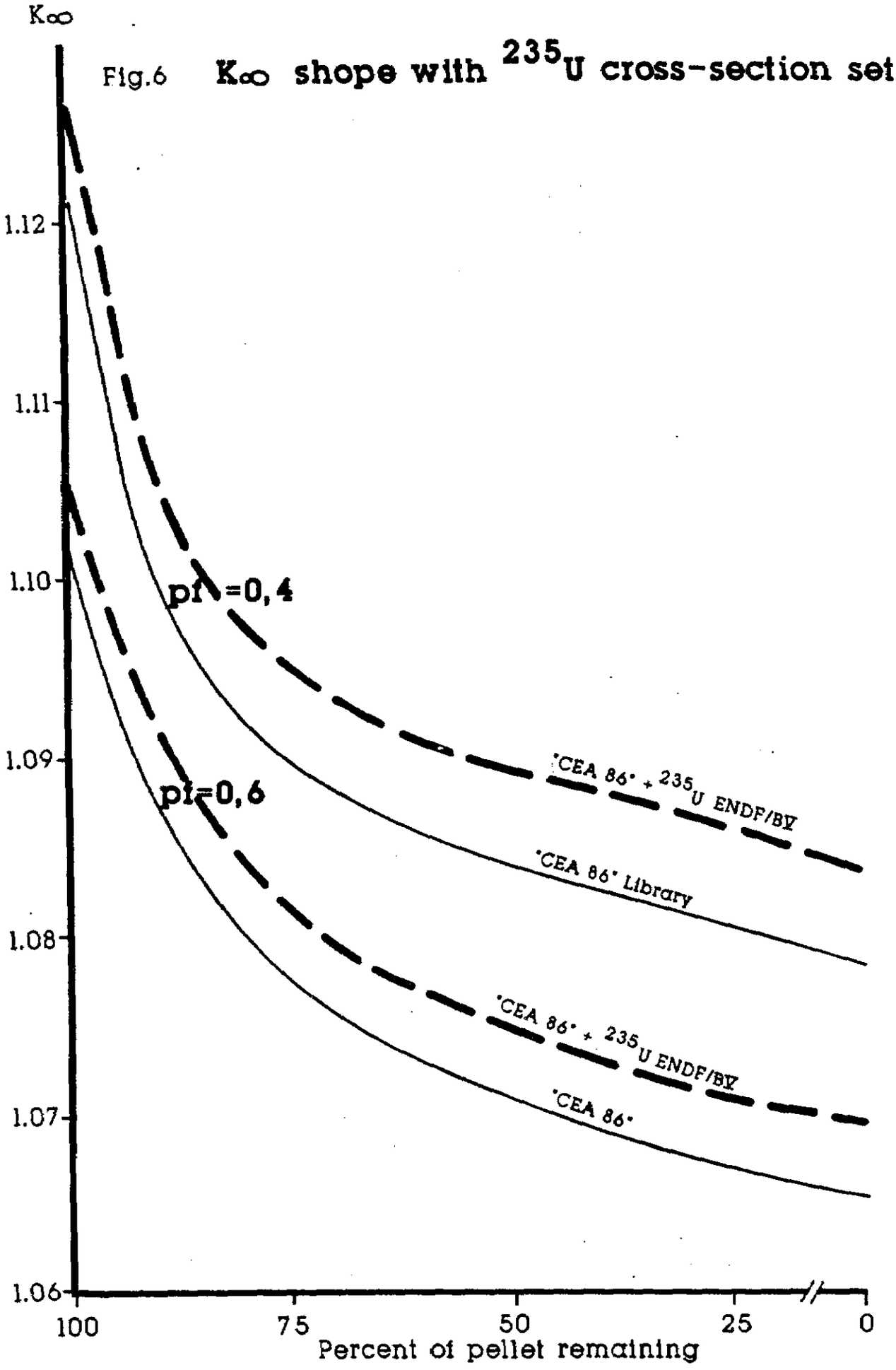

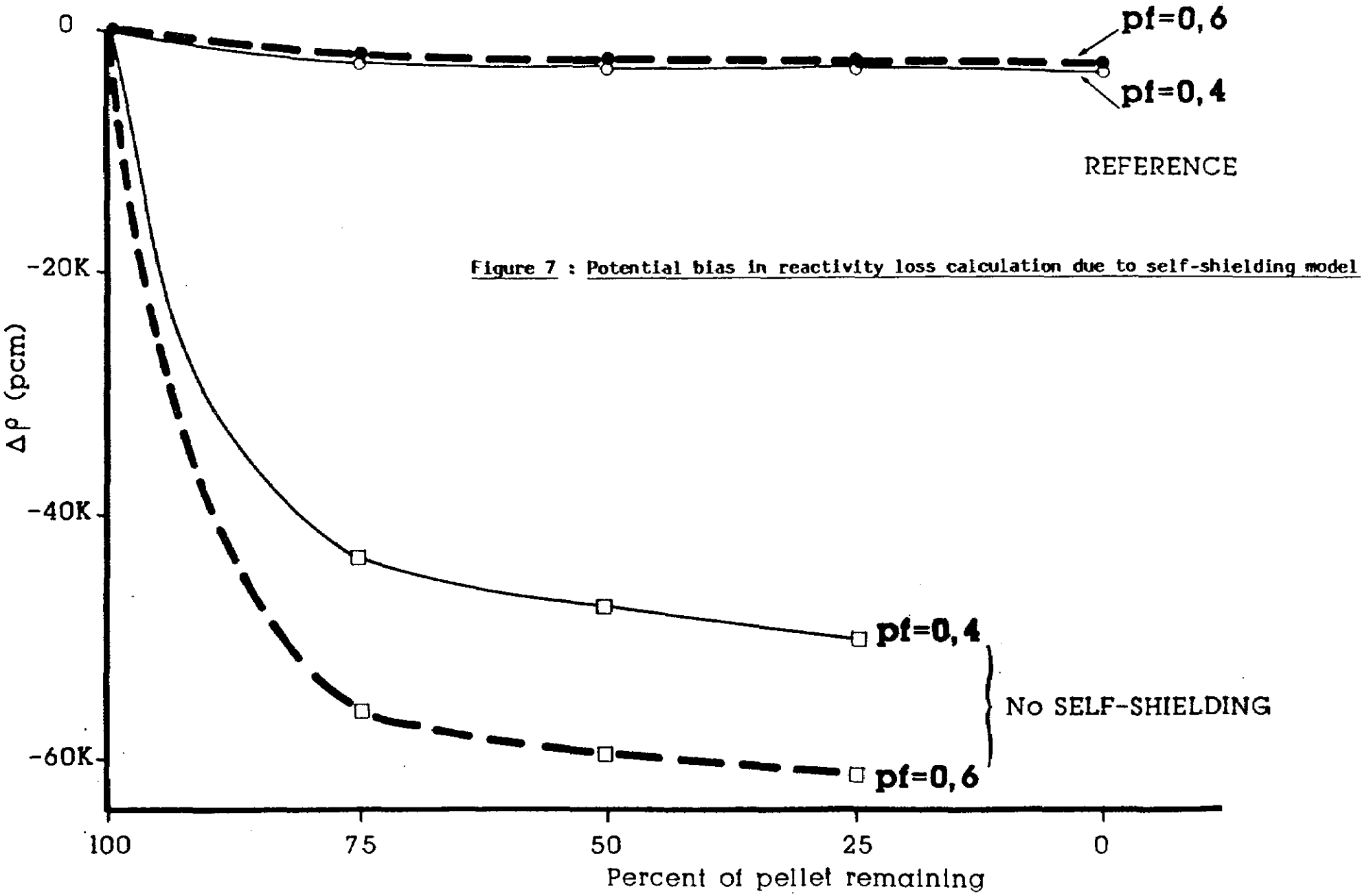

Figure 7 : Potential bias in reactivity loss calculation due to self-shielding model

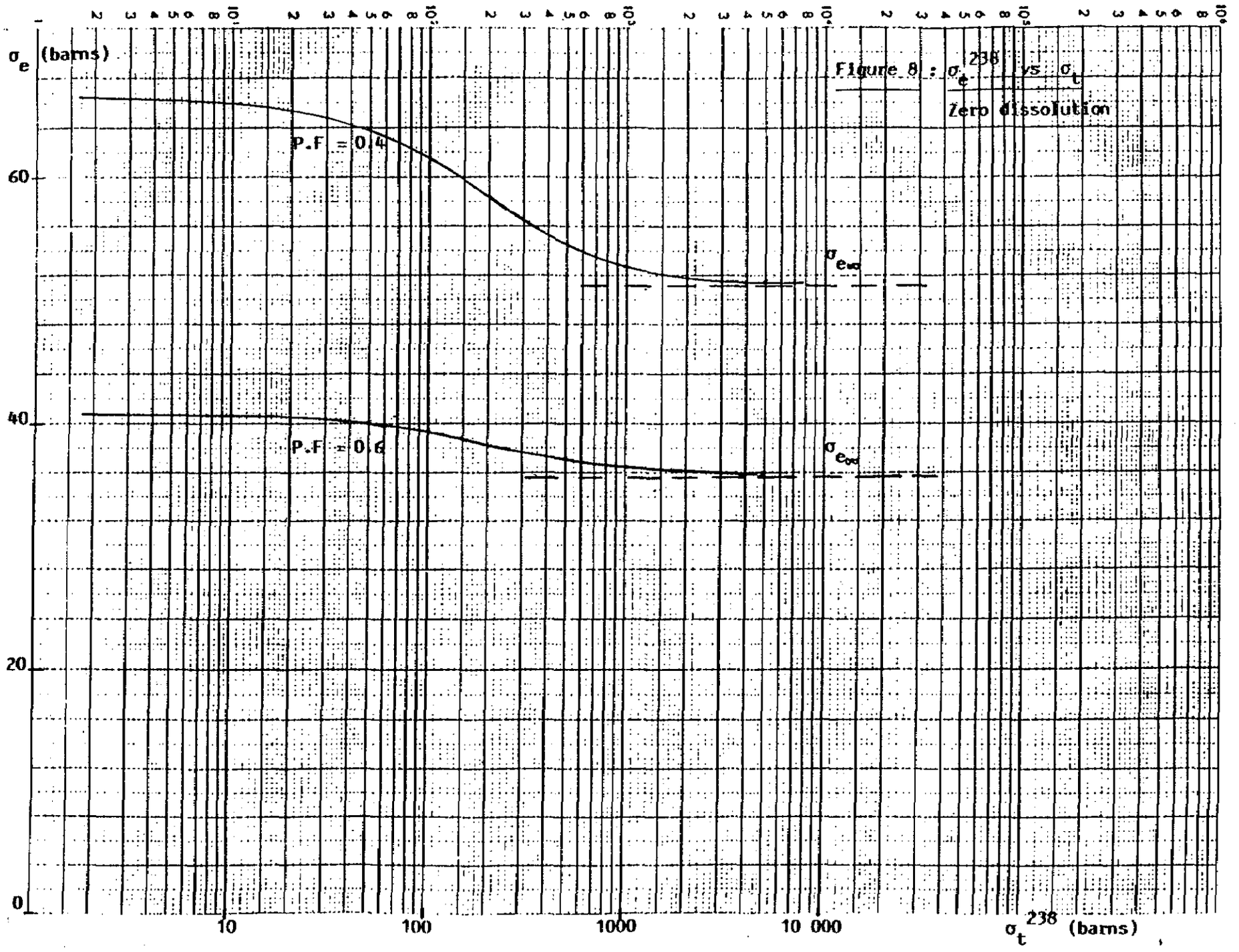

Figure 8 : σ_e 238 vs σ_t

Zero dissolution

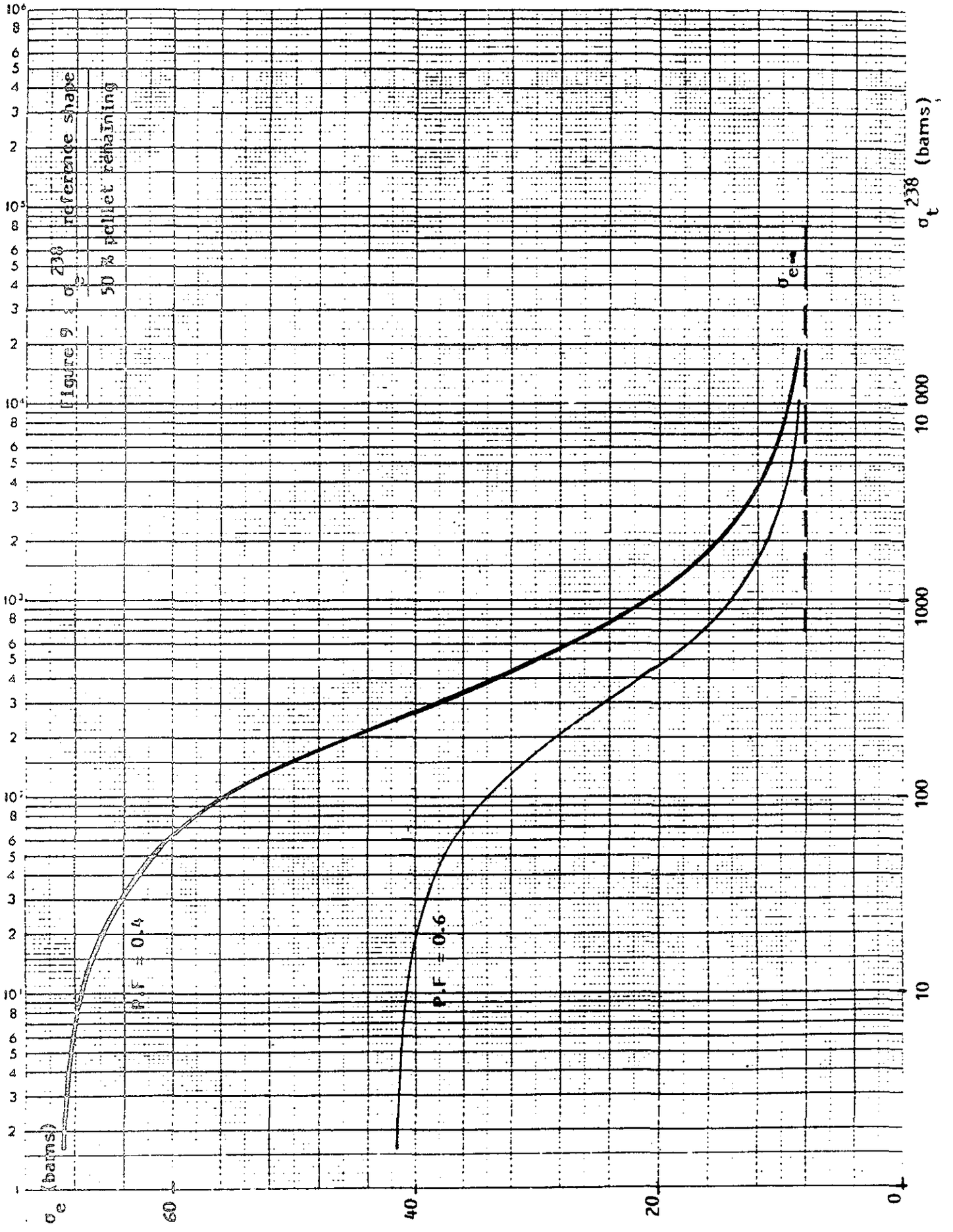
Figure 9 : σ_e of 238 reference shape
50 % pellet remaining
σ_e (barns)
σ_t 238 (barns)
P.F = 0.4
P.F = 0.6
$\sigma_{e=1}$
60
40
20
0
10 000
1000
100
10

Figure 10 : Reactivity loss as a function of pellet dissolution for various models of self-shielding

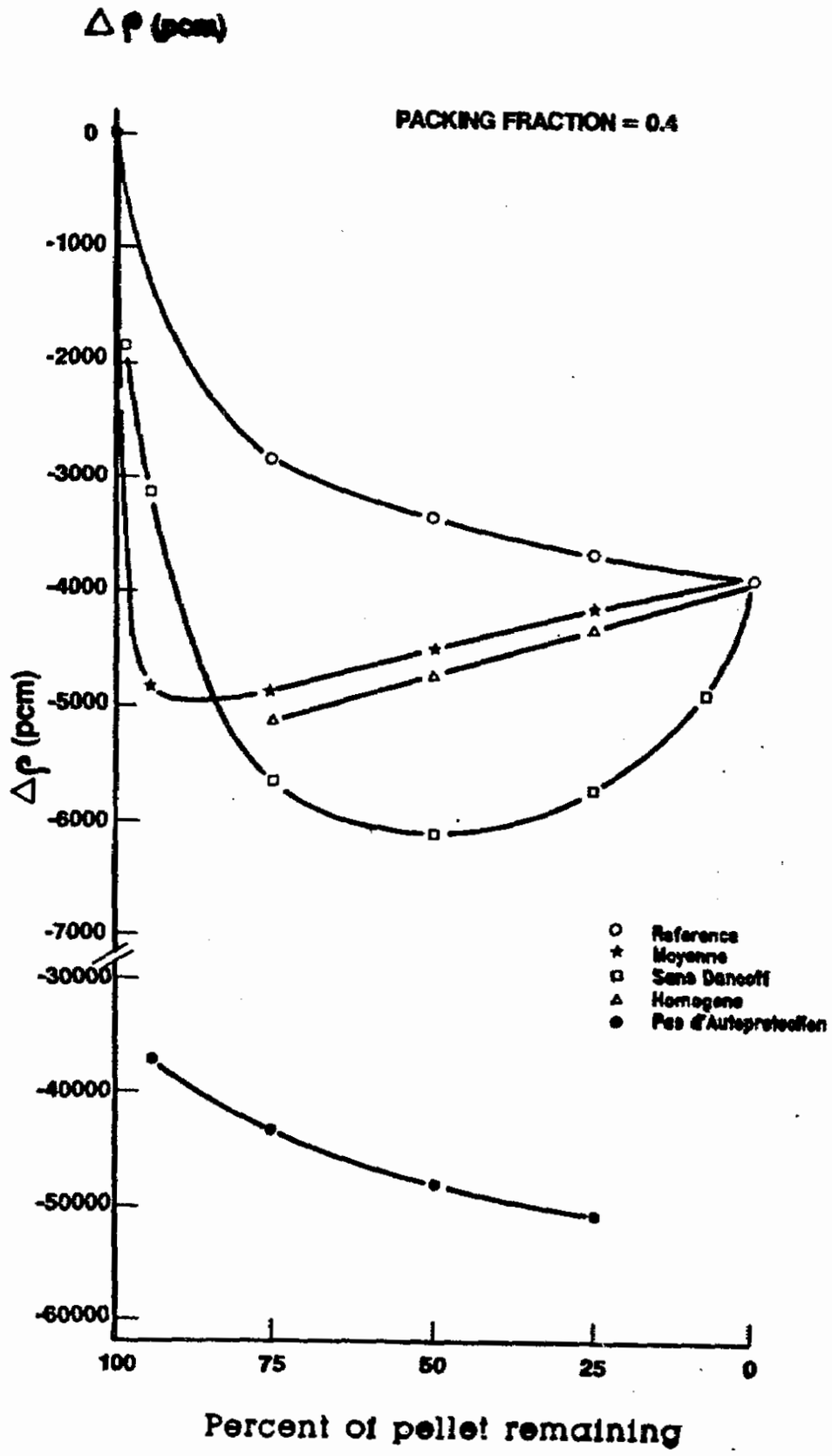

Figure 11 : Reactivity loss as afunction of pellet dissolution for various models of self-shielding

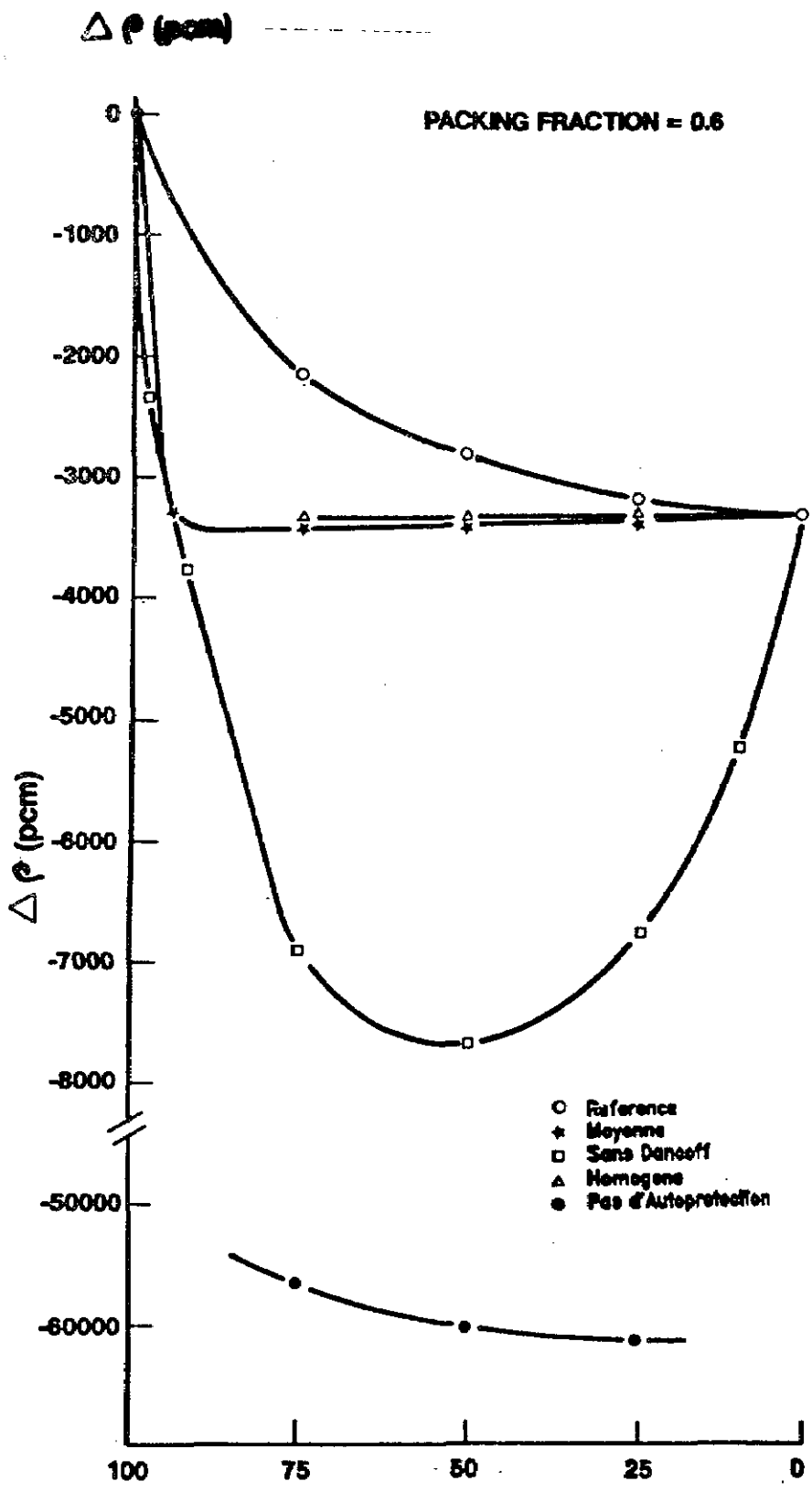

Figure 12 : Reference calculations

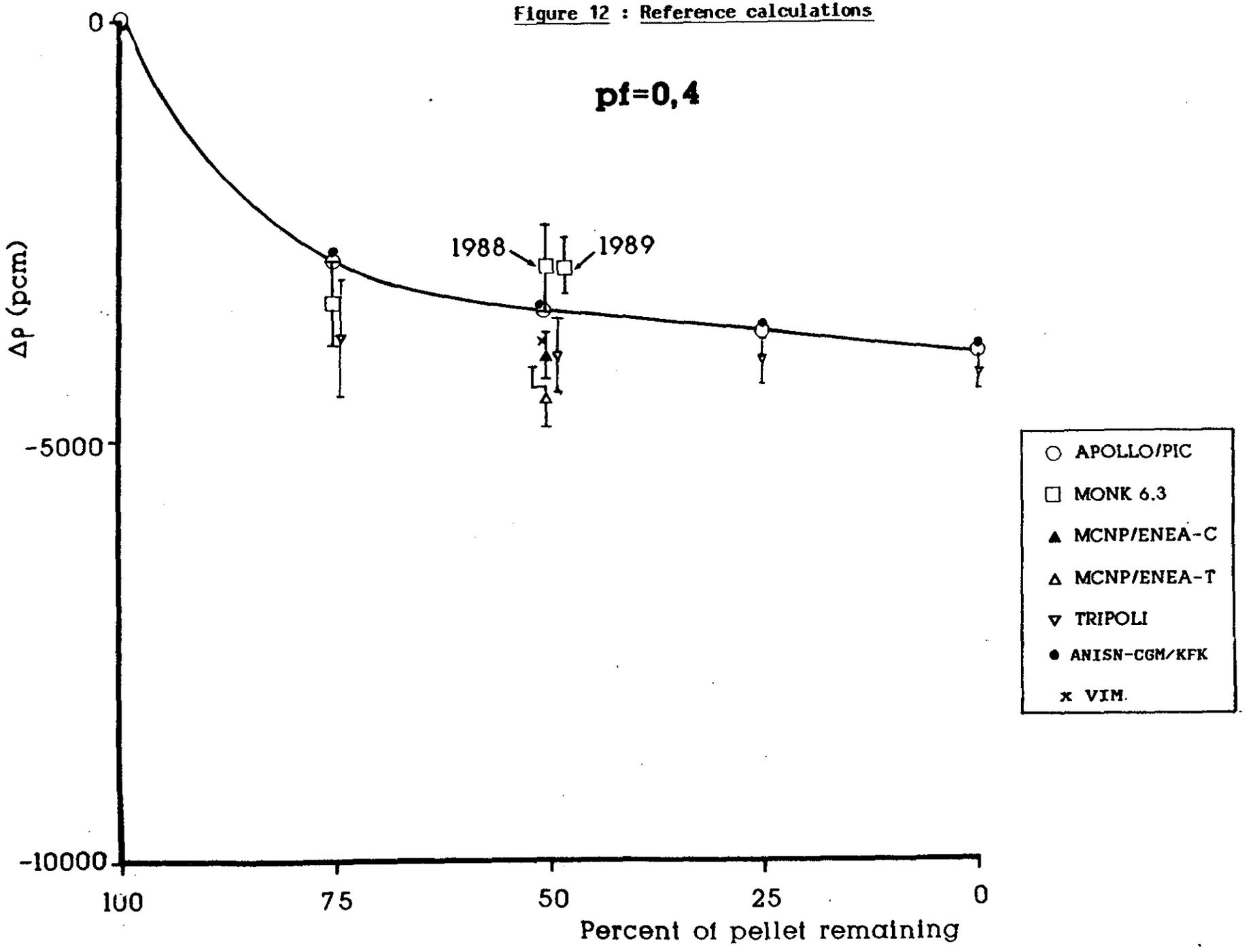

Figure 13 : Reference calculations

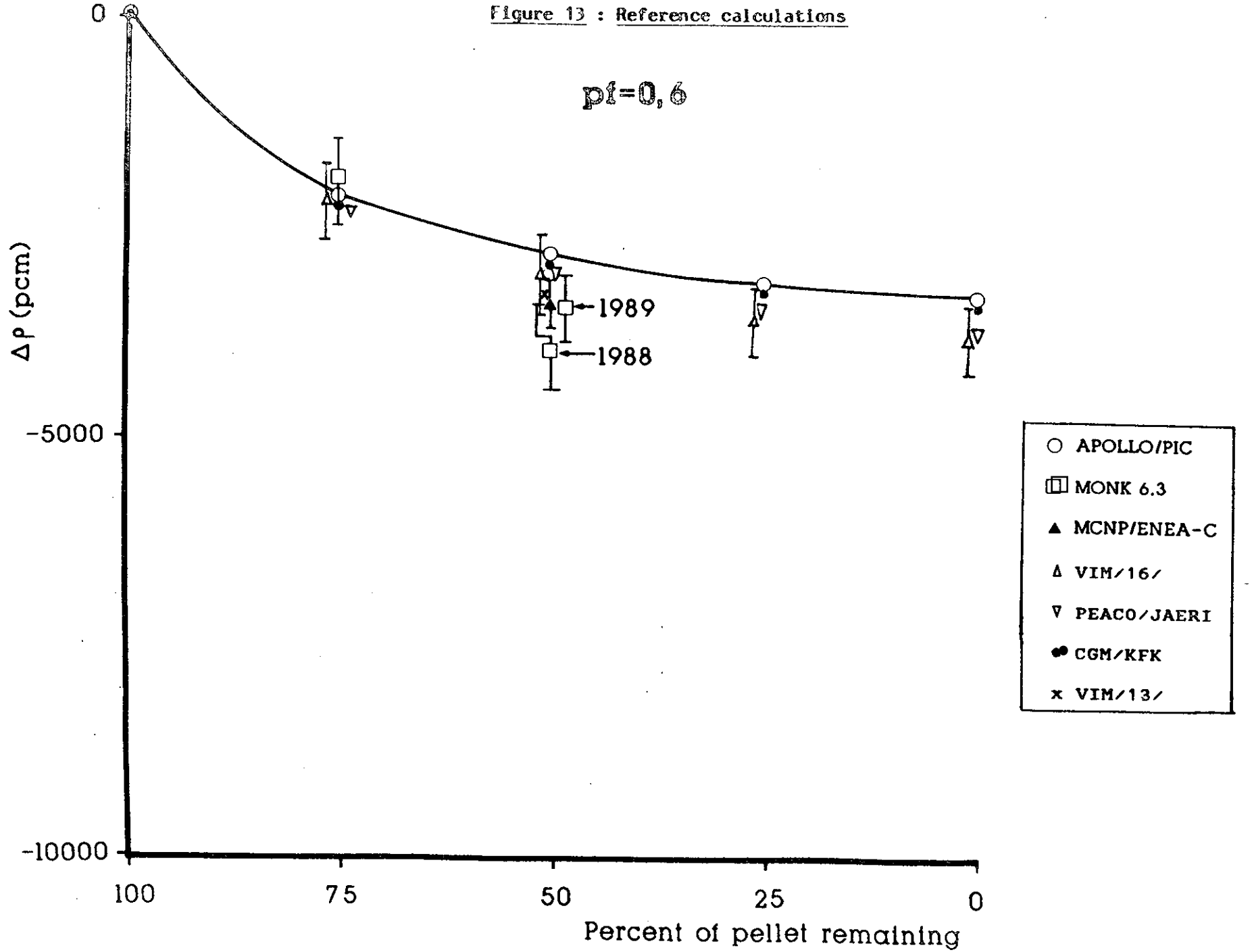

B - AN ANALYSIS OF THE RESULTS OF THE OECD CRITICALITY WORKING GROUP BY NEUTRON BALANCE METHODS

ABSTRACT

The OECD/NEA Criticality Benchmark Exercise of June 1988 showed that for many classes of problems satisfactory agreement (reactivity differences less than 4000 pcm (10^{-5} in $\Delta k/k$ can be achieved among the results of various contributors, however, the results for fuel dissolver calculations are highly discrepant (reactivity differences as high as 25000 pcm). The aim of this paper is to understand the origin of the wide spread in results from the various laboratories for this class of problems.

To achieve this objective we focussed on problem 20 of the benchmarking exercise as being the most discrepant case. From the range of variables covered by problem 20 we chose cases with a boron concentration of 1500 ppm and pellet concentrations at the two extreme values of triangular pitch. It can be shown that the other conditions described in problem 20 contribute no new information to the analysis.

For the cases thus defined we requested that the participants complete a standard table of all relevant reaction rates in three energy groups based on their calculations of June 1988.

This paper presents a comprehensive summary of all reaction rates (June 1988 study, reference APOLLO-PIC values, new results) contributed to the present time.

We have carried out a physics analysis of these data by means of a neutron balance based on the reaction rates. The multiplication factor was evaluated by three methods of decomposition : phenomenological (eg. resonance escape probability etc), historical (by energy group) and spatial. In this manner, a comparison of the participants results enabled us to identify the origin of the discrepancies ; the major factor is shown to be the resonance escape probability. This result is consistent with the conclusions of the theoretical study presented in chapter A.

SUMMARY

INTRODUCTION

The OECD/NEA Criticality Benchmark Exercise of June 1988, [1], showed that for many classes of criticality problems satisfactory agreement, i.e. reactivity differences less than 4000 pcm (10^{-5} in $\Delta k/k$), can be achieved among the results of calculations from different laboratories. It also showed, however, that for calculations on fuel dissolvers, widely different results may be obtained with reactivity differences as high as 25000 pcm, depending upon the conditions in the dissolver. The aim of this paper is to understand the origin of the wide spread in results from the various laboratories for this class of problems.

To achieve this objective we focussed our attention on problem 20 of the benchmarking exercise, [1], as being the most discrepant case. From the range of variables covered by problem 20 we chose a subset that we felt would adequately demonstrate the various facets of the problem with the minimum amount of computation. To this end we limited the cases to those with a boron concentration of 1500 ppm, pellet concentrations at the two extreme values of triangular pitch and two levels of dissolution, zero percent (100 % of fuel remains in the pellets) and 50 percent (50 % of the fuel is in the pellet, 50 % of the fuel is distributed uniformly throughout the solution). It can be shown that the other conditions described in problem 20 contribute no new information to this analysis.

For the cases thus defined we solicited from the participants a listing, in a standard table mailed to them, of all relevant reaction rates, in three energy groups, from their calculations of June 1988.

This paper presents a comprehensive summary of the reaction rates and an in-depth analysis of the factors which determine the value of k_∞. The analysis consists of a series of neutron balance formulations which view k_∞ from different perspectives ; phenomenological, historical (age theory/energy group), spatial. In this manner one can probe the origins of the discrepancies. The

results show that the problem rests primarily with improperly self-shielded ^{238}U resonance cross-sections when calculating situations that involve a double-heterogeneity. The results also show that XSDRNPM is capable of enormous errors in the calculation of reactivity losses which can be mitigated to some extent by the use of ROLAIDS.

Two other data sets from MCNP calculations were submitted as potential reference calculations. These data are included in this report. They were analyzed and are examined separately from the benchmark results.

1 - FRAMEWORK OF THE CALCULATIONS

The four cases treated in this study were given identification codes in the original benchmark study to facilitate discussion. They are defined as follows :

3B zero dissolution, packing fraction (pf) = 0.4
3F 50 % dissolution, cell size based on pf = 0.4
1B zero dissolution, packing fraction = 0.6
1F 50 % dissolution, cell size based on pf = 0.6

where the packing fraction is defined as $V(UO_2)/V(cell)$.

We note that the conditions in case 3B are typical of those found in light water reactors (PWRs) whereas the conditions in case 1B represent a significantly undermoderated reactor.

Reference calculations on these cases were carried out by the authors using the P_{IC} formalism in the APOLLO code as described in part A of this report. Reference calculations were also carried out to total dissolution of the pellets to define the limits of variation and to check for continuity of results. The discussion in this paper refers, for the most part, to deviations from these reference calculations. Reactivity differences are defined as $\ln(k_x/k_{ref})$ and are given in units of pcm where 1 pcm = 10^{-5} $\Delta k/k$.

The problem is illustrated in figures 1 to 4. Figures 1 and 2 present the k_∞ data, as functions of the percent of the fuel remaining in the pellet, from the June 1988 exercise [1]. These figures also include the results of the reference calculations for this study. Figure 1 shows the reasonably close agreement of most results for the 3B case. This is to be expected since these codes have evolved in the PWR context. Figure 2 shows an increase in the spread of results as the lattice becomes undermoderated and both figures show a very large increase in the spread of results as the fuel pellets are dissolved thereby introducing the double-heterogeneity.

Figures 3 and 4 present the same data in terms of reactivity losses from the cases at zero dissolution. Both figures now show a clustering effect based on the rate of reactivity loss with dissolution. In the first group are results from the codes APOLLO/CEAREF, R-XSDRNPM, MONK 6.3 and WIMSE. In the second group are results from the codes XSDRNPM/ENEA, KENO-IV, APOLLO/CEA and XSDRNPM/GAR. and in the third group are results from XSDRNPM/PNC and XSDRNPM/ORNL (i.e. no ROLAIDS treatment).

The data presented in Figures 1 to 4 are summarized in Table 1.

2 - TREATMENT AND IDENTIFICATION OF SUBMITTED DATA

As reaction rate data sheets were received from participants the value of the ratio of the sum of the production rates to the sum of the absorption rates was evaluated as a preliminary test to check for inconsistencies. The value of k_∞ thus obtained was also used as an internal check to ensure that data had not been improperly transcribed when creating the computer files. The standard forms that were mailed to the participants also permitted a certain amount of latitude in the presentation of the data and occasionally some manipulation was required to achieve a uniform presentation for data entry. For example, absorption rates of materials such as natural boron and water may be presented as the rates of individual isotopes. When the format of the submitted data did not match the required format it would have to be altered. Thus copies of the data sheets, as submitted, were reported at the 1989 Meeting [2] (Report [2] also contains the data that were used for data entry. A header page precedes each participants data set with notations that identify the participant, the laboratory, the code and the data library used and that describe the alterations to the submitted data). The value of the ratio of the sum of the production rates to the sum of the absorption rates was reevaluated to check for errors. The data was analyzed by a computer program which executed the neutron balance breakdown from the normalized reaction rates (Appendix I).

Data sets were received from the eight participants who were involved in the June 1988 problem 20 calculations. Since two different laboratories from each country, except the USA, contributed to the exercise an identification scheme was devised. Table 2 shows the identifier for each participant.

Some codes were used by different laboratories. The various cases were distinguished by appending part of the identifier to the code name e.g. XSDRNPM/PNC. The use of the ROLAIDS treatment prior to XSDRNPM calculations is designated as R-XSDRNPM.

In most cases the k_∞'s of the submitted reaction rates did not match exactly the results from June 1988. Therefore Table 3 summarizes and compares the k_∞'s and the reactivity losses from zero dissolution to 50 % dissolution for the June 1988 and June 1989 data. It can be seen that there are no substantial differences. Thus the data submitted for this analysis reflects the problems perceived in the original benchmark exercise.

3 - K SYNTHESIS TECHNIQUES AND THE ANALYSIS OF DEVIATIONS FROM THE REFERENCE CASE

A computer program was written to synthesize k_∞ from the participants reaction rates by three methods to provide insight into the nature and origin of the discrepancies. These methods are described below with the derivations and definitions of the various quantities used.

The authors felt that the root of the problem lay in the calculation of k_∞ since k_{eff} is basically achieved as a result of a multiplicative leakage correction to k_∞, which should, in general, be well treated by all codes. The validity of this assumption was demonstrated in the first part of this report.

3.1 - Phenomenological Model

The phenomenological method synthesizes the value of k_∞ from the types of parameters used in the four-factor formula. In this manner one can search for systematic discrepancies in calculation of physical processes. k_∞ is defined as :

$$k_\infty = \epsilon_8 \cdot \epsilon_5 \cdot p \cdot f \cdot \eta$$

where the various factors are defined in terms of the reaction rates as follows :

$\epsilon_8 = (P_8^1 + P_5^{tot})/P_5^{tot}$	^{238}U Fast Fission Factor
$\epsilon_5 = P_5^{tot}/P_5^2$	^{235}U Fast Fission Factor
$p = A_{tot}^2/A_{tot}^{tot}$	Resonance Escape Probability
$f = A_{fuel}^2/A_{tot}^2$	Thermal Utilization Factor
$\eta = P_5^2/A_{fuel}^2$	Eta-factor (thermal neutrons per thermal absorption in the fuel)

and the reaction rate symbols follow the conventions :

P = productions
A = absorptions and
P_i^j = productions for isotope i in group j etc...

The deviations from the values of the reference case, of each factor, for the results of each participant, were calculated in pcm, using the following formula :

$$\frac{\Delta k_\infty}{k} = \frac{\Delta \epsilon_8}{\epsilon_8} + \frac{\Delta \epsilon_5}{\epsilon_5} + \frac{\Delta p}{p} + \frac{\Delta f}{f} + \frac{\Delta \eta}{\eta}$$

where the quantities $\frac{\Delta x}{x}$ were calculated as $\ln(x/x_{ref})$

3.2 - Historical Model

The historical model synthesizes k_∞ as the sum of contributions from each energy group with appropriate weighting factors. The objective of the derivation was to achieve a separation into factors that could be classified cleanly as dependent or not-dependent on a single energy group. It can be shown that k_∞ can be expressed as a summation of contributions from each energy group weighted by two factors which describe the probability of arrival in each group and the probability of absorption in each group. Clearly the probability of arrival in group i is independent of group i events whereas the probability of absorption in group i is a function of the group i properties. In this formulation k_∞ can be expressed as follows :

$$k_\infty = k1.(1-p1) + p1.k2.(1-p2) + p1.p2.k3\ (1-p3) + \ldots$$

where, for example, in the third term, p1.p2, (the probability of escaping both groups 1 and 2 without absorption) represents the probability of arrival in group 3, (1-p3) represents the probability of absorption in group 3 and k3 represents the group 3 contribution to the neutron multiplication factor (productions/absorptions).

The deviations from the values of the reference case, of each factor, for the results of each participant were calculated, in pcm, using the following formula :

$$\frac{\Delta k_\infty}{k_\infty} = \sum_{g=1}^{ngp} \left(\frac{\Delta k_g}{k_g} + \frac{\Delta (1-p_g)}{(1-p_g)} + \frac{\Delta \prod_{m=1}^{g-1} p_m}{\prod_{m=1}^{g-1} p_m} \right) \cdot W_g$$

where the quantities $\frac{\Delta x}{x}$ were calculated as $\ln(x/x_{ref})$ and the W_g were calculated as :

$$W_g = (w_{gref} + w_{gi})/2 \qquad \begin{array}{l}(\text{ref = reference value,} \\ \quad i \quad = \text{participant's value})\end{array}$$

and

$$w_{gi} = \frac{k_g \cdot (1 - p_g) \cdot \prod_{m=1}^{g-1} p_m}{\sum_{g=1}^{ngp} k_g \cdot (1 - p_g) \cdot \prod_{m=1}^{g-1} p_m}$$

Deviations are tabulated as $W_g \cdot \ln (x/x_{ref})$ to preserve the pcm totals. The W_g are essentially constant with variation less than 2 %.

3.3 - Spatial Model

The spatial model synthesizes k_∞ as the sum of contributions from each spatial region in the cell with appropriate weighting factors. It can be shown that k_∞ can be expressed as :

$$k_\infty = k1 \,.\, W1 + k2 \,.\, W2$$

where k1 and k2 are the contributions to the neutron multiplication factor from the pellet and the solution regions respectively and W1 and W2 are weighting factors defined below :

$$W1 = \frac{A1}{A1 + A2} \qquad W2 = \frac{A2}{A1 + A2}$$

The deviations from the values of the reference case, of each factor, for the results or each participant were calculated, in pcm, using the following formula :

$$\frac{\Delta k_\infty}{k_\infty} = \frac{W1.k1}{W1.k1 + W2.k2} \cdot \left[\frac{\Delta W1}{W1} + \frac{\Delta k1}{k1}\right] + \frac{W2.k2}{W1.k1 + W2.k2} \cdot \left[\frac{\Delta W2}{W2} + \frac{\Delta k2}{k2}\right]$$

where the quantities $\frac{\Delta x}{x}$ were calculated as $\ln(x/x_{ref})$.

Deviations are tabulated as the product of the weighting function and $\ln(x/x_{ref})$.

4 - RESULTS OF THE SYNTHESIS CALCULATIONS

The results of the computer synthesis program are summarized in a series of tables and graphs. Tables 4 to 7 present the calculated values of the parameters described in section 3 for each of the three syntheses for cases 3B, 3F, 1B and 1F respectively. While three-group data were submitted a two-group analysis is presented here. Tables 4.1 to 7.1 present the deviations, in pcm, from the reference values, of the calculated values of the parameters described in section 3 for each of the three syntheses for cases 3B, 3F, 1B and 1F respectively. All input reaction rates were normalized to one absorption in the cell and expressed as a percent of that one absorption. The results are presented in Appendix I where sections I .1 to I .4 refer to cases 1B, 3B, 1F and 3F respectively.

The variation of each parameter in the syntheses was plotted in a series of graphs.

Figures 5 to 9 present the variation with dissolution of the five phenomenological factors ϵ_8, ϵ_5, p, f and η respectively, of all participants. Each figure contains the results for pf = 0.4 and pf = 0.6.

Figures 10 to 13 present the variation with dissolution of the k1, PAB(1), k2 and PAR(2) factors of the Historical Model. Each figure contains the results for pf = 0.4 and pf = 0.6.

Figures 14 to 19 present the variation with dissolution of the k1, W(1), k2 and W(2) factors of the Spatial Model. The k_∞ figures contain the results for pf = 0.4 and pf = 0.6. The scale differences for the W factors at zero dissolution and 50 % dissolution required that the data for pf = 0.4 and pf = 0.6 appear on separate pages. For k2, in this model only, a series of points are presented at 50 % dissolution since k2 at zero dissolution is zero. The data points for ANISN are so far off the graphs that the data point is not located according to the scale.

5 - OBSERVATIONS

In discussing the results of the synthesis calculations it is useful to talk about the magnitude of various parameters at zero dissolution wherein 100 % of the fuel remains in the pellet, and the rate of change of the parameters leading to the values when the pellets are 50 % dissolved. The discussion is also separated according to the packing fraction of the pellets.

5.1 - General observations

The 3B and 3F cases, based on a packing fraction of 0.4, represent a level of moderation that is similar to that found in pressurized light water reactors (PWR). As such, it is expected that all the codes used in the benchmark study are capable of achieving a reasonable level of agreement for these cases, where differences in the calculated k_∞ values are due largely to differences in the libraries of nuclear data. An evaluation of the spread in results from problems 1 to 18 [3] which do not involve a double-heterogeneity shows that differences in calculated neutron multiplication factors are in the range of 3000 to 4000 pcm. From the data presented in Table 4.1 one can see that this is also the situation for case 3B (spread 4364 pcm) which is similar in nature. The case 3F is based on the same packing fraction as case 3B but the pellets are 50 % dissolved with the other 50 % of the fuel dispersed uniformly throughout the solution i.e. case 3F introduces the double-heterogeneity problem. In case 3F the calculated k_∞ values exhibit a spread of 18225 pcm.

Case 1B is similar to case 3B in that 100 % of the fuel is in the pellets, but the pellets are much more densely packed creating an undermoderated assembly. In case 1B the calculated k_∞ values exhibit a spread of 7141 pcm where approximately 3000 pcm (after removal of the potential spread due to library differences) are due to differences in the ways in which the codes calculate undermoderated assemblies. Case 1F adds the complication of the dissolved fuel in the moderator and the calculated k_∞ values exhibit a spread of 26677 pcm or 22313 pcm when the potential spread due to library differences is removed.

Clearly the agreement between the various codes is slightly worse when calculating an undermoderated assembly without the double-heterogeneity and much worse when there is a double-heterogeneity present. Furthermore the spread in results due to the double-heterogeneity is increased as the level of moderation is reduced.

When the results of June 1988 are plotted as normalized deviations from the reference APOLLO calculations (figures 3 and 4), the general observations described above are easily discerned. However, one also sees that the deviations fall into three distinct groups :

- those that are in reasonable agreement with the reference calculation regarding reactivity loss (MONK 6.3, WIMSE and R-XSDRNPM/ORNL),

- those that overestimate the reactivity loss with dissolution of the pellet by approximately 3000 pcm at pf = 0.4 and by 6500 pcm at pf = 0.6 (KENO-IV, XSDRNPM/ENEA, APOLLO-ND , XSDRNPM/GARC.),

- those that overestimate the reactivity loss with dissolution of the pellet by approximately 13000 pcm at pf = 0.4 and by 20000 pcm at pf = 0.6 (XSDRNPM in automated SCALE calculations).

It has been shown in the companion paper A that the differences in the rate of reactivity loss for the second group can be explained on the basis of inappropriate modelling of the effective cross-sections wherein the calculations have not taken into account that different equivalent cross-sections must be calculated for each resonance absorber in the fuel pellet and in the solution and that one must also account for a "DANCOFF-like" effect between the pellets and the solution. Chapter A also shows that the codes in group 3 have additional problems to suffer such large reactivity losses but that the origin may still rest with the calculation of the self-shielding effect. It remains to be shown that this explanation has merit in the individual cases of the benchmark study.

6 - DISCUSSION

Using the reaction rate tables submitted by the participants and the k_∞ synthesis program, the various factors which contribute to k_∞ were evaluated and compared. It should be noted that : one should expect results from MONK 6.3 which may exhibit apparently erratic behaviour due to the statistical variation that is inherent in Monte Carlo calculations, that data were not available to reproduce all calculations from the June 1988 exercise and that the MCNP results submitted by ENEA/Trisaia [4] and ENEA/Casaccia [5] are not discussed at this time.

The various factors are discussed below in the order of occurrence in Tables 4 to 7.

6.1 - Phenomenological Model

6.1.1 - ^{238}U Fast Fission Factor

Figure 5 shows that there is generally good agreement on the magnitude of the ^{238}U Fast Fission Factor. The largest deviations from the reference values are + 644 pcm for ANISN and + 516 pcm for WIMSE at pf = 0.4 (zero dissolution) and + 701 pcm for ANISN and + 1076 pcm for WIMSE at pf = 0.6 (zero dissolution).

For pf = 0.4 and pf = 0.6 all codes except XSDRNPM/PNC exhibit only slight differences in the rate of change with dissolution. The maximum spreads for the ^{238}U fission factor calculated by these codes thus remain in the narrow bands discerned at zero dissolution. Automated SCALE calc. shows a much stronger rate of increase in value with dissolution and differs from the reference value by 951 pcm (pf = 0.4) and 4208 pcm (pf = 0.6) at 50 % dissolution. A review of the normalized reaction rates in Appendix I shows that the total ^{238}U fast production rates in both the solution and pellet are correct ; ε^{238} is biased by the bad slowing-down density calculation.

6.1.2 - ^{235}U Fast Fission Factor

Figure 6 shows that there is generally good agreement on the magnitude of the ^{235}U Fast Fission Factor except in the cases of R-XSDRNPM and XSDRNPM/PNC. The deviations from the reference values for these codes are + 2700 pcm for R-XSDRNPM and + 2549 pcm for XSDRNPM/PNC at pf = 0.4 (zero dissolution) and + 5333 pcm for R-XSDRNPM and + 4818 pcm for XSDRNPM/PNC at pf = 0.6 (zero dissolution). A review of the normalized reaction rates in Appendix I shows that the ratio of ^{235}U epi-thermal and thermal fission rates and thus the ratio of epi-thermal and thermal production rates is the major contributor to the deviation. The difference is unacceptable at zero dissolution.

For pf = 0.4 and pf = 0.6 all codes except XSDRNPM/PNC exhibit only slight differences in the rate of change with dissolution including R-XSDRNPM. The maximum spreads for the ^{235}U fission factor calculated by all codes except the automated SCALE calculation thus remain in the narrow bands discerned at zero. One more time, the poor result of automatic SCALE sequence on this ε factor is the consequence of the low thermal reaction rates due to inaccurate ^{238}U resonant capture calculation.

6.1.3 - Resonance Escape Probability

From Figure 7, where the resonance escape probabilities are presented, it is apparent that the values behave in the same general manner as k_∞ as discussed above. However, the scale is quite insensitive and to enhance the separation the data were replotted in figure 20 as the relative contribution of the resonance escape probability to the reactivity loss. The ordinate on the graph is defined as :

$$y = (p(50\ \%) - p(100\ \%)) * 100 / p(100\ \%)\ \text{pcm}$$

The clustering of results for the relative contributions to reactivity loss is now seen to clearly follow the pattern established in the k_∞ data. The codes APOLLO/CEAREF, MONK 6.3, WIMSE and R-XSDRNPM exhibit almost identical reactivity losses with dissolution of the pellets. Figure 20 shows that they also have essentially identical relative resonance escape contributions (5.2 % to 5.7 % at pf = 0.4 and 4.1 % to 4.7 % at pf = 0.6). That is not to say, however, that they calculate identical values of the resonance escape probability. The p-factors calculated by MONK 6.3 are very similar to the reference values, differing in a range of - 354 pcm to + 708 pcm. The p-factors calculated by WIMSE show somewhat larger though still acceptable deviations with differences in a range of - 854 pcm to - 1893 pcm. On the other hand the p-factors calculated by R-XSDRNPM show deviations from the reference cases that range from - 4586 pcm to-8894 pcm. The deviations are lowest for the case of zero dissolution and a moderation level appropriate to a PWR (3B) becoming worse both with the lower level of moderation (1B) and with the double-heterogeneity (1F) and taking their maximum values in the case of both undermoderation and double-heterogeneity (1F).

The codes APOLLO-"ND", XSDRNPM/ENEA-C and ANISN form a second group wherein the calculated relative contributions of the p-factors are similar (- 8.7 % to - 9.3 %, at pf = 0.4 and - 9.6 % to - 12.6 % at pf = 0.6). Both APOLLO/CEA and XSDRNPM/ENEA-C k_∞ values from the June 1988 exercise (ANISN results were not reported) are in the corresponding group (Figure 20) as are XSDRNPM/GAR and KENO/ENEA (reaction rates not available for this study).

The automated SCALE forms a third "group" wherein the relative contribution to reactivity loss is - 18.6 % at pf = 0.4 and - 29.6 % at pf = 0.6. Deviations from the reference values are - 4363 pcm to - 19647 pcm for pf = 0.4 and - 7872 pcm to - 38755 pcm for pf = 0.6. In the June 1988 exercise XSDRNPM/PNC was joined in this group by XSDRNPM/ORNL (reaction rates not available for this study).

6.1.4 - Thermal Utilization Factor

Figure 8 shows that there is generally excellent agreement on the magnitude of the Thermal Utilization Factor. The largest deviations from the reference values are + 309 pcm and + 316 pcm for XSDRNPM and R-XSDRNPM respectively and - 701 pcm for MONK 6.3 at pf = 0.4 (zero dissolution) and + 293 pcm and + 295 pcm for XSDRNPM and R-XSDRNPM respectively and - 360 pcm for MONK 6.3 at pf = 0.6 (zero dissolution).

For pf = 0.4 and pf = 0.6 all codes except MONK 6.3 exhibit only slight differences in the rate of change with dissolution. The maximum spreads for the Thermal Utilization Factor calculated by these codes thus remain in the narrow bands discerned at zero dissolution. MONK 6.3, however, shows a stronger rate of increase in value with dissolution but started at a lower value at zero dissolution and thus has a value at 50 % dissolution that is very close to the values calculated by the other codes. Some of the deviation may be due to statistical variation.

6.1.5 - Eta - Thermal Neutrons Produced per Thermal Absorption in the Fuel

Figure 9 shows that there is generally good agreement on the magnitude of the Eta-factor. The largest deviations from the reference values are + 1210 pcm and + 864 pcm for MONK 6.3 and WIMSE respectively at pf = 0.4 (zero dissolution) and + 1102 pcm and + 772 pcm for MONK 6.3 and WIMSE respectively at pf = 0.6 (zero dissolution).

For pf = 0.4 and pf = 0.6 all codes except MONK 6.3 exhibit only slight differences in the rate of change with dissolution. The maximum spreads for the Eta-factor calculated by these codes thus remain in the narrow bands discerned at zero dissolution. MONK 6.3, however, shows a strong rate of decrease in value with dissolution but started at a higher value at zero dissolution and thus has a value at 50 % dissolution that is very close to the values calculated by the other codes. Some of the deviation may be due to statistical variation.

6.2 - Historical Model

6.2.1 - KINF(1) and PAB(1)

Figure 10 shows that there is generally good agreement on the magnitude of KINF(1) (group 1 productions/group 1 absorptions) at zero dissolution for both pf = 0.4 and 0.6 except for ANISN where deviations from the reference cases of 2463 pcm and 2622 pcm respectively are recorded. The difference is more than 250 % greater than the next worst case at zero dissolution and pf = 0.4. In general the level of agreement deteriorates with the dissolution of the pellets. At 50 % dissolution the values of KINF(1) as calculated by MONK 6.3, WIMSE, R-XSDRNPM and ANISN are in good agreement with the reference calculation (deviations of about or less than 1000 pcm). ANISN has achieved this agreement by means of a very much larger rate of change with dissolution than all other contributors to compensate for the very much larger initial value. The APOLLO and XSDRNPM/ENEA-C KINF(1) values change at a somewhat higher rate than the reference case leading to deviations at 50 % dissolution and pf = 0.4 of 1710 pcm and 2988 pcm respectively, while the XSDRNPM/PNC value changes more rapidly to give a deviation of 5640 pcm at 50 % dissolution. The pattern is repeated for pf = 0.6 with the deviations being correspondingly larger in the undermoderated case.

Figure 11 shows that at zero dissolution, for both pf = 0.4 and 0.6, there is quite good agreement for PAB(1) among all the contributors except R-XSDRNPM and XSDRNPM/PNC. Both codes show much stronger initial group 1 absorptions than all other contributors. Differences in the rate of change of PAB(1) again cause a clustering of values that mirrors the behaviour observed in figures 3 and 4. The slopes for the reference, MONK 6.3, WIMSE and R-XSDRNPM curves are essentially identical. However due to the much higher initial absorption rate, PAB(1) for R-XSDRNPM remains high. The curves for APOLLO, ANISN and XSDRNPM/ENEA-C form a second group with almost identical rates of change. SCALE-Auto is in a class by itself. It not only starts with a high value of PAB(1) it has a rate of change which is very much larger than all other contributors leading to values of PAB(1) that deviate from the reference values by 5940 pcm and 8973 pcm at pf = 0.4 and 0.6 respectively. This level of deviation is 300 % to 400 % higher than the deviations of the intermediate group of codes.

6.2.2 - KINF(2) and PAR(2)

Figure 12 shows that there is generally excellent agreement on the magnitude of KINF(2) (group 2 productions/group 2 absorptions) at zero dissolution for both pf = 0.4 and 0.6 including ANISN. The highest deviations come from MONK 6.3 and WIMSE. Only MONK 6.3 shows a significant difference in the slope of the curve. This result may again be caused by statistical scatter since the deviations are small in any case. Thus the codes all agree on the behaviour of KINF(2).

Figure 13 shows that PAR(2) has the same clustering characteristics as PAB(1) only the deviations are larger. This is to be expected since the probability of arriving in group 2 is proportional to the probability of being absorbed in group 1. Note that deviations in PAR(2) are in the opposite sense of deviations in PAB(1).

6.3 - Spatial Model

6.3.1 - KINF(1) and W(1)

Figure 14 shows that the magnitudes of KINF(1) (pellet productions/pellet absorptions) values at zero dissolution for both pf = 0.4 and 0.6 reflect the major portion of the discrepancies in k_∞. Figure 14 shows that as dissolution proceeds the reference, MONK 6.3, WIMSE and R-XSDRNPM calculations exhibit an increase in KINF(1) with almost identical slopes, while ANISN, XSDRNPM/ENEA-C, XSDRNPM/PNC and APOLLO exhibit a decrease in KINF(1) with almost identical slopes. This leads to spreads in KINF (1) of 5710 pcm and 8283 pcm for pf = 0.4 and 0.6 respectively at 50 % dissolution. The very high KINF(1) value of ANISN at zero dissolution is compensated in each case by the negative rate of change with dissolution to the point where at 50 % dissolution it agrees very well with the reference calculation.

Figures 15 and 16 also show that at zero dissolution there is little disagreement arising from the weighting factor W(1) except for ANISN at pf = 0.6. The reference calculation, MONK 6.3, XSDRNPM/ENEA-C, ANISN and APOLLO all calculate a similar rate of change for W(1). R-XSDRNPM and WIMSE calculate a similar rate of change which is greater than the reference calculation and XSDRNPM/PNC calculates a very much greater rate of change than all other codes. XSDSRNPM/PNC shows the largest deviation from the reference values at 50 % dissolution, - 2133 pcm at pf = 0.4 and - 4271 pcm at pf = 0.6.

6.3.2 - KINF(2) and W(2)

Figure 17 shows only the KINF(2) (solution productions/ solution absorptions) at 50 % dissolution for pf = 0.4 and 0.6 since the value is 0. at zero dissolution. MONK 6.3, WIMSE, APOLLO and ANISN agree very closely with the reference calculation on the value of KINF(2). R-XSDRNPM and XSDRNPM/ENEA-C show deviations of - 1375 pcm and - 1809 pcm respectively at pf = 0.4 and XSDRNPM/PNC has a deviation of - 9120 pcm at pf = 0.4. At pf = 0.6, MONK 6.3,

WIMSE and ANISN still agree well with the reference calculation of KINF(2) while APOLLO, R-XSDRNPM and XSDRNPM/ENEA-C have deviations of - 1449 pcm, - 1565 pcm and - 2565 pcm respectively. XSDRNPM/PNC has a deviation of - 15910 pcm on the value of KINF(2).

Figures 18 and 19 show that there is excellent agreement on the value of W(2) for all codes except XSDRNPM/PNC and XSDRNPM/ENEA-C. It is also interesting to note that the deviations of XSDRNPM/PNC and XSDRNPM/ENEA-C have opposite senses. W(2) has a zero value due to the zero value of the weighting function.

6.4 - SUMMARY

6.4.1 - Phenomenological Model

The ^{235}U Fast Fission Factor points to problems with the calculated values of ^{235}U fissions and productions for R-XSDRNPM and XSDRNPM/PNC at zero dissolution. Appendix I shows that epithermal fissions and productions are higher than the reference case and almost all the other codes by 12% while the thermal fissions and productions are low by an amount that makes total fissions and productions equal to all the other codes. This may be an indication of differences in nuclear data since we do not feel that the small difference in the thermal energy boundary quoted for R-XSDRNPM could have this large an effect. Since XSDRNPM/PNC did not indicate a different thermal boundary from that requested (0.0625 eV) and shows a 10% difference on epithermal fission rates the shift in thermal boundary may cause an effect of the order of 2%.

The greatly different rate of change with dissolution of ε^8, fast fission factor and ε^5, epithermal fission factor, in the automated SCALE calculation is only the consequence of a poor slowing-down density at thermal cut-off (strong overestimation of the ^{238}U resonant capture).

The clustering of the calculated p-factors in a manner which imitates the clustering of calculated values in figure 20 as well as the deviation values recorded in tables 4.1 to 7.1 show that this is the major factor in the $k\infty$ discrepancies (the dominant factor is seen to be the ^{238}U capture rate). Reference self-shielding methods used in APOLLO-PIC, WIMSE, ROLAIDS and continuous-energy MC code MONK6, lead to consistent p variations with pellet dissolution. The standard ND model used in design calculations induces a bias amounting to -4000 pcm (standard APOLLO, XSDRNPM-ENEA, ANISN). The NITAWL module in SCALE calculations introduces an overestimation of the reactivity loss which amounts to -13000 pcm (pf =0.4; 50% UO_2 in pellet - 50% UO_2 in solution).

There is no significant disagreement in the calculation of the thermal utilization. The identical values calculated, at zero dissolution, for both pf = 0.4 and pf = 0.6 by XSDRNPM/PNC and R-XSDRNPM indicate that the library data are identical and cause a slightly higher f-factor than the other codes.

There is no significant disagreement in the calculation of the eta-factor. The consistently high values, at zero dissolution, for MONK 6.3 and to a lesser degree WIMSE indicate the possibility of library data that results in a higher than normal thermal neutron production rate.

6.4.2 - Historical Model

Since the cases at zero dissolution represent, for the most part, differences in nuclear data, the highly discrepant KINF(1) value from ANISN shows that there is clearly a problem in the ratio of group 1 productions to group 1 absorptions. On the other hand the rate of change of KINF(1) with dissolution is solely a function of the rate of change effective ^{235}U and ^{238}U cross-sections since the group 1 flux plays no part in the value of KINF(1).

Owing to the same physical effect, i.e. the underestimation of the resonant reaction rates, the discrepancies on the variations of KINF(1) and absorption probability W(1) as a function of pellet dissolution are of opposite sense, leading consequently to a high level of cancellation.

KINF(2) depends only on thermal properties. It is clear that quantities that depend solely on group 2 or thermal cross-sections exhibit a high degree of agreement both in magnitude and rate of change with dissolution. KINF(2) therefore contributes very little to observed k_∞ discrepancies.

The slowing-down density at thermal cut-off, PAR(2), appears as the main contribution to the disagreement in the rate of the reactivity loss : the bias corresponding to this parameter amounts to -15140 pcm nd -23500 pcm (respectively for pf = 0.4 and pf = 0.6) in the automated SCALE calculation using the NITAWL Nordheim Integral self-shielding method.

6.4.3 - Spatial Model

The rate of change of KINF(1), the ratio of pellet productions to pellet absorptions, is clearly handled in different ways by the different codes. APOLLO-PIC, MONK 6.3, WIMSE and ROLAIDS calculate an increase with dissolution of the pellet while SCALE, ANISN and APOLLO-ND calculate a decrease. The dominant factor is once again the ^{238}U epithermal absorptions, which is only correctly accounted for by the reference self-shielding formalisms.

The main interest of this kind of neutron balance breakdown was to point out that the automatic sequence in SCALE introduces an additional bias due to the reactivity of the fissile liquor, -9120 pcm to -16000 pcm for packing fractions pf = 0.4 to 0.6 (probably due to infinite dilution cross-sections being used in the liquor).

7 - MCNP "REFERENCE" CALCULATIONS

Two data sets were submitted by the ENEA laboratories at Casaccia and Trisaia as potential reference calculations. We will not discuss all parameters in detail although they were evaluated and included in the tables. The results of the calculations indicate that these calculations also experience problems in calculating the reactivity loss with fuel dissolution and that the major source of the discrepancies is the resonance escape probability.

8 - CONCLUSIONS

This study has shown that despite the reasonable agreement among the various codes when modelling cases that resemble pressurized light water reactor conditions, for which they were designed, there are significant differences in the physics of a fuel dissolver that were not forseen in the original formulation of methods viz. the double-heterogeneity. We believe that the APOLLO/PIC reference calculations represent a rigorous approach to the physics of the fuel dissolver and the CEA 86 data library has been extensively validated in the context of High Conversion Reactors. As such we feel that the results obtained by the reference calculation method are reliable. The detailed examination of each parameter in the various k_∞ syntheses indicates in the strongest manner that the source of the largest deviations from the reference calculations is the effective ^{238}U capture cross-sections. As was shown in the companion paper the origin of the problem seems to be the failure to calculate correctly effective ^{238}U capture cross-sections in both the pellet and the fuel bearing solution (which have widely different self shielding levels) and to provide an adequate representation of a "DANCOFF-like" effect between the pellet and solution because the standard DANCOFF formulation does not apply when there is fuel in the moderator.

The codes MONK 6.3, WIMSE and R-XSDRNPM all calculate reactivity losses with fuel dissolution that agree well with the reference calculation. Of these, only MONK 6.3 shows consistently good agreement in almost all factors with the largest disagreement reflecting a difference in the ^{235}U production cross-sections. While WIMSE shows consistently good agreement with the reference values of k_∞ this is a result of compensation of deviations in several factors. For example in case 1f, WIMSE has a deviation of - 1893 pcm on the resonance escape probability which is compensated by deviations of + 1082 pcm and + 800 pcm on the ^{238}U Fast Fission Factor and the eta-factor respectively. The differences on ^{235}U production rates generate higher absolute k_∞ values than the reference calculation for both MONK 6.3 and WIMSE. R-XSDRNPM is a

hybrid code. The absolute reactivity levels are determined by XSDRNPM and its library, used also by PNC. The application of the ROLAIDS treatment corrects the variation of the effective cross-sections with dissolution but perturbs other parameters as discussed in A. Without the ROLAIDS treatment XSDRNPM does an extremely poor job of calculating self-shielding effects under dissolution. We demonstrated in part A with calculations that included no self-shielding that reactivity losses with dissolution as high as 60000 pcm are possible. The companion paper A shows that the ORNL and PNC calculations probably used infinite dilution cross-sections accounting for the excessive absorption rate in ^{238}U.

On the other hand the codes APOLLO, ANISN and XSDRNPM/ENEA-C calculate reactivity losses with dissolution that can be explained, for the most part, on the basis of faulty effective capture ^{238}U cross-sections due to an inappropriate DANCOFF correction.

The authors feel that differences in the SCALE0 and SCALE2 packages create the observed differences in XSDRNPM results between ORNL/PNC and ENEA-C. The former apparently uses infinite dilution cross-sections for the solution while the latter imposes a DANCOFF factor of 0 for the solution.

REFERENCES

[1] OECD/NEA - Criticality Calculations Working Group Meeting.
PARIS - June 27-30, 1988.

[2] H.J. SMITH - A. SANTAMARINA
"An analysis of the results of an international OECD/NEA criticality benchmark calculation on fuel dissolvers".
OECD Criticality Meeting - PARIS - June 27-29 1989.

[3] G.E. WHITESIDES
Report of the OECD - Criticality Calculations Working Group.
NEACRP - L - 306 - April 1990.

[4] P. LANDEYRO.
Personal communication.

[5] F. SICILIANO.
Personal communication.

TABLE 1

A SUMMARY OF K-INFINITY AND DELTA RHO VALUES
FOR BENCHMARK EXERCISE 20 CALCULATIONS (JUNE 1988)
AND REFERENCE VALUES (JUNE 1989)

		K-INFINITY		DELTA RHO	
		PF=0.4	PF=0.6	PF=0.4	PF=0.6
FRANCE/CEAREF					
APOLLOREF	100	1.12101	1.10081	0	0
	75	1.08936	1.07732	- 2864	- 2157
	50	1.08393	1.07042	- 3364	- 2800
	25	1.08042	1.06670	- 3688	- 3148
	0	1.07811	1.06512	- 3902	- 3296
USA/ORNL					
R-XSDRNPM	100	1.10407	1.07135	0	0
	75	1.07054	1.04809	- 3083	- 2194
	50	1.06390	1.04143	- 3707	- 2832
USA/ORNL					
XSDRNPM	100	1.10727	1.07730	0	0
	75	0.96494	0.87158	-13758	-21191
	50	0.94147	0.83829	-16222	-25084
FRANCE/CEA					
APOLLO	100	1.12450	1.10340	0	0
	75	1.05680	1.01450	- 6210	- 8400
	50	1.05200	1.00870	- 6664	- 8973
UK/SRD					
MONK 6.3	100	1.14980	1.13620	0	0
	75	1.11200	1.11410	- 3343	- 1964
	50	1.11700	1.09260	- 2894	- 3912
UK/BNFL					
WIMSE	100	1.12950	1.11290	0	0
	75	1.09760	1.08990	- 2864	- 2088
	50	1.09150	1.08370	- 3422	- 2650
ITALY/ENEA-T					
XSDRNPM	100	1.10195	1.08300	0	0
	75	1.04010	1.01100	- 5777	- 7688
	50	1.02826	0.98380	- 6921	- 9430
ITALY/ENEA-C					
KENO-IV	100	1.10070	1.07842	0	0
	75	1.04552	0.99835	- 5143	- 7715
	50	1.02986	0.98412	- 6652	- 9126
JAPAN/PNC					
XSDRNPM	100	1.10568	1.07501	0	0
	75	0.96359	0.86987	-13753	-21175
	50	0.94020	0.83677	-16213	-25054
FRG/GARCHING					
XSDRNPM	100	1.13000	1.12000	0	0
	75	1.06174	1.02003	- 6231	- 8417
	50	1.04329	1.00110	- 7984	-10290

TABLE 2

IDENTIFICATION SYMBOLS FOR THE PARTICIPANTS

France,	Commissariat à l'Energie Atomique, Institut de Recherche et Développement Industriel - Reference Calculation	FRANCE/CEAREF
France,	Commissariat à l'Energie Atomique, Institut de Protection et Sécurité Nucléaire	FRANCE/CEA
USA,	Oak-Ridge National Laboratory	USA/ORNL
UK,	Safety and Reliability Directorate	UK/SRD
UK,	British Nuclear Fuels Limited	UK/BNFL
Italy,	Energia Nucleare e Energia Alternative, Trisaia	ENEA-T
Italy,	Energia Nucleare e Energia Alternative, Casaccia	ENEA-C
Japan,	Power Reactor and Nuclear Fuel Development Corporation	JAPAN/PNC
Japan,	Japan Atomic Energy Research Institute	JAPAN/JAERI
Germany,	Gesellschaft fur Reaktorsichereit Garching/Munchen	FRG/GARCHING

TABLE 3

A COMPARISON OF K-INFINITY AND DELTA RHO VALUES
FOR BENCHMARK EXERCISE 20 CALCULATIONS
(JUNE 1988/89)

		K-INFINITY		DELTA RHO	
		1988	1989	1988	1989
USA/ORNL					
R-XSDRNPM	1B	1.07135	1.07280	0	0
	3B	1.10407	1.10400	0	0
	1F	1.04143	1.04310	- 2832	- 2808
	3F	1.06390	1.06440	- 3706	- 3706
FRANCE/CEA					
APOLLO	1B	1.10340	1.10210	0	0
	3B	1.12450	1.12270	0	0
	1F	1.00870	1.02230	- 8973	- 7516
	3F	1.05200	1.05650	- 6665	- 6077
UK/SRD					
MONK 6.3	1B	1.13620	1.12340	0	0
	3B	1.14980	1.13440	0	0
	1F	1.09260	1.08530	- 3912	- 3450
	3F	1.11700	1.10200	- 2894	- 2898
UK/BNFL					
WIMSE	1B	1.11290	1.10320	0	0
	3B	1.12950	1.12690	0	0
	1F	1.08370	1.07270	- 2650	- 2804
	3F	1.09150	1.08640	- 3422	- 3660
ITALY/ENEA-C					
XSDRNPM	1B	1.07637	1.07420	0	0
	3B	1.10610	1.10600	0	0
	1F	0.98124	0.97829	- 9253	- 9353
	3F	1.03022	1.02790	- 7107	- 7323
JAPAN/PNC					
XSDRNPM	1B	1.07501	1.07410	0	0
	3B	1.10568	1.10460	0	0
	1F	0.83677	0.83605	-25054	-25055
	3F	0.94020	0.93934	-16212	-16206
JAPAN/JAERI					
ANISN	1B		1.12950		0
	3B		1.15470		0
	1F		1.06040		- 6313
	3F		1.07900		- 6781
ITALY/ENEA-T					
MCNP	1B		1.10310		0
	3B		1.12230		0
	1F		1.05290		- 4658
	3F		1.07320		- 4474
ITALY/ENEA-C					
MCNP	1B		1.07490		0
	3B		1.10280		0
	1F		1.03890		- 3407
	3F		1.05960		- 3996

TABLE 4

A SUMMARY OF THE KINFINITY SYNTHESIS FACTORS

CASE 3B (PF=0.4, 100% UO2 IN PELLET - 0% UO2 IN SOLUTION)

PHENOMENOLOGICAL MODEL (4 - FACTOR)

USER	KINF	FF8	FF5	PESC	F	ETA
FRANCE/CEAREF APOLLO	1.12100	1.08310	1.16180	0.65767	0.76339	1.77450
USA/ORNL R-XSDRNPM	1.10400	1.08410	1.19360	0.62819	0.76581	1.77330
FRANCE/CEA APOLLO	1.12270	1.08410	1.16130	0.65631	0.76278	1.78140
UK/SRD MONK 6.3	1.13440	1.08150	1.16320	0.66234	0.75806	1.79610
UK/BNFL WIMSE	1.12690	1.08870	1.16140	0.65208	0.76359	1.78990
ITALY/ENEA C XSDRNPM	1.10600	1.08280	1.15600	0.65345	0.76380	1.77040
JAPAN/PNC XSDRNPM	1.10460	1.08420	1.19180	0.62959	0.76575	1.77330
JAPAN/JAERI ANISN	1.15470	1.09010	1.17200	0.66791	0.76453	1.77000
ITALY/ENEA CB4 MCNP	1.10280	1.08640	1.16390	0.64450	0.76441	1.77020
ITALY/ENEA T MCNP	1.12230	1.08590	1.15810	0.65926	0.75941	1.78260

HISTORICAL MODEL

		BY GROUP					
USER	KINF	KINF(1)	PAR(1)	PAB(1)	KINF(2)	PAR(2)	PAB(2)
FRANCE/CEAREF APOLLO	1.12100	0.67224	1.00000	0.34233	1.35460	0.65767	1.00000
USA/ORNL R-XSDRNPM	1.10400	0.67472	1.00000	0.37181	1.35800	0.62819	1.00000
FRANCE/CEA APOLLO	1.12270	0.67190	1.00000	0.34369	1.35880	0.65631	1.00000
UK/SRD MONK 6.3	1.13440	0.68897	1.00000	0.33766	1.36150	0.66234	1.00000
UK/BNFL WIMSE	1.12690	0.67749	1.00000	0.34792	1.36670	0.65208	1.00000
ITALY/ENEA C XSDRNPM	1.10600	0.64183	1.00000	0.34655	1.35220	0.65345	1.00000
JAPAN/PNC XSDRNPM	1.10460	0.67416	1.00000	0.37041	1.35790	0.62959	1.00000
JAPAN/JAERI ANISN	1.15470	0.75535	1.00000	0.33209	1.35320	0.66791	1.00000
ITALY/ENEA CB4 MCNP	1.10280	0.64903	1.00000	0.35550	1.35310	0.64450	1.00000
ITALY/ENEA T MCNP	1.12230	0.67454	1.00000	0.34074	1.35370	0.65926	1.00000

SPATIAL MODEL

		BY REGION			
USER	KINF	KINF(1)	W(1)	KINF(2)	W(2)
FRANCE/CEAREF APOLLO	1.12100	1.35850	0.82517	0.00000	0.17483
USA/ORNL R-XSDRNPM	1.10400	1.33160	0.82905	0.00000	0.17095
FRANCE/CEA APOLLO	1.12270	1.36100	0.82495	0.00000	0.17505
UK/SRD MONK 6.3	1.13440	1.38330	0.82009	0.00000	0.17991
UK/BNFL WIMSE	1.12690	1.36100	0.82798	0.00000	0.17202
ITALY/ENEA C XSDRNPM	1.10600	1.33310	0.82964	0.00000	0.17036
JAPAN/PNC XSDRNPM	1.10460	1.33310	0.82865	0.00000	0.17135
JAPAN/JAERI ANISN	1.15470	1.40550	0.82151	0.00000	0.17850
ITALY/ENEA CB4 MCNP	1.10280	1.33120	0.82847	0.00000	0.17153
ITALY/ENEA T MCNP	1.12230	1.36230	0.82383	0.00000	0.17617

TABLE 4.1

A SUMMARY OF DEVIATIONS FROM THE REFERENCE MODEL IN PCM

CASE 3B (PF=0.4, 100% UO2 IN PELLET - 0% UO2 IN SOLUTION)

PHENOMENOLOGICAL MODEL (4 - FACTOR)

USER	KINF	FF8	FF5	PESC	F	ETA
USA/ORNL R-XSDRNPM	-1528.	92.	2700.	-4586.	316.	-68.
FRANCE/CEA APOLLO	151.	92.	-43.	-207.	-80.	388.
UK/SRD MONK 6.3	1188.	-148.	120.	708.	-701.	1210.
UK/BNFL WIMSE	525.	516.	-34.	-854.	26.	864.
ITALY/ENEA C XSDRNPM	-1347.	-28.	-500.	-644.	54.	-231.
JAPAN/PNC XSDRNPM	-1474.	101.	2549.	-4363.	309.	-68.
JAPAN/JAERI ANISN	2962.	644.	874.	-545.	149.	-254.
ITALY/ENEA CB4 MCNP	-1637.	304.	181.	-2023.	134.	-243.
ITALY/ENEA T MCNP	116.	258.	-319.	241.	-523.	455.

HISTORICAL MODEL

		BY GROUP					
USER	KINF	KINF(1)	PAR(1)	PAB(1)	KINF(2)	PAR(2)	PAB(2)
USA/ORNL R-XSDRNPM	-1528.	80.	0.	1786.	196.	-3594.	0.
FRANCE/CEA APOLLO	151.	-10.	0.	81.	246.	-164.	0.
UK/SRD MONK 6.3	1188.	504.	0.	-282.	404.	562.	0.
UK/BNFL WIMSE	525.	161.	0.	336.	705.	-677.	0.
ITALY/ENEA C XSDRNPM	-1347.	-941.	0.	249.	-141.	-513.	0.
JAPAN/PNC XSDRNPM	-1474.	61.	0.	1700.	191.	-3422.	0.
JAPAN/JAERI ANISN	2962.	2463.	0.	-642.	-82.	1219.	0.
ITALY/ENEA CB4 MCNP	-1637.	-728.	0.	782.	-88.	-1604.	0.
ITALY/ENEA T MCNP	116.	70.	0.	-95.	-53.	192.	0.

SPATIAL MODEL

		BY REGION			
USER	KINF	KINF(1)	W(1)	KINF(2)	W(2)
USA/ORNL R-XSDRNPM	-1528.	-2000.	469.	0.	0.
FRANCE/CEA APOLLO	151.	184.	-27.	0.	0.
UK/SRD MONK 6.3	1188.	1809.	-618.	0.	0.
UK/BNFL WIMSE	525.	184.	340.	0.	0.
ITALY/ENEA C XSDRNPM	-1347.	-1887.	540.	0.	0.
JAPAN/PNC XSDRNPM	-1474.	-1887.	421.	0.	0.
JAPAN/JAERI ANISN	2962.	3401.	-445.	0.	0.
ITALY/ENEA CB4 MCNP	-1637.	-2030.	399.	0.	0.
ITALY/ENEA T MCNP	116.	279.	-163.	0.	0.

TABLE 5

A SUMMARY OF THE KINFINITY SYNTHESIS FACTORS

CASE 3F (PF=0.4, 50% UO2 IN PELLET - 50% UO2 IN SOLUTION)

PHENOMENOLOGICAL MODEL (4 - FACTOR)

USER	KINF	FF8	FF5	PESC	F	ETA
FRANCE/CEAREF APOLLO	1.08750	1.08820	1.16490	0.62363	0.77555	1.77380
USA/ORNL R-XSDRNPM	1.06440	1.08600	1.19830	0.59284	0.77778	1.77380
FRANCE/CEA APOLLO	1.05650	1.08620	1.16720	0.60335	0.77521	1.78180
UK/SRD MONK 6.3	1.10200	1.08460	1.16870	0.62448	0.77670	1.79250
UK/BNFL WIMSE	1.08640	1.09040	1.16590	0.61541	0.77567	1.79020
ITALY/ENEA C XSDRNPM	1.02790	1.08670	1.16460	0.59248	0.77428	1.77040
JAPAN/PNC XSDRNPM	0.93934	1.09860	1.20990	0.51239	0.77692	1.77530
JAPAN/JAERI ANISN	1.07900	1.09490	1.18280	0.60627	0.77534	1.77260
ITALY/ENEA CB4 MCNP	1.05960	1.08900	1.16970	0.60538	0.77570	1.77150
ITALY/ENEA T MCNP	1.07320	1.09000	1.17010	0.60957	0.77559	1.77990

HISTORICAL MODEL

		BY GROUP					
USER	KINF	KINF(1)	PAR(1)	PAB(1)	KINF(2)	PAR(2)	PAB(2)
FRANCE/CEAREF APOLLO	1.08750	0.61005	1.00000	0.37637	1.37570	0.62363	1.00000
USA/ORNL R-XSDRNPM	1.06440	0.60530	1.00000	0.40716	1.37970	0.59284	1.00000
FRANCE/CEA APOLLO	1.05650	0.56261	1.00000	0.39665	1.38120	0.60335	1.00000
UK/SRD MONK 6.3	1.10200	0.61943	1.00000	0.37552	1.39220	0.62448	1.00000
UK/BNFL WIMSE	1.08640	0.60293	1.00000	0.38459	1.38860	0.61541	1.00000
ITALY/ENEA C XSDRNPM	1.02790	0.52933	1.00000	0.40752	1.37080	0.59248	1.00000
JAPAN/PNC XSDRNPM	0.93935	0.47707	1.00000	0.48761	1.37930	0.51239	1.00000
JAPAN/JAERI ANISN	1.07900	0.62427	1.00000	0.39373	1.37440	0.60627	1.00000
ITALY/ENEA CB4 MCNP	1.05960	0.57715	1.00000	0.39462	1.37410	0.60538	1.00000
ITALY/ENEA T MCNP	1.07320	0.59352	1.00000	0.39043	1.38050	0.60957	1.00000

SPATIAL MODEL

		BY REGION			
USER	KINF	KINF(1)	W(1)	KINF(2)	W(2)
FRANCE/CEAREF APOLLO	1.08750	1.38500	0.37578	0.90846	0.62422
USA/ORNL R-XSDRNPM	1.06440	1.36420	0.37460	0.88479	0.62540
FRANCE/CEA APOLLO	1.05650	1.32170	0.38293	0.89201	0.61707
UK/SRD MONK 6.3	1.10200	1.41310	0.37732	0.91348	0.62263
UK/BNFL WIMSE	1.08640	1.39600	0.37370	0.90170	0.62630
ITALY/ENEA C XSDRNPM	1.02790	1.26660	0.38629	0.87756	0.61371
JAPAN/PNC XSDRNPM	0.93935	1.25450	0.35942	0.76250	0.64058
JAPAN/JAERI ANISN	1.07900	1.36600	0.37890	0.90399	0.62111
ITALY/ENEA CB4 MCNP	1.05960	1.35750	0.37477	0.88109	0.62523
ITALY/ENEA T MCNP	1.07320	1.37390	0.37557	0.89237	0.62443

TABLE 5.1

A SUMMARY OF DEVIATIONS FROM THE REFERENCE MODEL IN PCM

CASE 3F (PF=0.4, 50% UO2 IN PELLET - 50% UO2 IN SOLUTION)

PHENOMENOLOGICAL MODEL (4 - FACTOR)

USER	KINF	FF8	FF5	PESC	F	ETA
USA/ORNL R-XSDRNPM	-2147.	-202.	2827.	-5063.	287.	0.
FRANCE/CEA APOLLO	-2892.	-184.	197.	-3306.	-44.	450.
UK/SRD MONK 6.3	1325.	-331.	326.	136.	148.	1049.
UK/BNFL WIMSE	-101.	202.	86.	-1327.	15.	920.
ITALY/ENEA C XSDRNPM	-5636.	-138.	-26.	-5124.	-164.	-192.
JAPAN/PNC XSDRNPM	-14646.	951.	3790.	-19647.	176.	84.
JAPAN/JAERI ANISN	-785.	614.	1525.	-2823.	-27.	-68.
ITALY/ENEA CB4 MCNP	-2599.	73.	411.	-2970.	19.	-130.
ITALY/ENEA T MCNP	-1324.	165.	445.	-2280.	5.	343.

HISTORICAL MODEL

		BY GROUP					
USER	KINF	KINF(1)	PAR(1)	PAB(1)	KINF(2)	PAR(2)	PAB(2)
USA/ORNL R-XSDRNPM	-2147.	-173.	0.	1740.	226.	-3943.	0.
FRANCE/CEA APOLLO	-2892.	-1710.	0.	1108.	315.	-2608.	0.
UK/SRD MONK 6.3	1325.	322.	0.	-48.	941.	107.	0.
UK/BNFL WIMSE	-101.	-249.	0.	459.	735.	-1045.	0.
ITALY/ENEA C XSDRNPM	-5636.	-2988.	0.	1674.	-282.	-4045.	0.
JAPAN/PNC XSDRNPM	-14645.	-5640.	0.	5940.	201.	-15141.	0.
JAPAN/JAERI ANISN	-785.	506.	0.	990.	-74.	-2204.	0.
ITALY/ENEA CB4 MCNP	-2599.	-1181.	0.	1009.	-92.	-2337.	0.
ITALY/ENEA T MCNP	-1324.	-587.	0.	783.	274.	-1794.	0.

SPATIAL MODEL

		BY REGION			
USER	KINF	KINF(1)	W(1)	KINF(2)	W(2)
USA/ORNL R-XSDRNPM	-2147.	-725.	-151.	-1375.	98.
FRANCE/CEA APOLLO	-2892.	-2240.	902.	-952.	-600.
UK/SRD MONK 6.3	1325.	967.	197.	286.	-128.
UK/BNFL WIMSE	-101.	379.	-266.	-389.	173.
ITALY/ENEA C XSDRNPM	-5636.	-4265.	1317.	-1809.	-888.
JAPAN/PNC XSDRNPM	-14645.	-4743.	-2133.	-9120.	1347.
JAPAN/JAERI ANISN	-785.	-662.	396.	-257.	-260.
ITALY/ENEA CB4 MCNP	-2599.	-961.	-129.	-1593.	84.
ITALY/ENEA T MCNP	-1324.	-386.	-27.	-930.	17.

TABLE 6

A SUMMARY OF THE KINFINITY SYNTHESIS FACTORS

CASE 1B (PI=0.6, 100% UO2 IN PELLET - 0% UO2 IN SOLUTION)

PHENOMENOLOGICAL MODEL (4 - FACTOR)

USER	KINF	FF8	FF5	PESC	F	ETA
FRANCE/CEAREF APOLLO	1.10080	1.13640	1.34530	0.46299	0.87938	1.76850
USA/ORNL R-XSDRNPM	1.07280	1.14210	1.41900	0.42520	0.88198	1.76520
FRANCE/CEA APOLLO	1.10210	1.13870	1.34540	0.46182	0.87944	1.77110
UK/SRD MONK 6.3	1.12340	1.14330	1.35150	0.46406	0.87622	1.78810
UK/BNFL WIMSE	1.10320	1.14870	1.34340	0.45594	0.87977	1.78220
ITALY/ENEA C XSDRNPM	1.07420	1.13550	1.33840	0.45635	0.87978	1.76030
JAPAN/PNC XSDRNPM	1.07410	1.14210	1.41170	0.42794	0.88196	1.76510
JAPAN/JAERI ANISN	1.12950	1.14440	1.36870	0.46515	0.88012	1.76130
ITALY/ENEA CB4 MCNP	1.07490	1.14140	1.35840	0.44757	0.88026	1.75970
ITALY/ENEA T MCNP	1.10310	1.14450	1.33590	0.46387	0.87656	1.77450

HISTORICAL MODEL

		BY GROUP					
USER	KINF	KINF(1)	PAR(1)	PAB(1)	KINF(2)	PAR(2)	PAB(2)
FRANCE/CEAREF APOLLO	1.10080	0.70905	1.00000	0.53701	1.55520	0.46299	1.00000
USA/ORNL R-XSDRNPM	1.07280	0.71475	1.00000	0.57480	1.55690	0.42520	1.00000
FRANCE/CEA APOLLO	1.10210	0.71120	1.00000	0.53818	1.55760	0.46182	1.00000
UK/SRD MONK 6.3	1.12340	0.73949	1.00000	0.53594	1.56680	0.46406	1.00000
UK/BNFL WIMSE	1.10320	0.71363	1.00000	0.54406	1.56800	0.45594	1.00000
ITALY/ENEA C XSDRNPM	1.07420	0.67581	1.00000	0.54366	1.54870	0.45634	1.00000
JAPAN/PNC XSDRNPM	1.07410	0.71307	1.00000	0.57206	1.55670	0.42794	1.00000
JAPAN/JAERI ANISN	1.12950	0.76360	1.00000	0.53485	1.55020	0.46515	1.00000
ITALY/ENEA CB4 MCNP	1.07490	0.69085	1.00000	0.55243	1.54900	0.44757	1.00000
ITALY/ENEA T MCNP	1.10310	0.71176	1.00000	0.53613	1.55540	0.46387	1.00000

SPATIAL MODEL

		BY REGION			
USER	KINF	KINF(1)	W(1)	KINF(2)	W(2)
FRANCE/CEAREF APOLLO	1.10080	1.18320	0.93034	0.00000	0.06966
USA/ORNL R-XSDRNPM	1.07280	1.14960	0.93324	0.00000	0.06676
FRANCE/CEA APOLLO	1.10210	1.18450	0.93041	0.00000	0.06959
UK/SRD MONK 6.3	1.12340	1.21160	0.92722	0.00000	0.07278
UK/BNFL WIMSE	1.10320	1.18320	0.93232	0.00000	0.06768
ITALY/ENEA C XSDRNPM	1.07420	1.15150	0.93287	0.00000	0.06713
JAPAN/PNC XSDRNPM	1.07410	1.15140	0.93286	0.00000	0.06714
JAPAN/JAERI ANISN	1.12950	1.23660	0.91336	0.00000	0.08665
ITALY/ENEA CB4 MCNP	1.07490	1.15280	0.93245	0.00000	0.06755
ITALY/ENEA T MCNP	1.10310	1.18600	0.93012	0.00000	0.06988

TABLE 6.1

A SUMMARY OF DEVIATIONS FROM THE REFERENCE MODEL IN PCM

CASE 1B (PF=0.6, 100% UO2 IN PELLET - 0% UO2 IN SOLUTION)

PHENOMENOLOGICAL MODEL (4 - FACTOR)

USER	KINF	FF8	FF5	PESC	F	ETA
USA/ORNL R-XSDRNPM	-2577.	500.	5333.	-8515.	295.	-187.
FRANCE/CEA APOLLO	118.	202.	7.	-253.	7.	147.
UK/SRD MONK 6.3	2032.	605.	460.	231.	-360.	1102.
UK/BNFL WIMSE	218.	1076.	-141.	-1534.	44.	772.
ITALY/ENEA C XSDRNPM	-2446.	-79.	-514.	-1445.	45.	-465.
JAPAN/PNC XSDRNPM	-2455.	500.	4818.	-7872.	293.	-192.
JAPAN/JAERI ANISN	2574.	701.	1724.	465.	84.	-408.
ITALY/ENEA CB4 MCNP	-2381.	439.	969.	-3387.	100.	-499.
ITALY/ENEA T MCNP	209.	710.	-701.	190.	-321.	339.

DEVIATIONS FROM THE REFERENCE MODEL IN PCM

HISTORICAL MODEL

		BY GROUP					
USER	KINF	KINF(1)	PAR(1)	PAB(1)	KINF(2)	PAR(2)	PAB(2)
USA/ORNL R-XSDRNPM	-2577.	292.	0.	2478.	69.	-5412.	0.
FRANCE/CEA APOLLO	118.	105.	0.	75.	101.	-165.	0.
UK/SRD MONK 6.3	2032.	1468.	0.	-70.	484.	150.	0.
UK/BNFL WIMSE	218.	225.	0.	455.	534.	-999.	0.
ITALY/ENEA C XSDRNPM	-2446.	-1652.	0.	423.	-275.	-949.	0.
JAPAN/PNC XSDRNPM	-2455.	205.	0.	2294.	61.	-5016.	0.
JAPAN/JAERI ANISN	2574.	2622.	0.	-143.	-208.	301.	0.
ITALY/ENEA CB4 MCNP	-2381.	-911.	0.	992.	-259.	-2200.	0.
ITALY/ENEA T MCNP	209.	132.	0.	-57.	8.	124.	0.

SPATIAL MODEL

	BY REGION				
USER	KINF	KINF(1)	W(1)	KINF(2)	W(2)
USA/ORNL R-XSDRNPM	-2577.	-2881.	311.	0.	0.
FRANCE/CEA APOLLO	118.	110.	7.	0.	0.
UK/SRD MONK 6.3	2032.	2372.	-336.	0.	0.
UK/BNFL WIMSE	218.	0.	213.	0.	0.
ITALY/ENEA C XSDRNPM	-2446.	-2716.	272.	0.	0.
JAPAN/PNC XSDRNPM	-2455.	-2724.	270.	0.	0.
JAPAN/JAERI ANISN	2574.	4414.	-1842.	0.	0.
ITALY/ENEA CB4 MCNP	-2381.	-2603.	227.	0.	0.
ITALY/ENEA T MCNP	209.	236.	-24.	0.	0.

TABLE 7

A SUMMARY OF THE KINFINITY SYNTHESIS FACTORS

CASE 1F (PF=0.6, 50% UO2 IN PELLET - 50% UO2 IN SOLUTION)

PHENOMENOLOGICAL MODEL (4 - FACTOR)

USER	KINF	FF8	FF5	PESC	F	ETA
FRANCE/CEAREF APOLLO	1.07040	1.14000	1.35170	0.44372	0.88544	1.76810
USA/ORNL R-XSDRNPM	1.04310	1.14580	1.43110	0.40596	0.88786	1.76500
FRANCE/CEA APOLLO	1.02230	1.14520	1.36410	0.41726	0.88552	1.77110
UK/SRD MONK 6.3	1.08530	1.14070	1.37290	0.44215	0.88533	1.77030
UK/BNFL WIMSE	1.07270	1.15240	1.35420	0.43540	0.88577	1.78230
ITALY/ENEA C XSDRNPM	0.97829	1.14590	1.37410	0.39864	0.88558	1.75980
JAPAN/PNC XSDRNPM	0.83605	1.18900	1.49000	0.30116	0.88629	1.76810
JAPAN/JAERI ANISN	1.06040	1.15370	1.40210	0.41978	0.88531	1.76390
ITALY/ENEA CB4 MCNP	1.03890	1.14600	1.37420	0.42323	0.88542	1.76040
ITALY/ENEA T MCNP	1.05290	1.15400	1.36210	0.42803	0.88315	1.77190

HISTORICAL MODEL

		BY GROUP					
USER	KINF	KINF(1)	PAR(1)	PAB(1)	KINF(2)	PAR(2)	PAB(2)
FRANCE/CEAREF APOLLO	1.07040	0.67549	1.00000	0.55628	1.56550	0.44372	1.00000
USA/ORNL R-XSDRNPM	1.04310	0.68507	1.00000	0.59404	1.56710	0.40596	1.00000
FRANCE/CEA APOLLO	1.02230	0.63137	1.00000	0.58274	1.56830	0.41726	1.00000
UK/SRD MONK 6.3	1.08530	0.70331	1.00000	0.55785	1.56730	0.44215	1.00000
UK/BNFL WIMSE	1.07270	0.68244	1.00000	0.56460	1.57870	0.43540	1.00000
ITALY/ENEA C XSDRNPM	0.97829	0.59371	1.00000	0.60136	1.55840	0.39864	1.00000
JAPAN/PNC XSDRNPM	0.83605	0.52102	1.00000	0.69884	1.56710	0.30116	1.00000
JAPAN/JAERI ANISN	1.06040	0.69775	1.00000	0.58023	1.56160	0.41977	1.00000
ITALY/ENEA CB4 MCNP	1.03890	0.65747	1.00000	0.57677	1.55870	0.42323	1.00000
ITALY/ENEA T MCNP	1.05290	0.66972	1.00000	0.57197	1.56480	0.42803	1.00000

SPATIAL MODEL

		BY REGION			
USER	KINF	KINF(1)	W(1)	KINF(2)	W(2)
FRANCE/CEAREF APOLLO	1.07040	1.20980	0.42999	0.96528	0.57001
USA/ORNL R-XSDRNPM	1.04310	1.18590	0.42794	0.93632	0.57206
FRANCE/CEA APOLLO	1.02230	1.12920	0.43978	0.93845	0.56022
UK/SRD MONK 6.3	1.08530	1.22460	0.43069	0.97995	0.56931
UK/BNFL WIMSE	1.07270	1.21920	0.42762	0.96319	0.57238
ITALY/ENEA C XSDRNPM	0.97829	1.05070	0.45335	0.91826	0.54665
JAPAN/PNC XSDRNPM	0.83605	1.03280	0.39383	0.70820	0.60617
JAPAN/JAERI ANISN	1.06040	1.18720	0.43410	0.96309	0.56590
ITALY/ENEA CB4 MCNP	1.03890	1.18280	0.42683	0.93169	0.57317
ITALY/ENEA T MCNP	1.05290	1.19440	0.42864	0.94665	0.57136

TABLE 7.1

A SUMMARY OF DEVIATIONS FROM THE REFERENCE MODEL IN PCM

CASE 1F (PF=0.6, 50% UO2 IN PELLET - 50% UO2 IN SOLUTION)

PHENOMENOLOGICAL MODEL (4 - FACTOR)

USER	KINF	FF8	FF5	PESC	F	ETA
USA/ORNL R-XSDRNPM	-2584.	507.	5708.	-8894.	273.	-175.
FRANCE/CEA APOLLO	-4598.	455.	913.	-6148.	9.	170.
UK/SRD MONK 6.3	1382.	61.	1556.	-354.	-12.	124.
UK/BNFL WIMSE	215.	1082.	185.	-1893.	37.	800.
ITALY/ENEA C XSDRNPM	-8998.	516.	1644.	-10713.	16.	-471.
JAPAN/PNC XSDRNPM	-24710.	4208.	9741.	-38755.	96.	0.
JAPAN/JAERI ANISN	-939.	1194.	3661.	-5546.	-15.	-238.
ITALY/ENEA CB4 MCNP	-2987.	525.	1651.	-4728.	-2.	-436.
ITALY/ENEA T MCNP	-1648.	1221.	766.	-3600.	-259.	215.

HISTORICAL MODEL

		BY GROUP					
USER	KINF	KINF(1)	PAR(1)	PAB(1)	KINF(2)	PAR(2)	PAB(2)
USA/ORNL R-XSDRNPM	-2584.	522.	0.	2434.	64.	-5598.	0.
FRANCE/CEA APOLLO	-4598.	-2401.	0.	1652.	115.	-3963.	0.
UK/SRD MONK 6.3	1382.	1438.	0.	100.	74.	-228.	0.
UK/BNFL WIMSE	215.	363.	0.	527.	541.	-1221.	0.
ITALY/ENEA C XSDRNPM	-8998.	-4620.	0.	2790.	-292.	-6878.	0.
JAPAN/PNC XSDRNPM	-24710.	-10212.	0.	8973.	62.	-23514.	0.
JAPAN/JAERI ANISN	-939.	1188.	0.	1545.	-158.	-3515.	0.
ITALY/ENEA CB4 MCNP	-2987.	-968.	0.	1295.	-279.	-3035.	0.
ITALY/ENEA T MCNP	-1648.	-307.	0.	994.	-29.	-2313.	0.

SPATIAL MODEL

	BY REGION				
USER	KINF	KINF(1)	W(1)	KINF(2)	W(2)
USA/ORNL R-XSDRNPM	-2584.	-970.	-232.	-1565.	184.
FRANCE/CEA APOLLO	-4598.	-3350.	1094.	-1449.	-891.
UK/SRD MONK 6.3	1382.	591.	79.	775.	-63.
UK/BNFL WIMSE	215.	376.	-269.	-111.	213.
ITALY/ENEA C XSDRNPM	-8998.	-6859.	2573.	-2565.	-2149.
JAPAN/PNC XSDRNPM	-24710.	-7692.	-4271.	-15910.	3160.
JAPAN/JAERI ANISN	-939.	-916.	462.	-117.	-372.
ITALY/ENEA CB4 MCNP	-2987.	-1097.	-358.	-1821.	284.
ITALY/ENEA T MCNP	-1648.	-623.	-153.	-1001.	122.

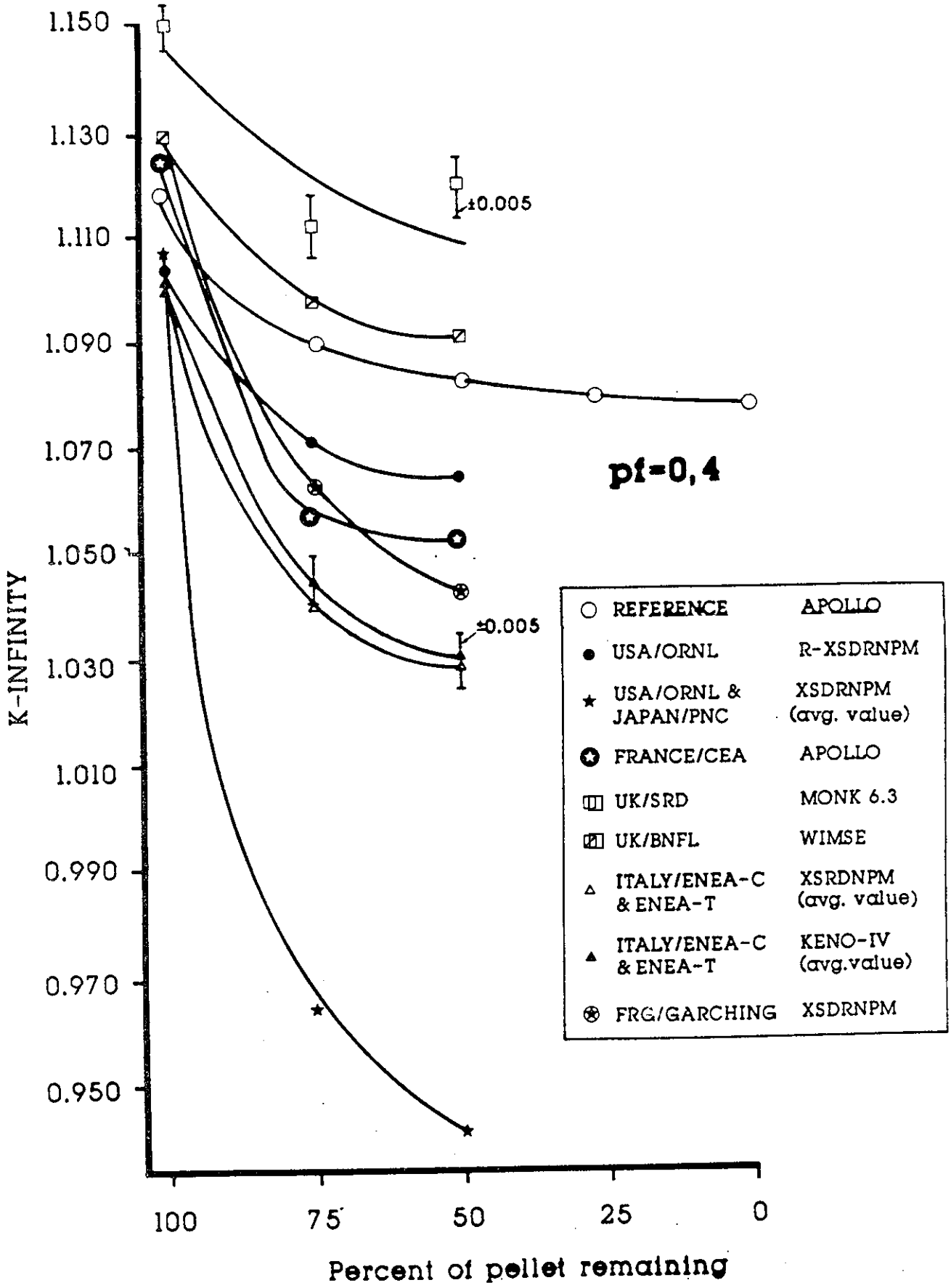

Figure 1: A comparison of the variation of k_∞ with pellet dissolution for the reference calculation and the June 1988 calculations. PF=0.4

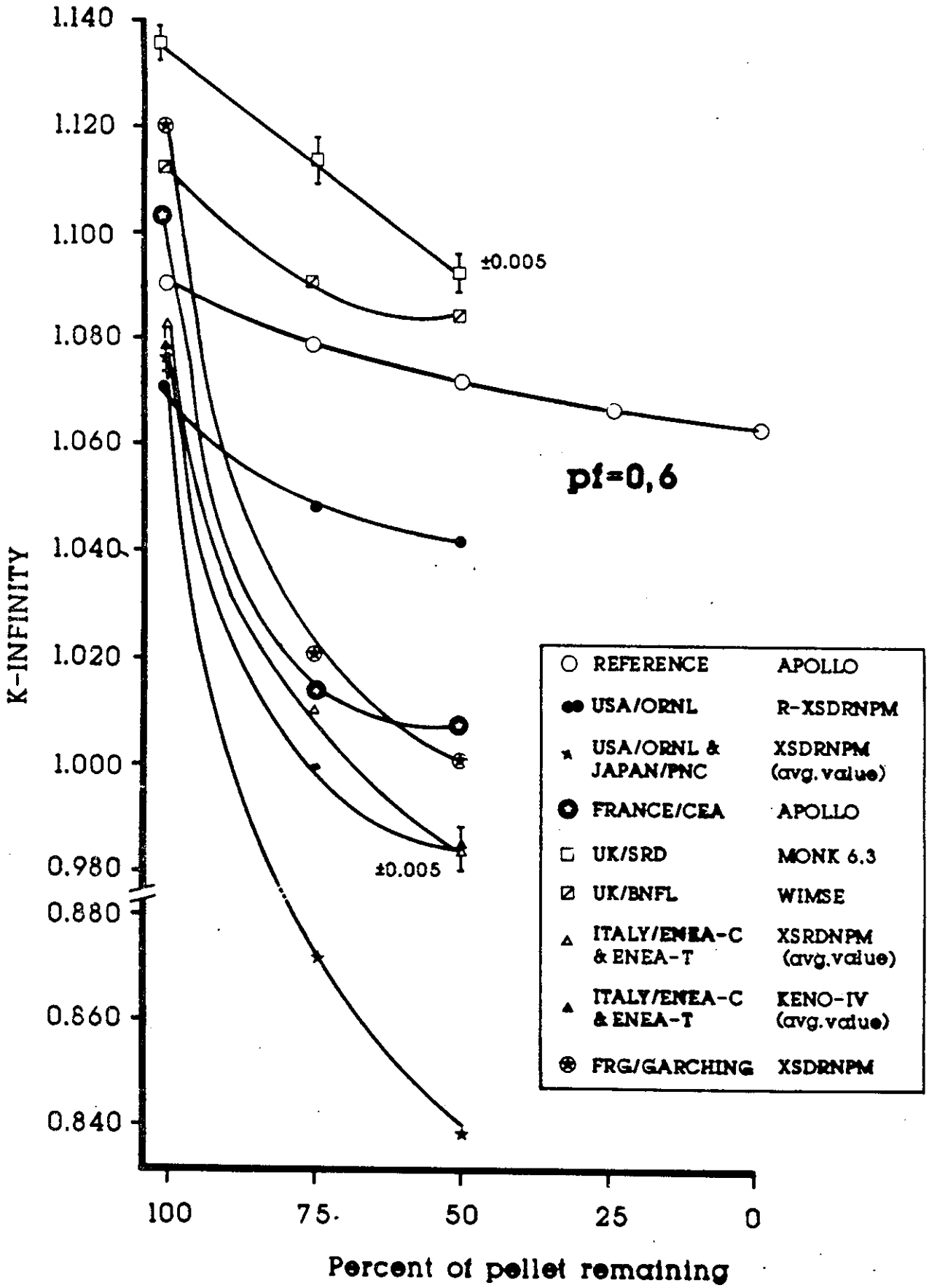

Figure 2: A comparison of the variation of k_∞ with pellet dissolution for the reference calculation and the June 1988 calculations. PF=0.6

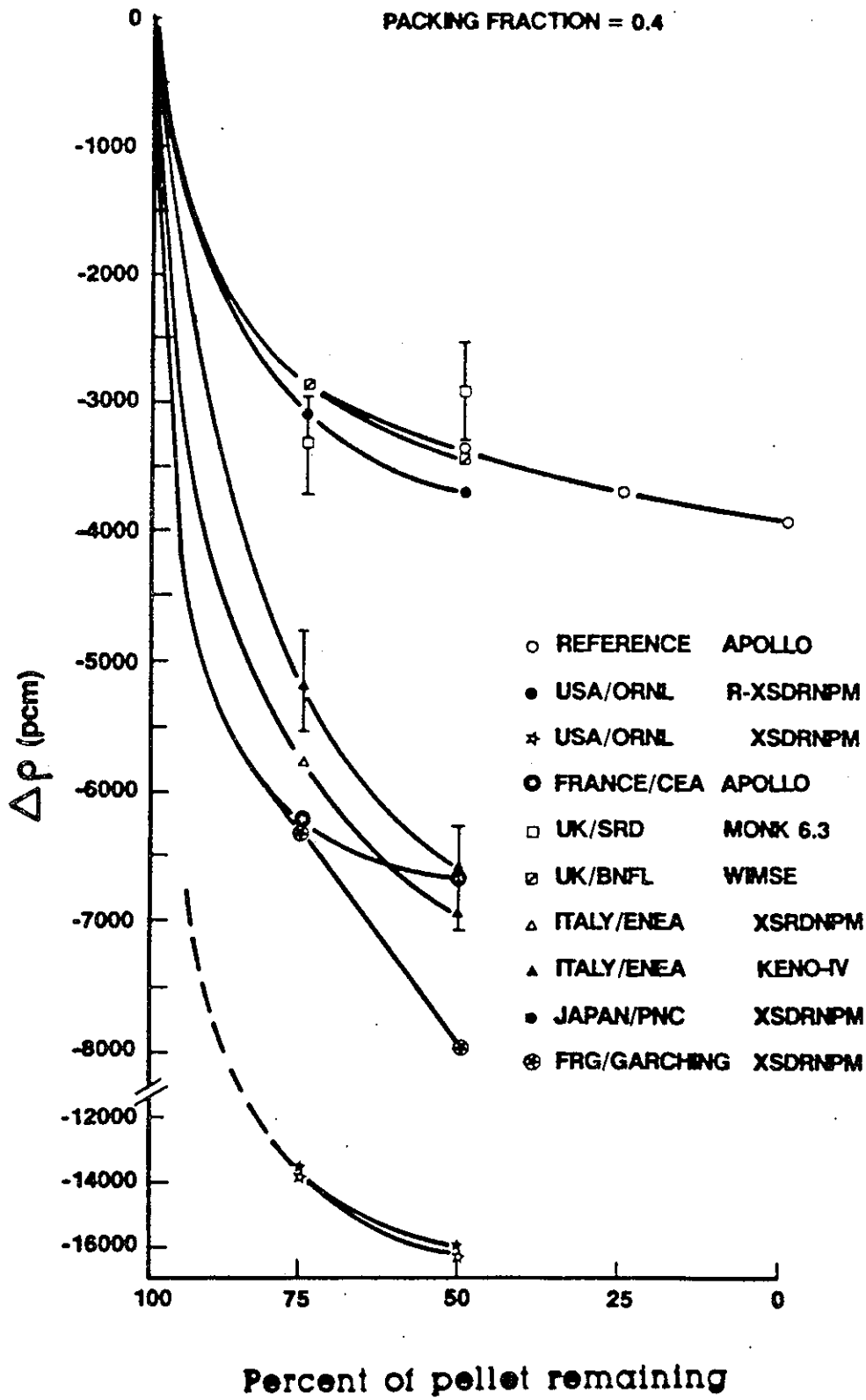

Figure 3: A comparison of the variation of $\Delta\rho$ with pellet dissolution for the reference calculation and the June 1988 calculations. PF=0.4

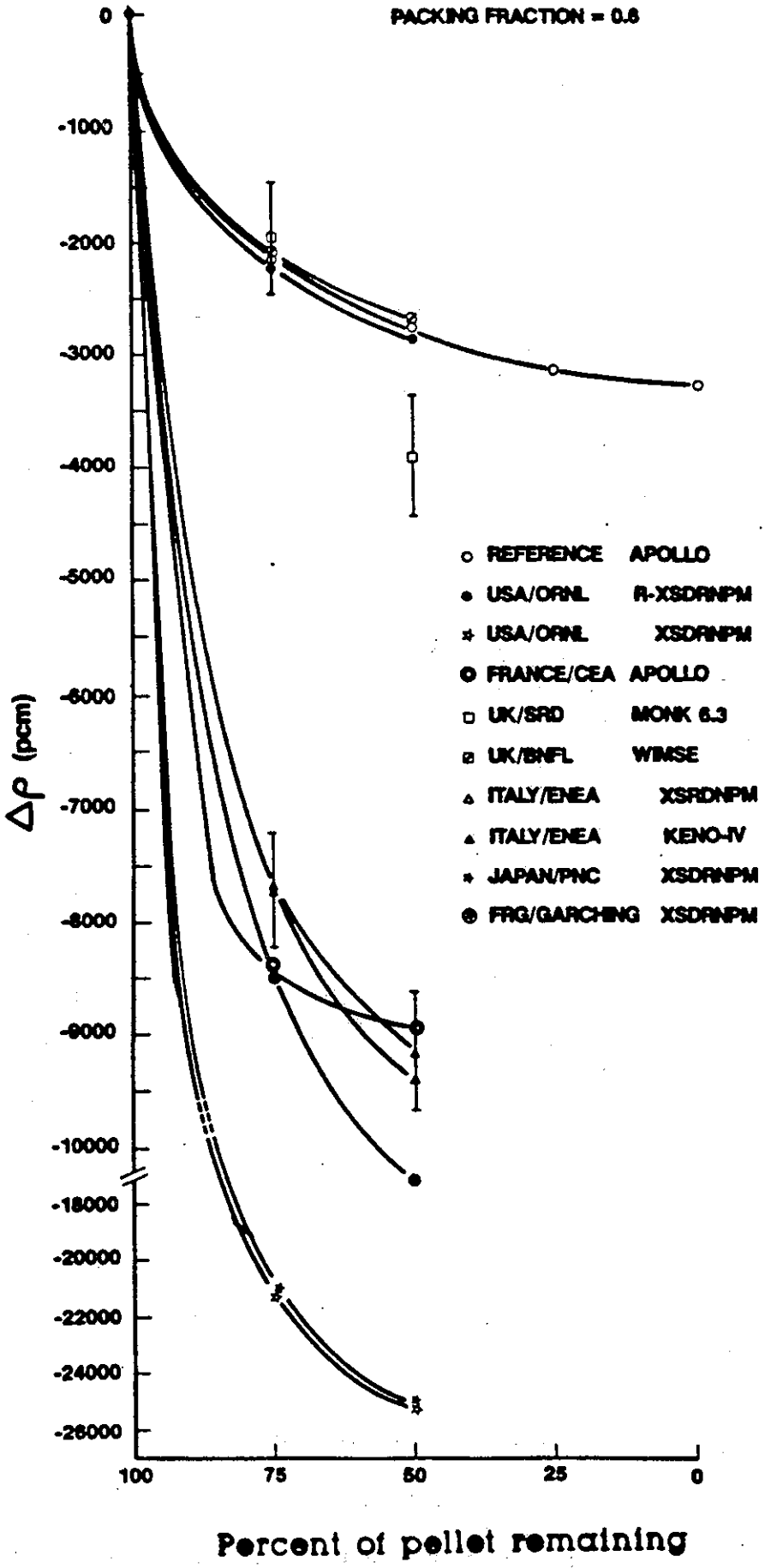

Figure 4: A comparison of the variation of $\Delta\rho$ with pellet dissolution for the reference calculation and the June 1988 calculations. PF=0.6

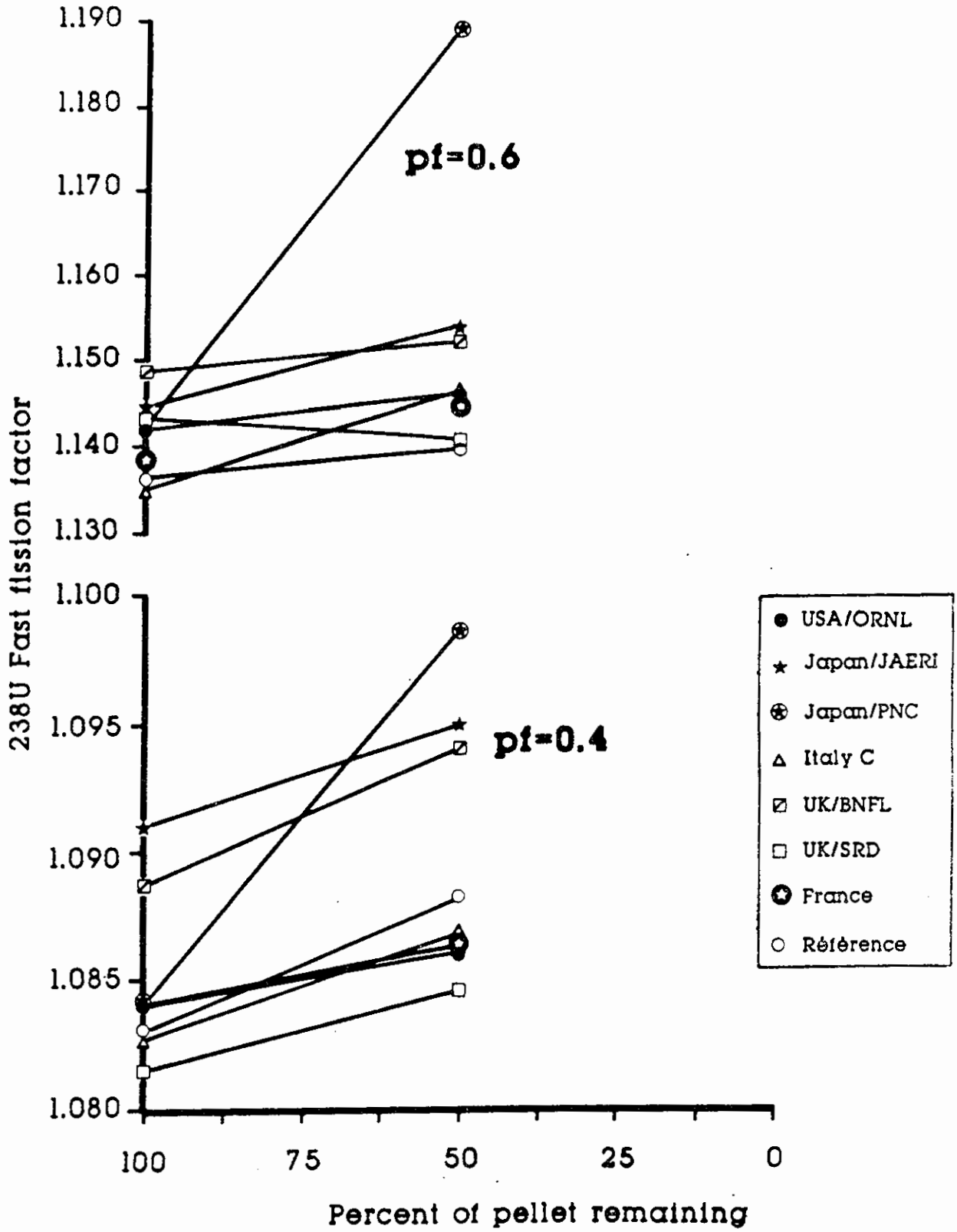

Figure 5: A comparison of the ^{238}U Fast Fission Factor as a function of pellet dissolution as calculated by the participants in the June 1989 exercise. PF=0.4 and PF=0.6.

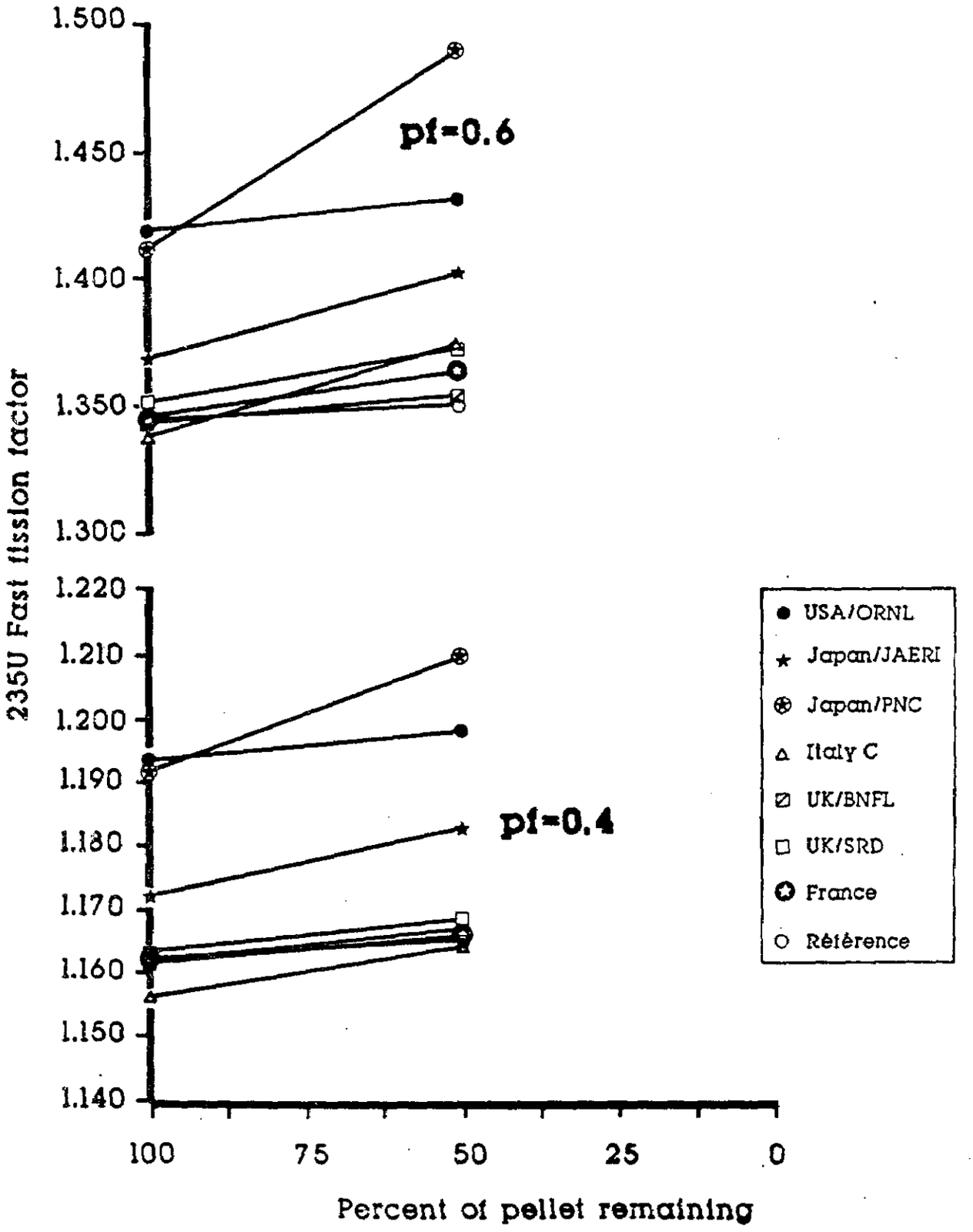

Figure 6: A comparison of the ^{235}U Fast Fission Factor as a function of pellet dissolution as calculated by the participants in the June 1989 exercise. PF=0.4 and PF=0.6.

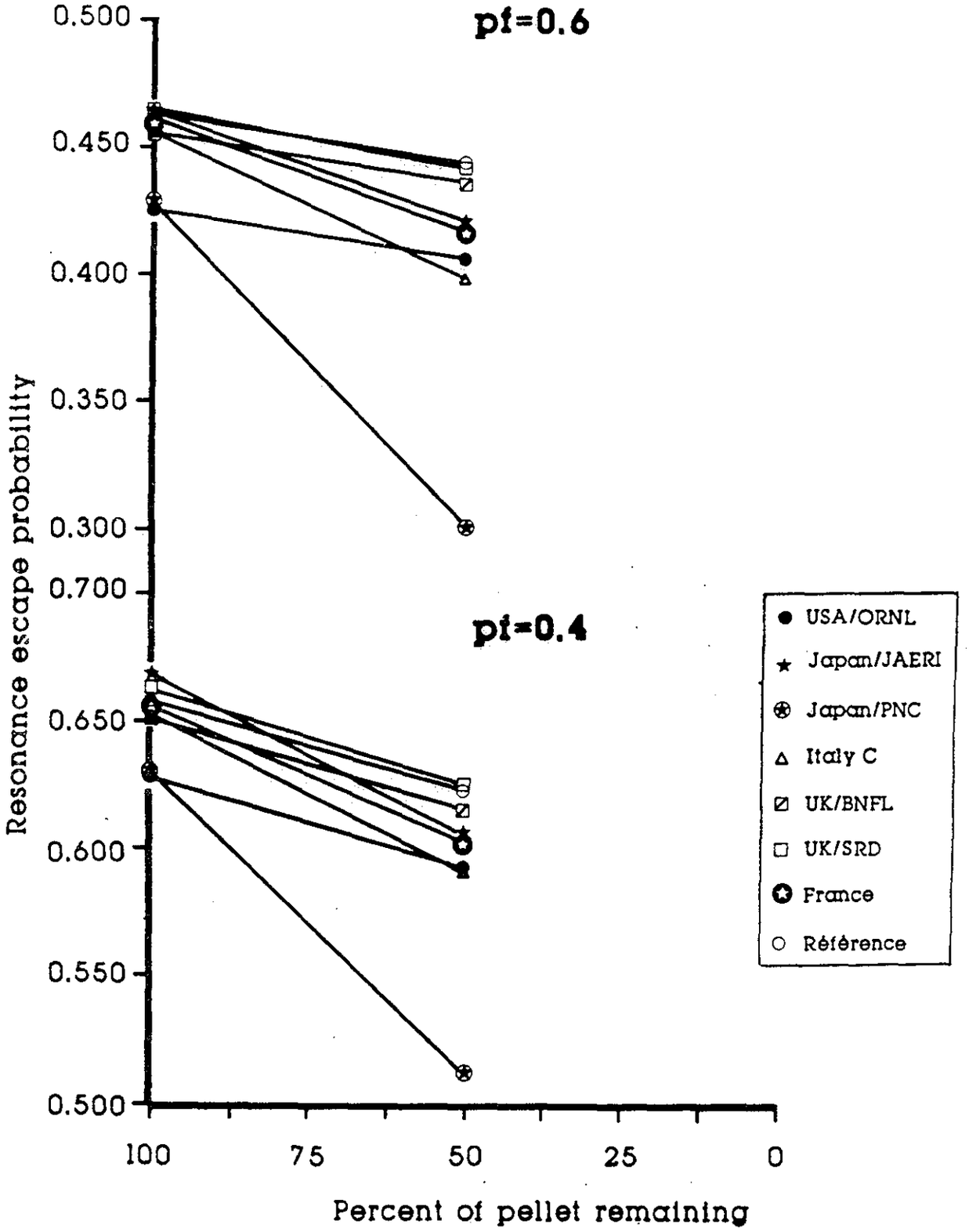

Figure 7: A comparison of the Resonance Escape Probability as a function of pellet dissolution as calculated by the participants in the June 1989 exercise. PF=0.4 and PF=0.6.

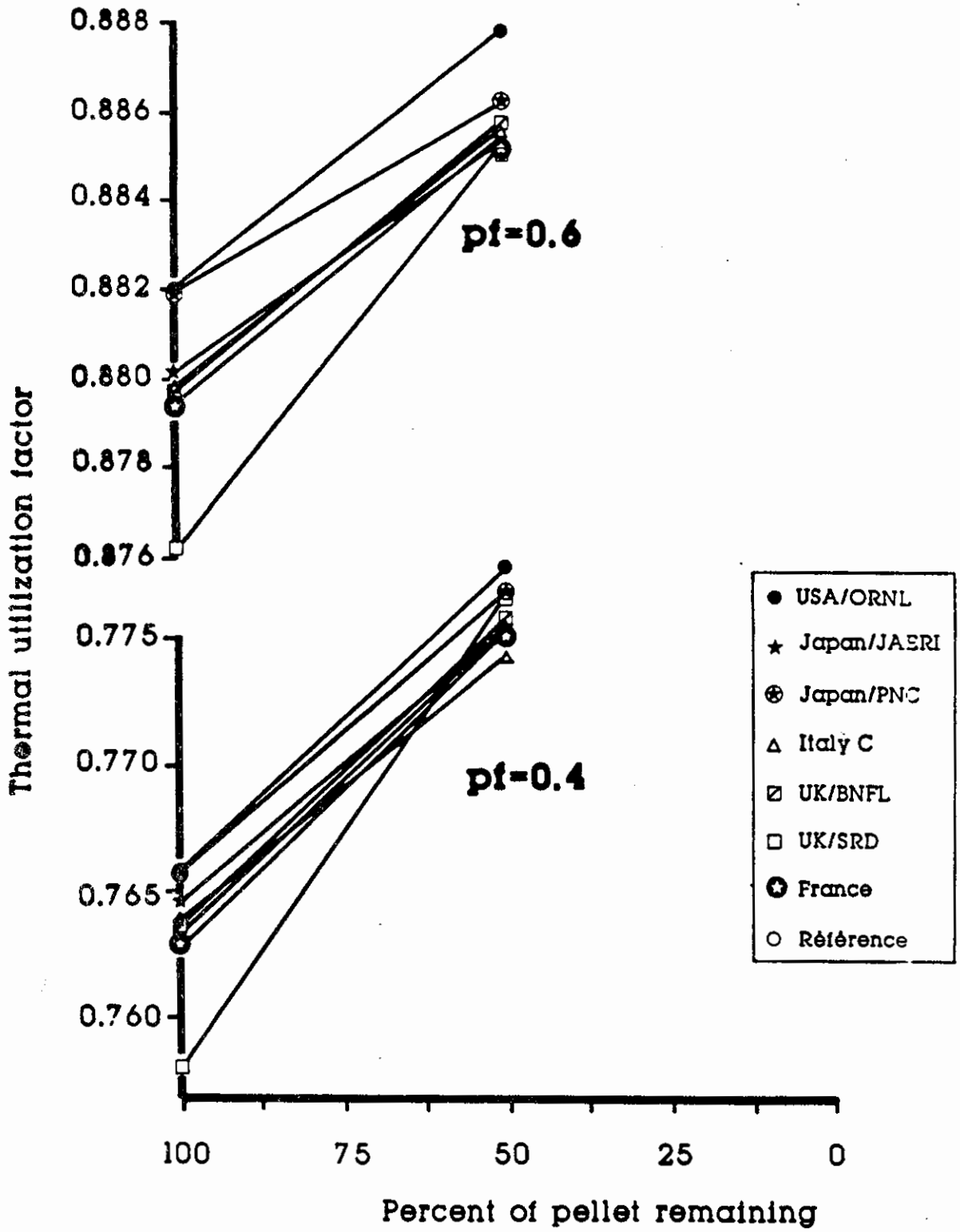

Figure 8: A comparison of the Thermal Utilization Factor as a function of pellet dissolution as calculated by the participants in the June 1989 exercise. PF=0.4 and PF=0.6.

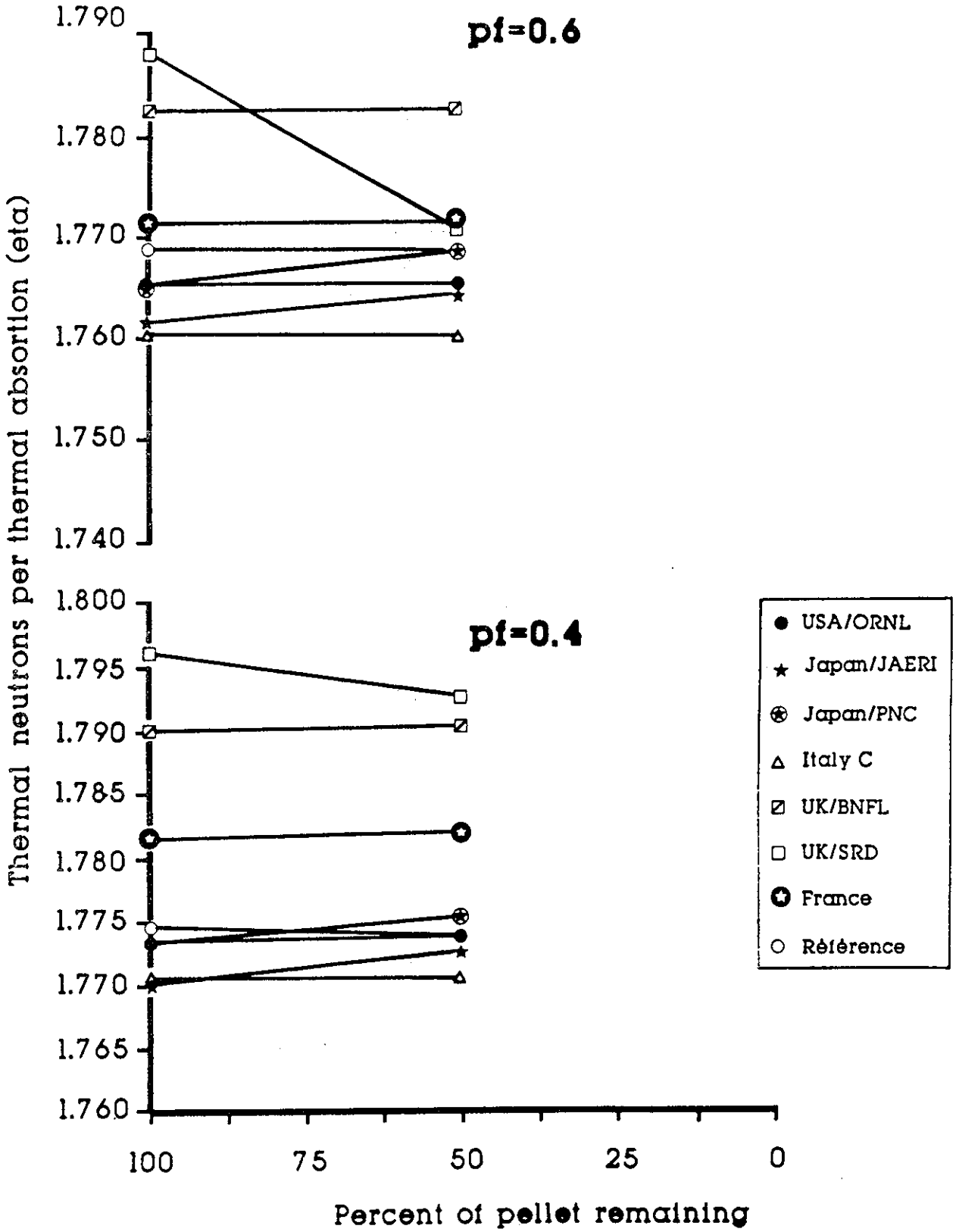

Figure 9: A comparison of the eta-Factor as a function of pellet dissolution as calculated by the participants in the June 1989 exercise. PF=0.4 and PF=0.6.

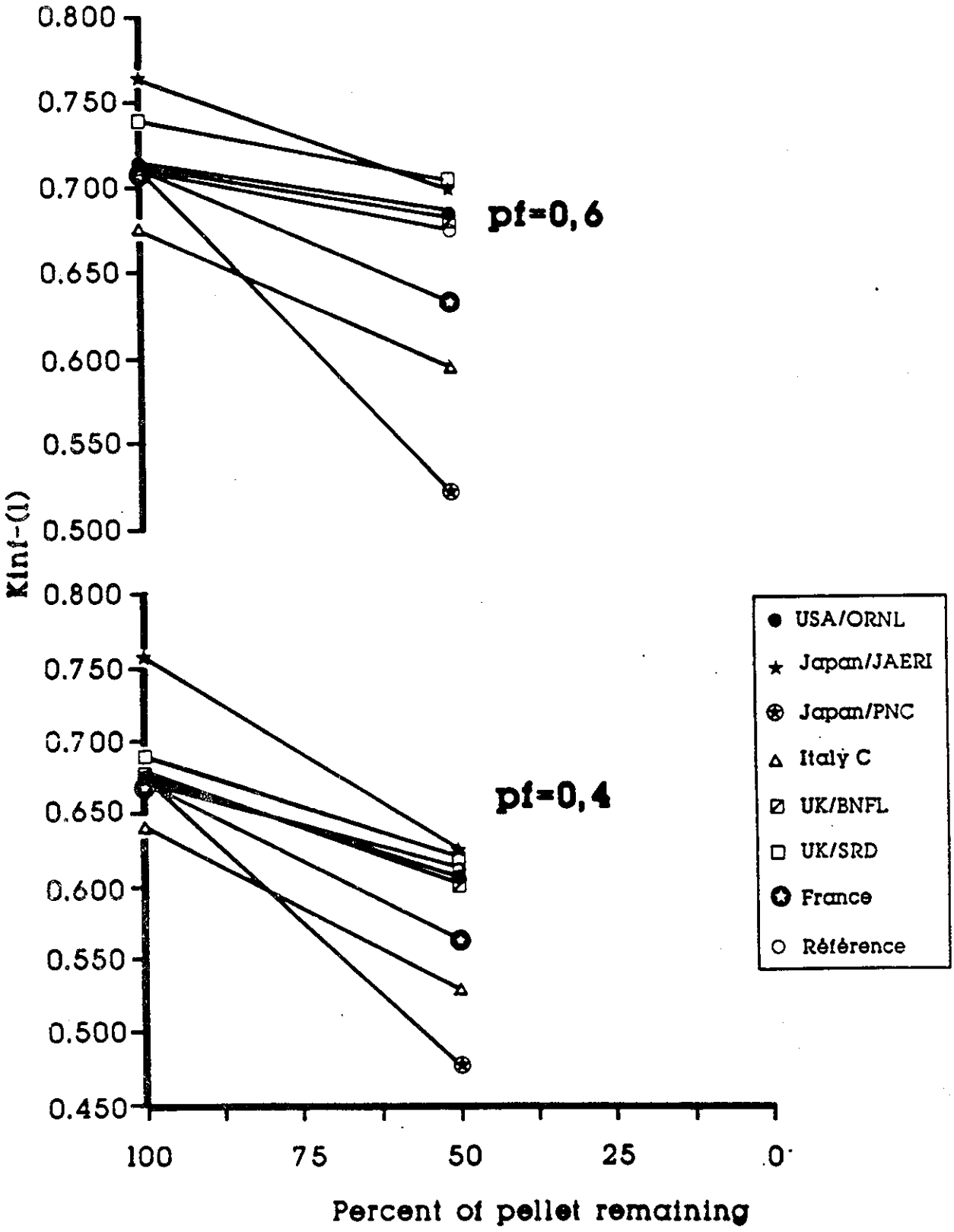

Figure 10: A comparison of the KINF(1) - Historical Model as a function of pellet dissolution as calculated by the participants in the June 1989 exercise. PF=0.4 and PF=0.6.

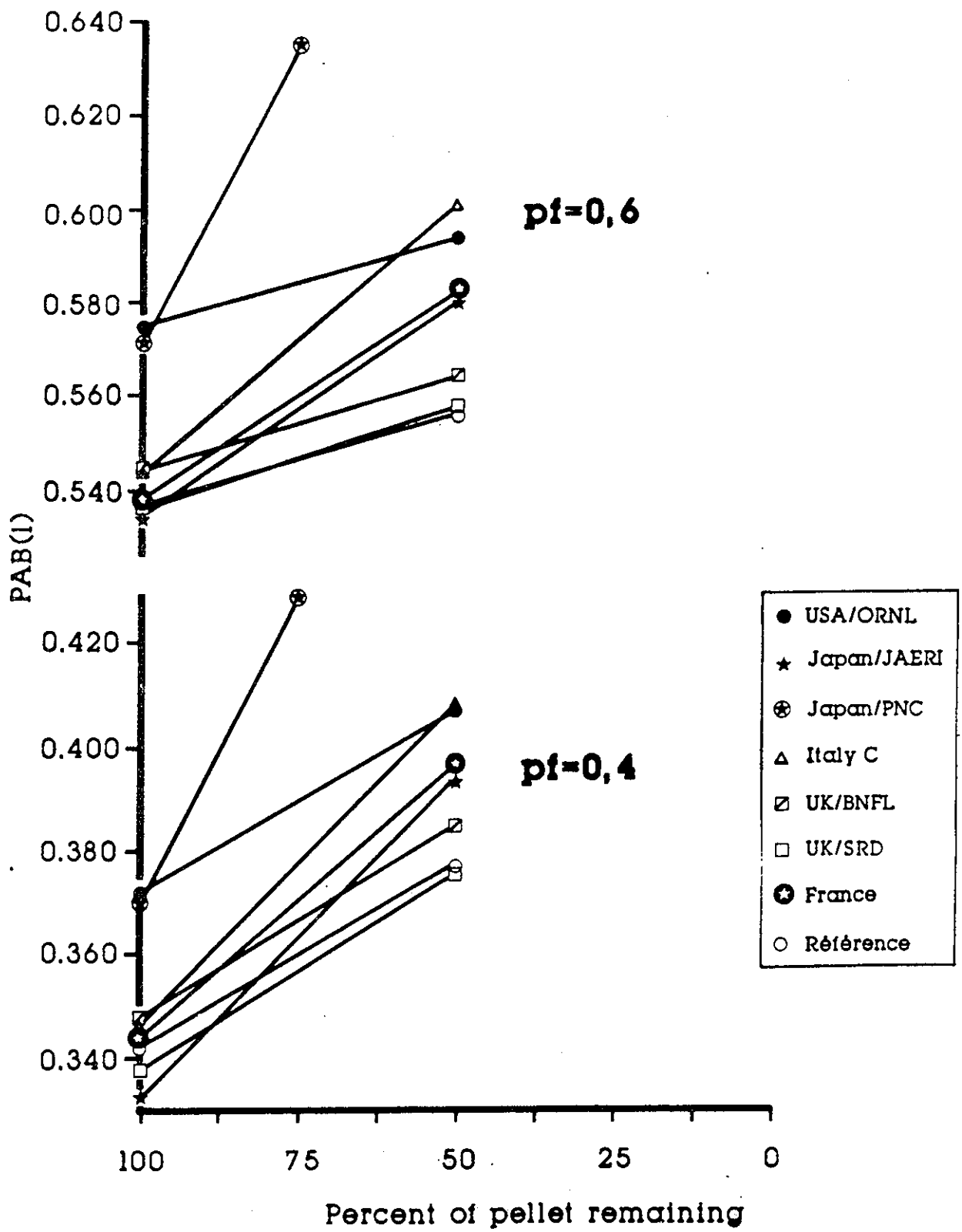

Figure 11: A comparison of the PAB(1) - Historical Model as a function of pellet dissolution as calculated by the participants in the June 1989 exercise. PF=0.4 and PF=0.6.

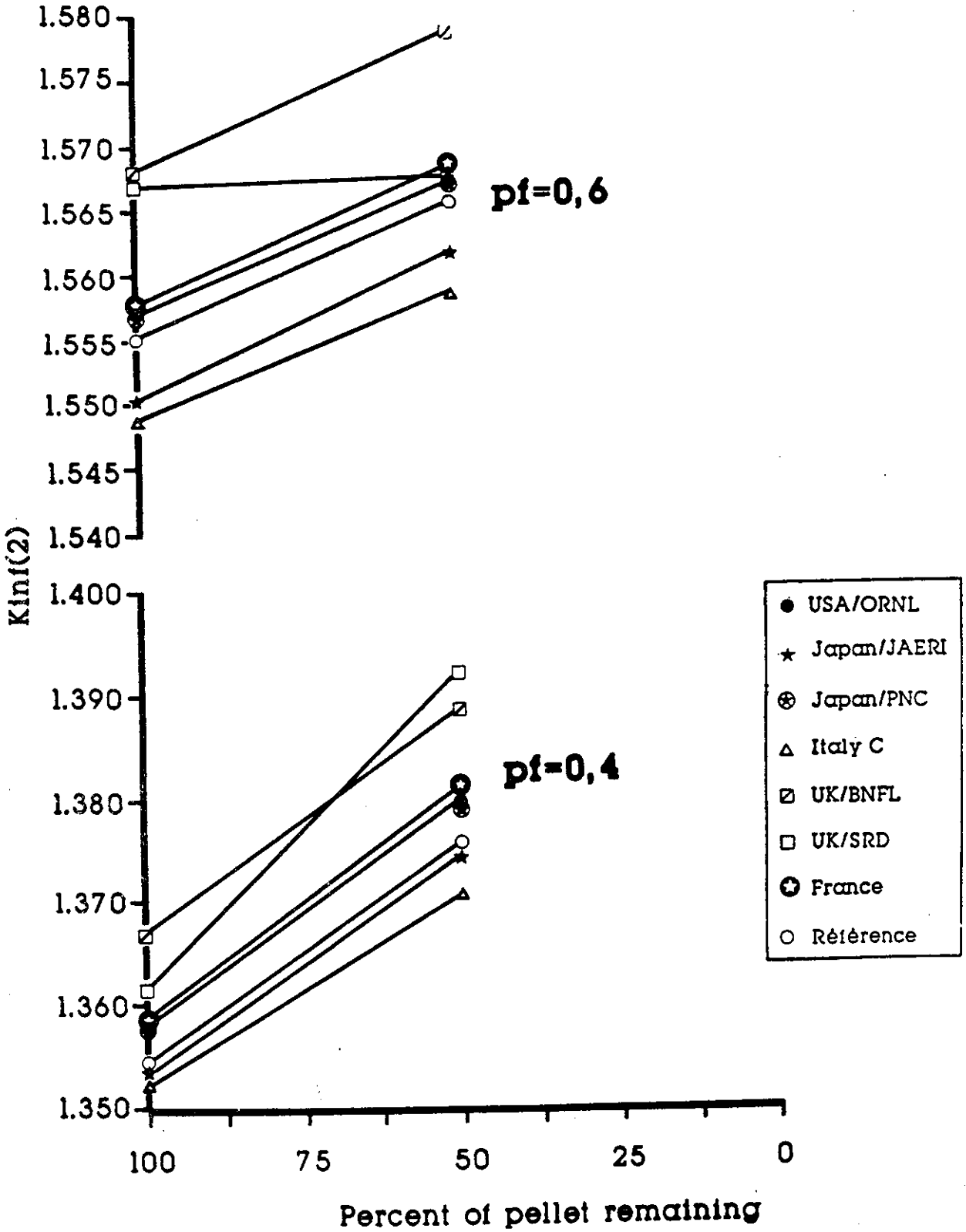

Figure 12: A comparison of the KINF(2) - Historical Model as a function of pellet dissolution as calculated by the participants in the June 1989 exercise. PF=0.4 and PF=0.6.

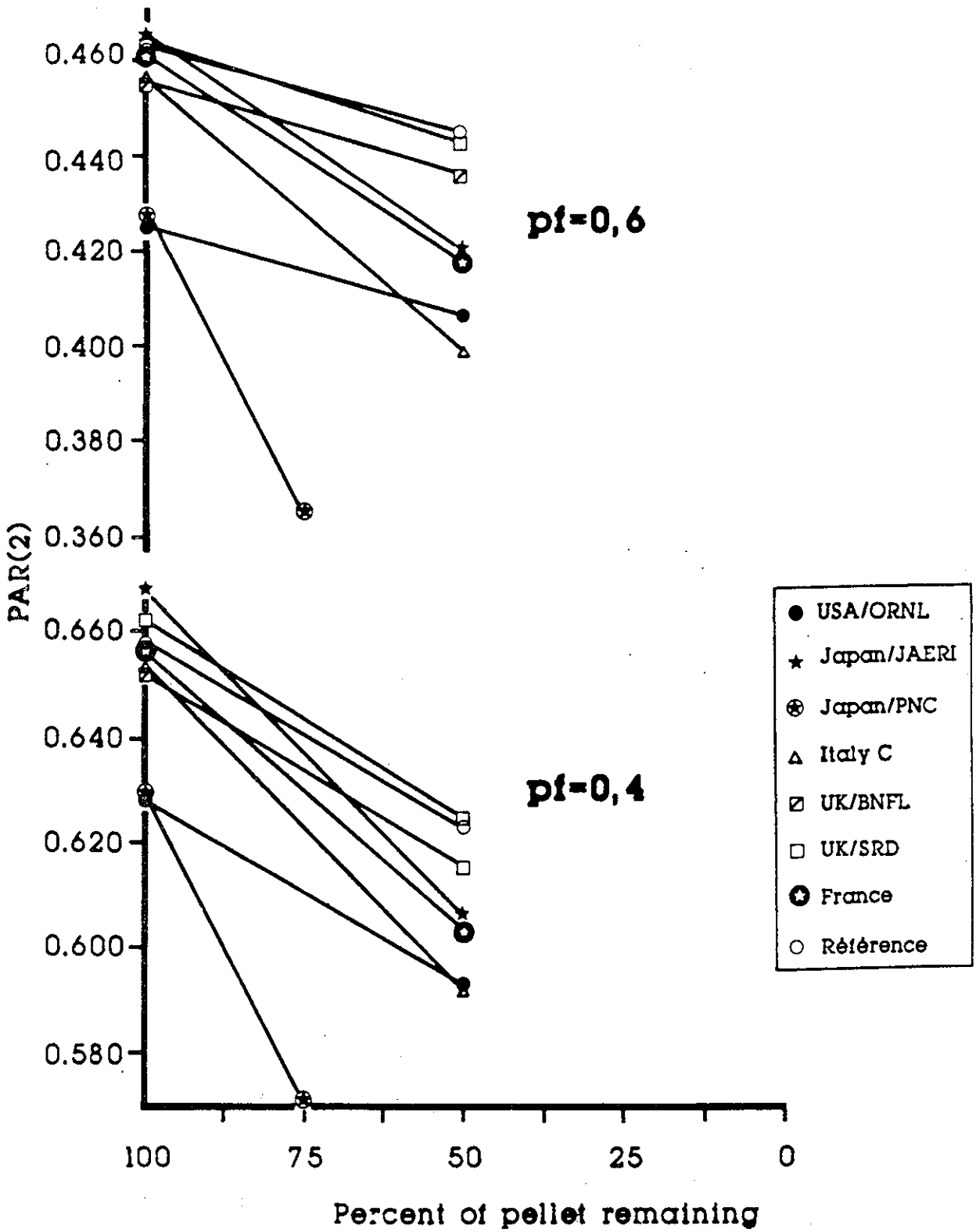

Figure 13: A comparison of the PAR(2) - Historical Model as a function of pellet dissolution as calculated by the participants in the June 1989 exercise. PF=0.4 and PF=0.6.

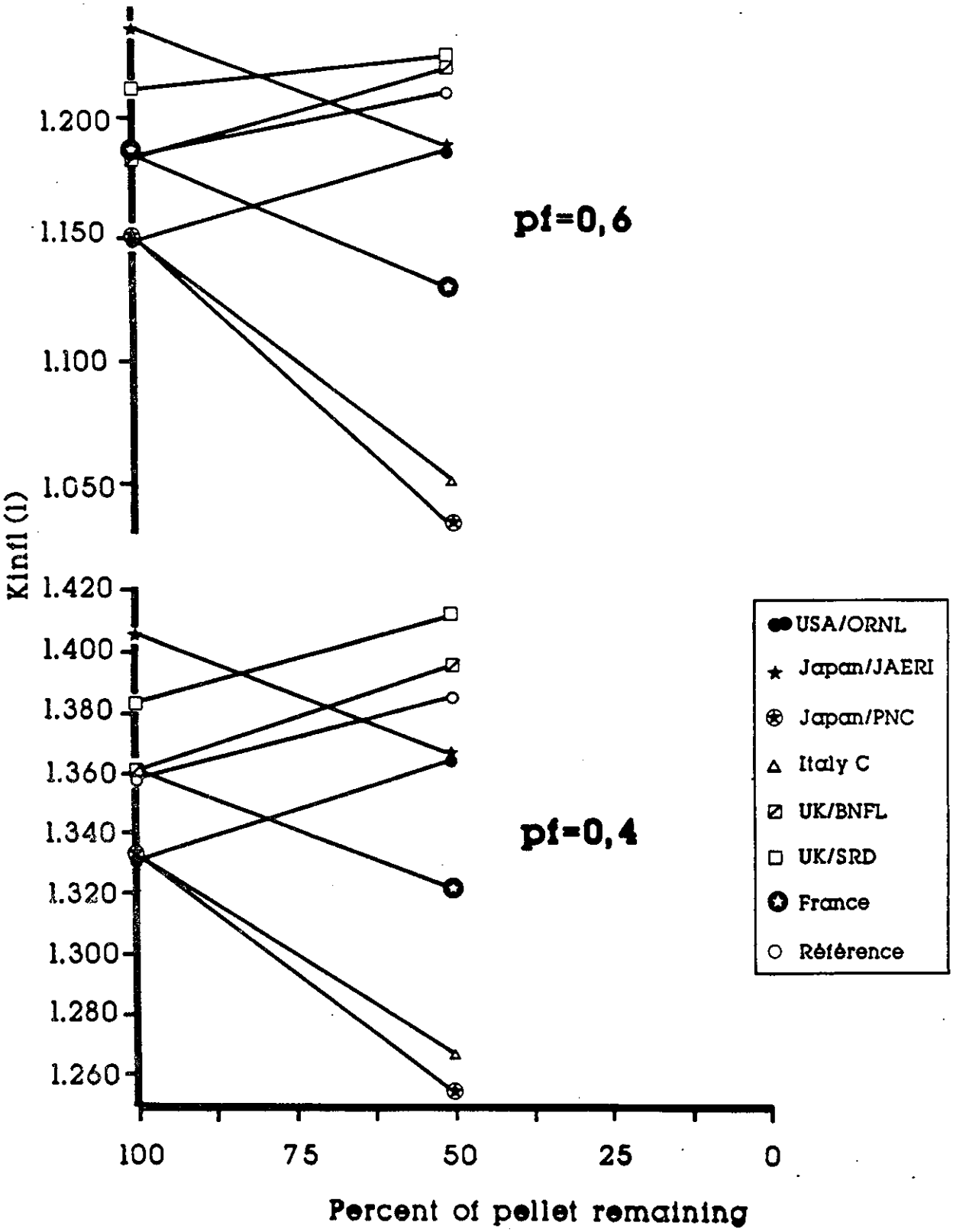

Figure 14: A comparison of the KINF(1) - Spatial Model as a function of pellet dissolution as calculated by the participants in the June 1989 exercise. PF=0.4 and PF=0.6.

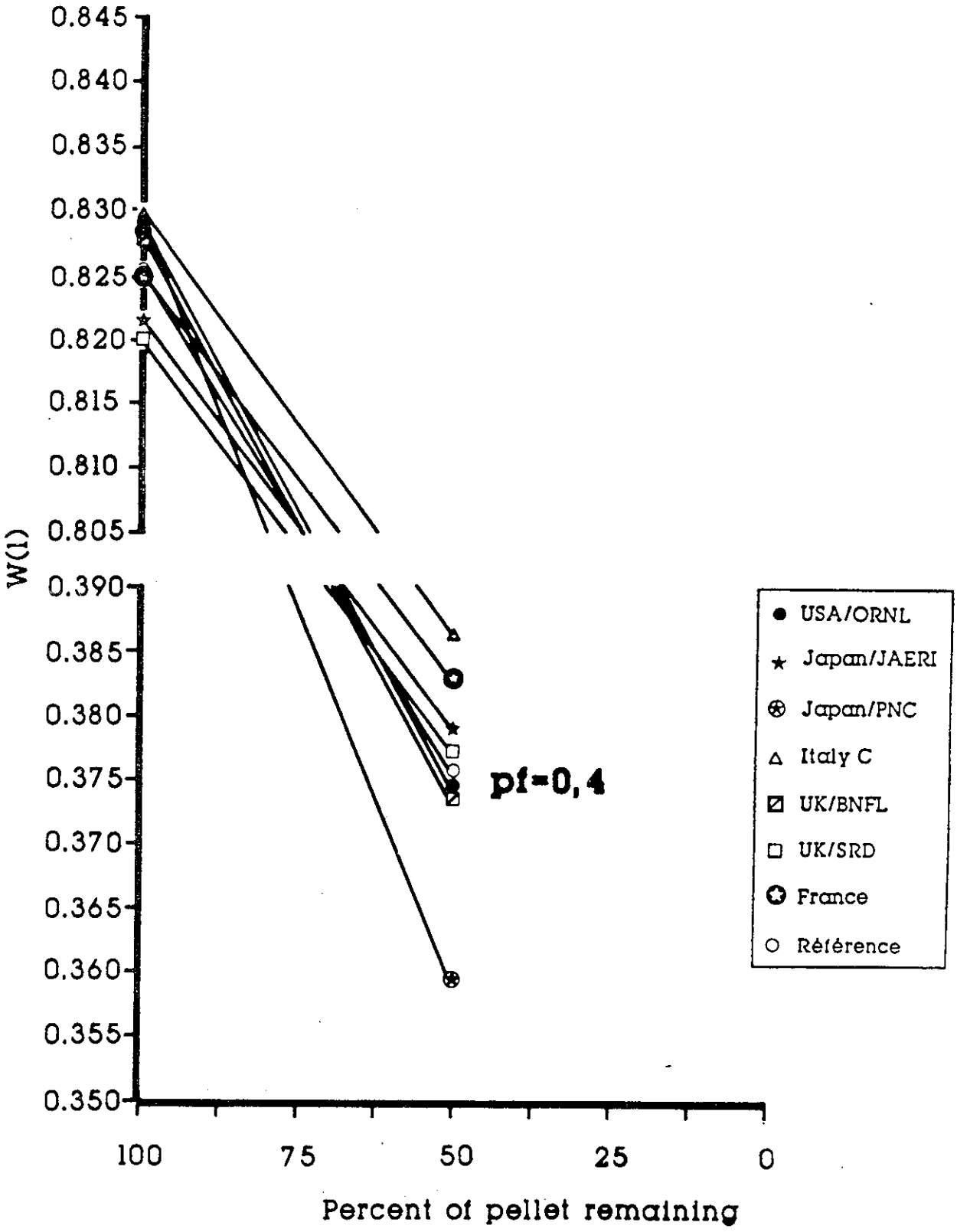

Figure 15: A comparison of the W(1) - Spatial Model as a function of pellet dissolution as calculated by the participants in the June 1989 exercise. PF=0.4.

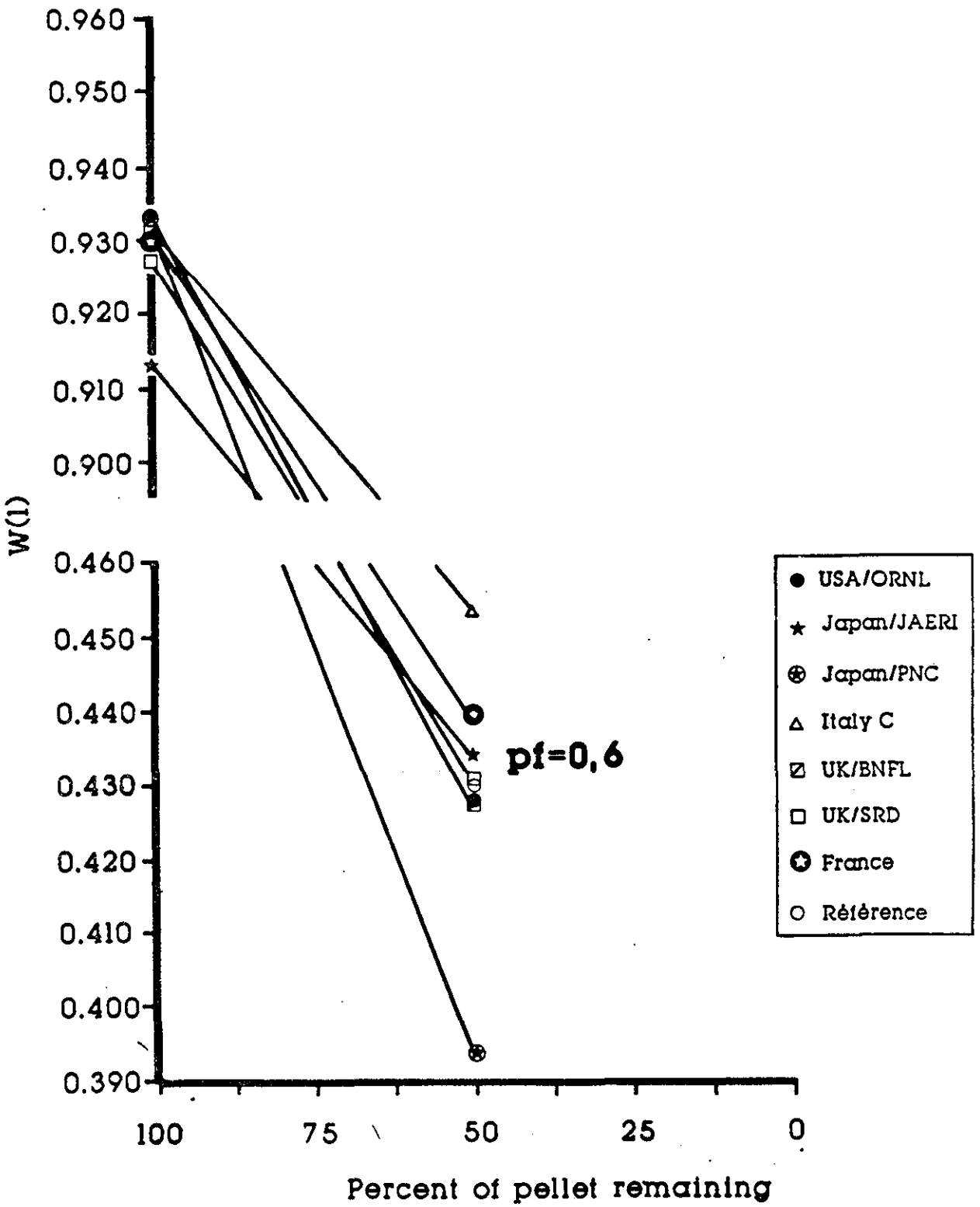

Figure 16: A comparison of the W(1) - Spatial Model as a function of pellet dissolution as calculated by the participants in the June 1989 exercise. PF=0.6.

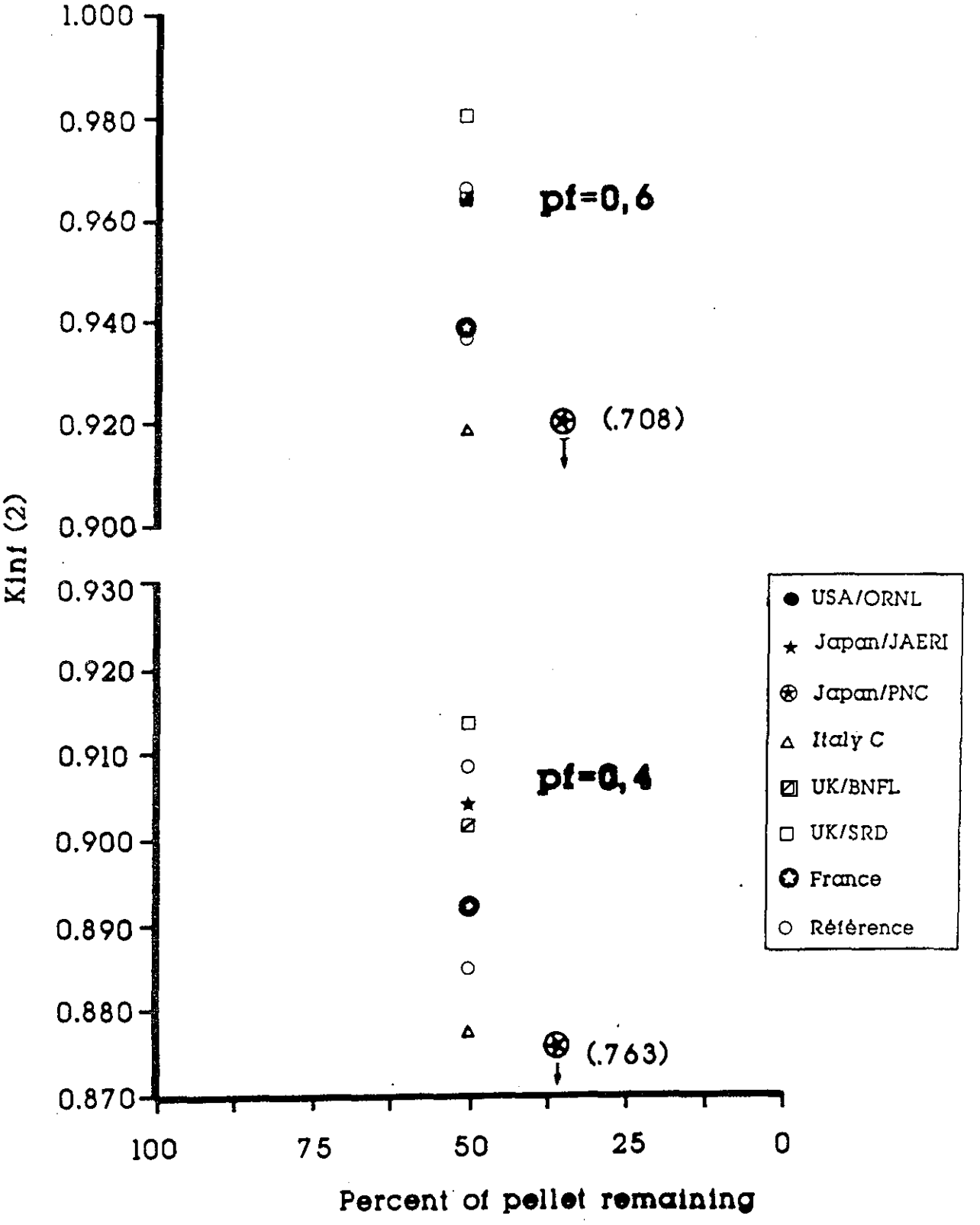

Figure 17: A comparison of the KINF(2) - Spatial Model as a function of pellet dissolution as calculated by the participants in the June 1989 exercise. PF=0.4 and PF=0.6.

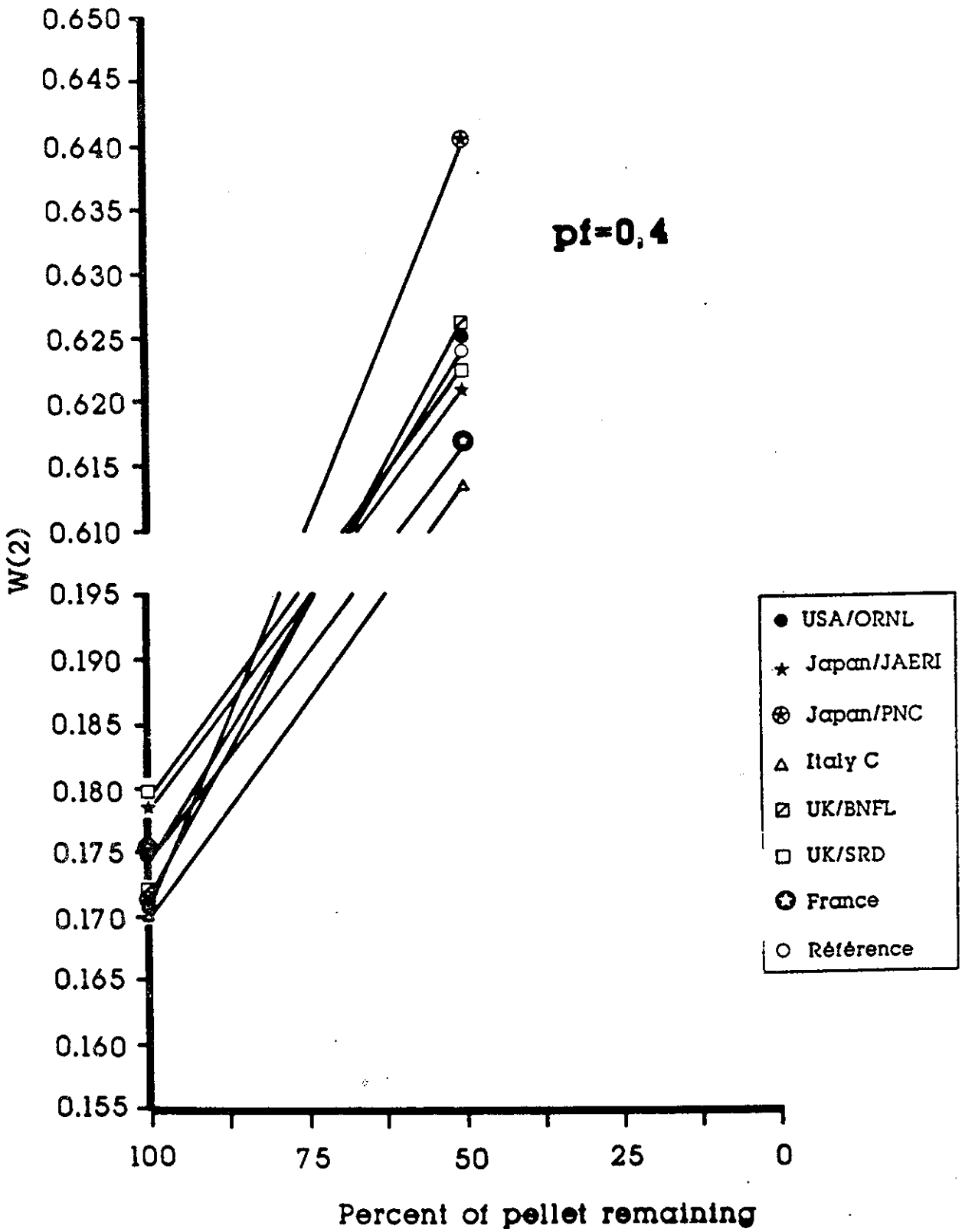

Figure 18: A comparison of the W(2) - Spatial Model as a function of pellet dissolution as calculated by the participants in the June 1989 exercise. PF=0.4.

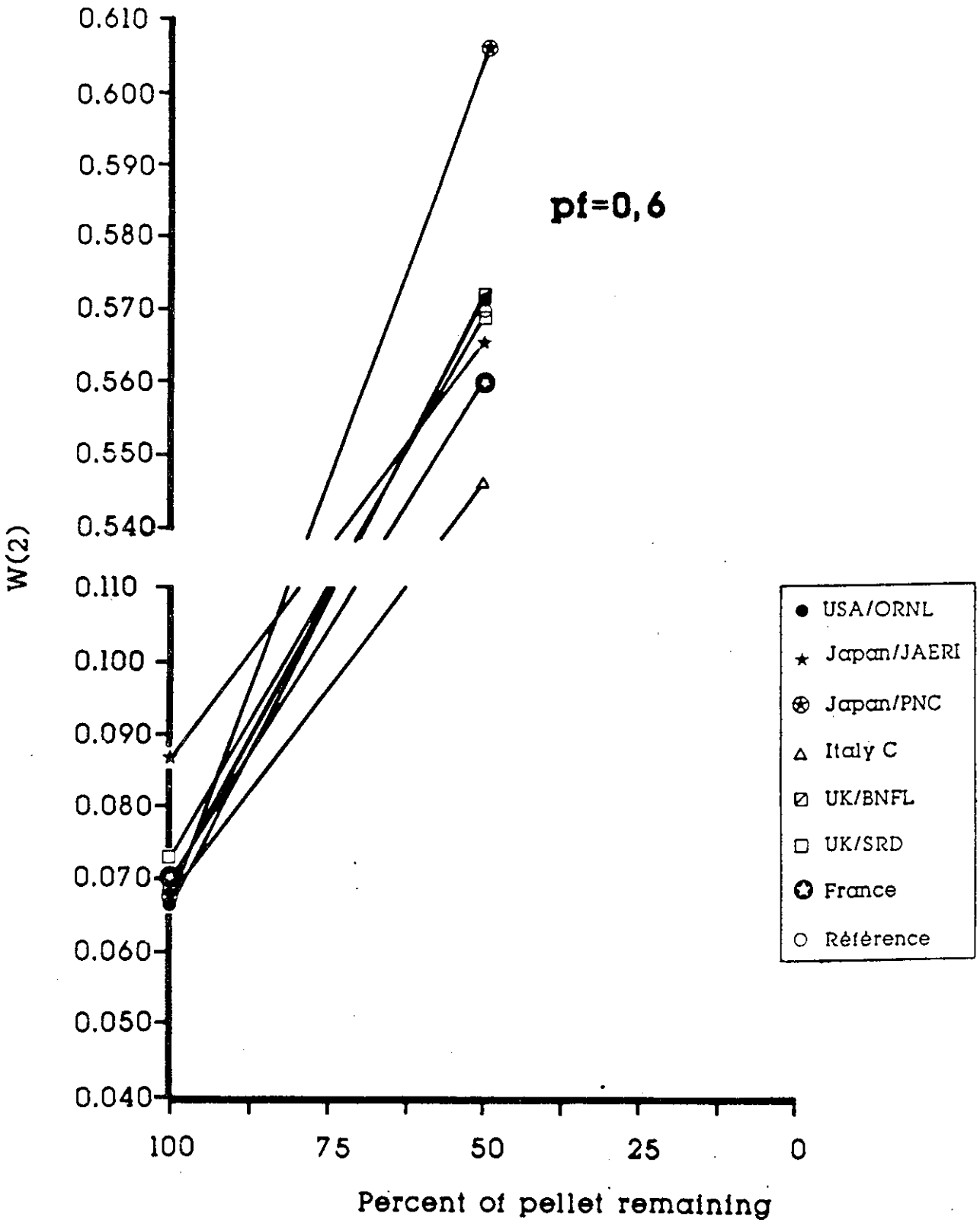

Figure 19: A comparison of the W(2) - Spatial Model as a function of pellet dissolution as calculated by the participants in the June 1989 exercise. PF=0.6.

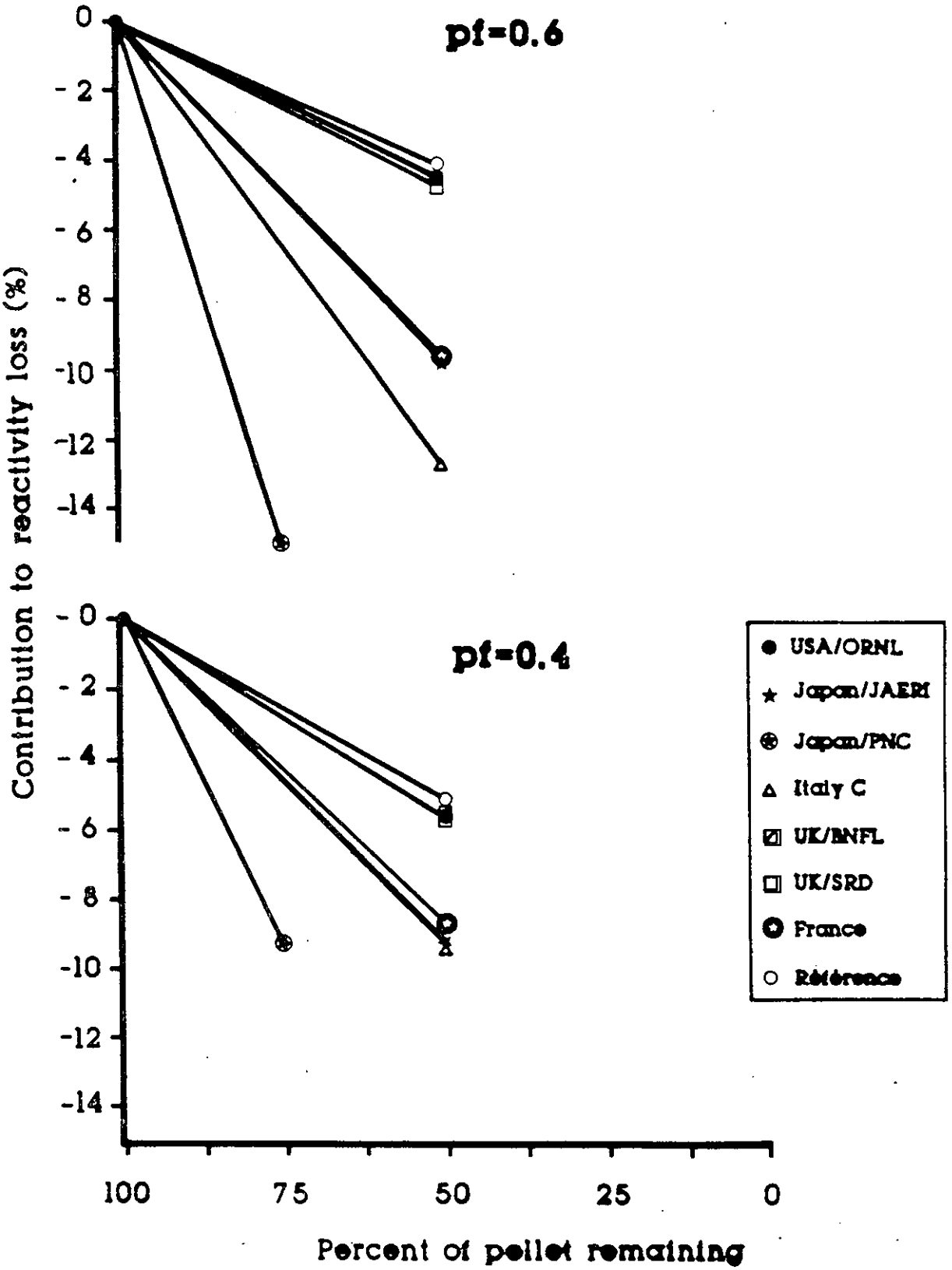

Figure 20: A comparison of the relative contribution to reactivity loss linked to the p-Factor as a function of pellet dissolution as calculated by the participants in the June 1989 exercise. PF=0.4 and PF=0.6.

APPENDIX I

NORMALIZED REACTION RATES

TABLE I .1

A SUMMARY OF PARTICIPANTS REACTION RATES
NORMALIZED TO ONE ABSORPTION IN THE CELL AND
EXPRESSED AS A PERCENTAGE OF THE ABSORPTION RATE

CASE 1B (PF=0.6, 100% UO2 IN PELLET - 0% UO2 IN SOLUTION)

FRANCE/CEAREF APOLLO PROD/ABS= 1.10076 NU= 2.46300

CAPTURES

		REGION 1				REGION 2			
	FAST	EPI	THERMAL	TOTAL	FAST	EPI	THERMAL	TOTAL
CAP 92235	0.2793	4.3994	5.2165	9.8952	0.0000	0.0000	0.0000	0.0000
CAP 92238	6.1472	26.3308	5.7409	38.2189	0.0000	0.0000	0.0000	0.0000
CAP 160	0.2217	0.0003	0.0025	0.2245	0.0000	0.0000	0.0000	0.0000
CAP H2O	0.0000	0.0000	0.0000	0.0000	0.0991	0.3185	1.4338	1.8513
CAP B(NAT)	0.0000	0.0000	0.0000	0.0000	0.0238	0.9404	4.1504	5.1147
TOTAL	6.6483	30.7305	10.9599	48.3387	0.1229	1.2590	5.5842	6.9660

FISSIONS

		REGION 1				REGION 2			
	FAST	EPI	THERMAL	TOTAL	FAST	EPI	THERMAL	TOTAL
FIS 92235	1.3079	8.9098	29.7536	39.9712	0.0000	0.0000	0.0000	0.0000
FIS 92238	4.7206	0.0000	0.0000	4.7206	0.0000	0.0000	0.0000	0.0000
FIS 160	0.0000	0.0000	0.0000	0.0000	0.0000	0.0000	0.0000	0.0000
FIS H2O	0.0000	0.0000	0.0000	0.0000	0.0000	0.0000	0.0000	0.0000
FIS B(NAT)	0.0000	0.0000	0.0000	0.0000	0.0000	0.0000	0.0000	0.0000
TOTAL	6.0284	8.9098	29.7536	44.6918	0.0000	0.0000	0.0000	0.0000

PRODUCTIONS

		REGION 1				REGION 2			
	FAST	EPI	THERMAL	TOTAL	FAST	EPI	THERMAL	TOTAL
PRD 92235	3.2984	21.5622	72.0032	96.8637	0.0000	0.0000	0.0000	0.0000
PRD 92238	13.2143	0.0000	0.0000	13.2143	0.0000	0.0000	0.0000	0.0000
PRD 160	0.0000	0.0000	0.0000	0.0000	0.0000	0.0000	0.0000	0.0000
PRD H2O	0.0000	0.0000	0.0000	0.0000	0.0000	0.0000	0.0000	0.0000
PRD B(NAT)	0.0000	0.0000	0.0000	0.0000	0.0000	0.0000	0.0000	0.0000
TOTAL	16.5126	21.5622	72.0032	110.0780	0.0000	0.0000	0.0000	0.0000

USA/ORNL R-XSDRNPM PROD/ABS= 1.07279 NU= 2.46449

CAPTURES

		REGION 1				REGION 2			
	FAST	EPI	THERMAL	TOTAL	FAST	EPI	THERMAL	TOTAL
CAP 92235	0.3199	4.4315	4.9028	9.6542	0.0000	0.0000	0.0000	0.0000
CAP 92238	7.4592	27.1762	5.2246	39.8600	0.0000	0.0000	0.0000	0.0000
CAP 160	0.2755	0.0002	0.0007	0.2764	0.0000	0.0000	0.0000	0.0000
CAP H2O	0.0000	0.0000	0.0000	0.0000	0.1317	0.3926	1.3003	1.8246
CAP B(NAT)	0.0000	0.0000	0.0000	0.0000	0.0274	1.1058	3.7175	4.8507
TOTAL	8.0545	31.6079	10.1281	49.7905	0.1591	1.4984	5.0178	6.6753

FISSIONS

		REGION 1				REGION 2			
	FAST	EPI	THERMAL	TOTAL	FAST	EPI	THERMAL	TOTAL
FIS 92235	1.4532	9.9517	27.3726	38.7775	0.0000	0.0000	0.0000	0.0000
FIS 92238	4.7524	0.0000	0.0000	4.7524	0.0000	0.0000	0.0000	0.0000
FIS 160	0.0000	0.0000	0.0000	0.0000	0.0000	0.0000	0.0000	0.0000
FIS H2O	0.0000	0.0000	0.0000	0.0000	0.0000	0.0000	0.0000	0.0000
FIS B(NAT)	0.0000	0.0000	0.0000	0.0000	0.0000	0.0000	0.0000	0.0000
TOTAL	6.2056	9.9517	27.3726	43.5299	0.0000	0.0000	0.0000	0.0000

PRODUCTIONS

		REGION 1				REGION 2			
	FAST	EPI	THERMAL	TOTAL	FAST	EPI	THERMAL	TOTAL
PRD 92235	3.6664	24.0712	66.1980	93.9355	0.0000	0.0000	0.0000	0.0000
PRD 92238	13.3443	0.0000	0.0000	13.3443	0.0000	0.0000	0.0000	0.0000
PRD 160	0.0000	0.0000	0.0000	0.0000	0.0000	0.0000	0.0000	0.0000
PRD H2O	0.0000	0.0000	0.0000	0.0000	0.0000	0.0000	0.0000	0.0000
PRD B(NAT)	0.0000	0.0000	0.0000	0.0000	0.0000	0.0000	0.0000	0.0000
TOTAL	17.0107	24.0712	66.1980	107.2798	0.0000	0.0000	0.0000	0.0000

ITALY/ENEA T MCNP PROD/ABS= 1.10316 NU= 2.48173

CAPTURES

		REGION 1				REGION 2			
	FAST	EPI	THERMAL	TOTAL	FAST	EPI	THERMAL	TOTAL
CAP 92235	0.2676	4.2487	5.2345	9.7509	0.0000	0.0000	0.0000	0.0000
CAP 92238	5.8497	27.1181	5.8458	38.8136	0.0000	0.0000	0.0000	0.0000
CAP 160	0.0000	0.0000	0.0000	0.0000	0.0000	0.0000	0.0000	0.0000
CAP H2O	0.0000	0.0000	0.0000	0.0000	0.0065	0.3197	1.4815	1.8078
CAP B(NAT)	0.0000	0.0000	0.0000	0.0000	0.0217	0.9144	4.2449	5.1810
TOTAL	6.1173	31.3669	11.0803	48.5645	0.0282	1.2341	5.7264	6.9888

FISSIONS

		REGION 1				REGION 2			
	FAST	EPI	THERMAL	TOTAL	FAST	EPI	THERMAL	TOTAL
FIS 92235	1.2637	8.6379	29.5826	39.4842	0.0000	0.0000	0.0000	0.0000
FIS 92238	4.9670	0.0000	0.0000	4.9670	0.0000	0.0000	0.0000	0.0000
FIS 160	0.0000	0.0000	0.0000	0.0000	0.0000	0.0000	0.0000	0.0000
FIS H2O	0.0000	0.0000	0.0000	0.0000	0.0000	0.0000	0.0000	0.0000
FIS B(NAT)	0.0000	0.0000	0.0000	0.0000	0.0000	0.0000	0.0000	0.0000
TOTAL	6.2308	8.6379	29.5826	44.4512	0.0000	0.0000	0.0000	0.0000

PRODUCTIONS

		REGION 1				REGION 2			
	FAST	EPI	THERMAL	TOTAL	FAST	EPI	THERMAL	TOTAL
PRD 92235	3.2018	21.0335	72.1559	96.3912	0.0000	0.0000	0.0000	0.0000
PRD 92238	13.9259	0.0000	0.0000	13.9259	0.0000	0.0000	0.0000	0.0000
PRD 160	0.0000	0.0000	0.0000	0.0000	0.0000	0.0000	0.0000	0.0000
PRD H2O	0.0000	0.0000	0.0000	0.0000	0.0000	0.0000	0.0000	0.0000
PRD B(NAT)	0.0000	0.0000	0.0000	0.0000	0.0000	0.0000	0.0000	0.0000
TOTAL	17.1277	21.0335	72.1559	110.3171	0.0000	0.0000	0.0000	0.0000

TABLE I .2

A SUMMARY OF PARTICIPANTS REACTION RATES
NORMALIZED TO ONE ABSORPTION IN THE CELL AND
EXPRESSED AS A PERCENTAGE OF THE ABSORPTION RATE

CASE 3B (PF=0.4, 100% UO2 IN PELLET - 0% UO2 IN SOLUTION)

FRANCE/CEAREF APOLLO PROD/ABS= 1.12101 NU= 2.44763

CAPTURES

		REGION 1				REGION 2			
	FAST	EPI	THERMAL	TOTAL	FAST	EPI	THERMAL	TOTAL
CAP 92235	0.1367	2.6050	6.3728	9.1146	0.0000	0.0000	0.0000	0.0000
CAP 92238	3.0778	17.3562	7.0174	27.4513	0.0000	0.0000	0.0000	0.0000
CAP 160	0.1505	0.0002	0.0029	0.1537	0.0000	0.0000	0.0000	0.0000
CAP H2O	0.0000	0.0000	0.0000	0.0000	0.1479	0.4433	3.9978	4.5890
CAP B(NAT)	0.0000	0.0000	0.0000	0.0000	0.0263	1.3041	11.5635	12.8939
TOTAL	3.3650	19.9614	13.3931	36.7196	0.1742	1.7474	15.5613	17.4829

FISSIONS

		REGION 1				REGION 2			
	FAST	EPI	THERMAL	TOTAL	FAST	EPI	THERMAL	TOTAL
FIS 92235	0.6900	5.2315	36.8141	42.7356	0.0000	0.0000	0.0000	0.0000
FIS 92238	3.0637	0.0000	0.0000	3.0637	0.0000	0.0000	0.0000	0.0000
FIS 160	0.0000	0.0000	0.0000	0.0000	0.0000	0.0000	0.0000	0.0000
FIS H2O	0.0000	0.0000	0.0000	0.0000	0.0000	0.0000	0.0000	0.0000
FIS B(NAT)	0.0000	0.0000	0.0000	0.0000	0.0000	0.0000	0.0000	0.0000
TOTAL	3.7537	5.2315	36.8141	45.7993	0.0000	0.0000	0.0000	0.0000

PRODUCTIONS

		REGION 1				REGION 2			
	FAST	EPI	THERMAL	TOTAL	FAST	EPI	THERMAL	TOTAL
PRD 92235	1.7535	12.6607	89.0904	103.5046	0.0000	0.0000	0.0000	0.0000
PRD 92238	8.5988	0.0000	0.0000	8.5988	0.0000	0.0000	0.0000	0.0000
PRD 160	0.0000	0.0000	0.0000	0.0000	0.0000	0.0000	0.0000	0.0000
PRD H2O	0.0000	0.0000	0.0000	0.0000	0.0000	0.0000	0.0000	0.0000
PRD B(NAT)	0.0000	0.0000	0.0000	0.0000	0.0000	0.0000	0.0000	0.0000
TOTAL	10.3523	12.6607	89.0904	112.1035	0.0000	0.0000	0.0000	0.0000

USA/ORNL R-XSDRNPM PROD/ABS= 1.10397 NU= 2.44757

CAPTURES

		REGION 1				REGION 2			
	FAST	EPI	THERMAL	TOTAL	FAST	EPI	THERMAL	TOTAL
CAP 92235	0.1565	2.6699	6.1904	9.0168	0.0000	0.0000	0.0000	0.0000
CAP 92238	3.6984	18.2578	6.6408	28.5969	0.0000	0.0000	0.0000	0.0000
CAP 160	0.1871	0.0001	0.0009	0.1881	0.0000	0.0000	0.0000	0.0000
CAP H2O	0.0000	0.0000	0.0000	0.0000	0.1940	0.5659	3.8108	4.5707
CAP B(NAT)	0.0000	0.0000	0.0000	0.0000	0.0301	1.5939	10.9010	12.5250
TOTAL	4.0420	20.9279	12.8321	37.8019	0.2241	2.1598	14.7118	17.0957

FISSIONS

		REGION 1				REGION 2			
	FAST	EPI	THERMAL	TOTAL	FAST	EPI	THERMAL	TOTAL
FIS 92235	0.7562	6.0347	35.2764	42.0673	0.0000	0.0000	0.0000	0.0000
FIS 92238	3.0376	0.0000	0.0000	3.0376	0.0000	0.0000	0.0000	0.0000
FIS 160	0.0000	0.0000	0.0000	0.0000	0.0000	0.0000	0.0000	0.0000
FIS H2O	0.0000	0.0000	0.0000	0.0000	0.0000	0.0000	0.0000	0.0000
FIS B(NAT)	0.0000	0.0000	0.0000	0.0000	0.0000	0.0000	0.0000	0.0000
TOTAL	3.7938	6.0347	35.2764	45.1049	0.0000	0.0000	0.0000	0.0000

PRODUCTIONS

		REGION 1				REGION 2			
	FAST	EPI	THERMAL	TOTAL	FAST	EPI	THERMAL	TOTAL
PRD 92235	1.9226	14.5969	85.3113	101.8307	0.0000	0.0000	0.0000	0.0000
PRD 92238	8.5682	0.0000	0.0000	8.5682	0.0000	0.0000	0.0000	0.0000
PRD 160	0.0000	0.0000	0.0000	0.0000	0.0000	0.0000	0.0000	0.0000
PRD H2O	0.0000	0.0000	0.0000	0.0000	0.0000	0.0000	0.0000	0.0000
PRD B(NAT)	0.0000	0.0000	0.0000	0.0000	0.0000	0.0000	0.0000	0.0000
TOTAL	10.4908	14.5969	85.3113	110.3990	0.0000	0.0000	0.0000	0.0000

FRANCE/CEA APOLLO PROD/ABS= 1.12270 NU= 2.45713

CAPTURES

	REGION 1				REGION 2			
	FAST	EPI	THERMAL	TOTAL	FAST	EPI	THERMAL	TOTAL
CAP 92235	0.1360	2.7237	6.2910	9.1507	0.0000	0.0000	0.0000	0.0000
CAP 92238	3.1129	17.3193	7.0672	27.4994	0.0000	0.0000	0.0000	0.0000
CAP 160	0.1499	0.0002	0.0029	0.1531	0.0000	0.0000	0.0000	0.0000
CAP H20	0.0000	0.0000	0.0000	0.0000	0.1470	0.4468	3.9994	4.5933
CAP B(NAT)	0.0000	0.0000	0.0000	0.0000	0.0271	1.3148	11.5694	12.9112
TOTAL	3.3989	20.0432	13.3612	36.8032	0.1741	1.7616	15.5688	17.5045

FISSIONS

	REGION 1				REGION 2			
	FAST	EPI	THERMAL	TOTAL	FAST	EPI	THERMAL	TOTAL
FIS 92235	0.7422	5.1439	36.7007	42.5868	0.0000	0.0000	0.0000	0.0000
FIS 92238	3.1050	0.0000	0.0000	3.1050	0.0000	0.0000	0.0000	0.0000
FIS 160	0.0000	0.0000	0.0000	0.0000	0.0000	0.0000	0.0000	0.0000
FIS H20	0.0000	0.0000	0.0000	0.0000	0.0000	0.0000	0.0000	0.0000
FIS B(NAT)	0.0000	0.0000	0.0000	0.0000	0.0000	0.0000	0.0000	0.0000
TOTAL	3.8471	5.1439	36.7007	45.6917	0.0000	0.0000	0.0000	0.0000

PRODUCTIONS

	REGION 1				REGION 2			
	FAST	EPI	THERMAL	TOTAL	FAST	EPI	THERMAL	TOTAL
PRD 92235	1.8857	12.5000	89.1816	103.5673	0.0000	0.0000	0.0000	0.0000
PRD 92238	8.7066	0.0000	0.0000	8.7066	0.0000	0.0000	0.0000	0.0000
PRD 160	0.0000	0.0000	0.0000	0.0000	0.0000	0.0000	0.0000	0.0000
PRD H20	0.0000	0.0000	0.0000	0.0000	0.0000	0.0000	0.0000	0.0000
PRD B(NAT)	0.0000	0.0000	0.0000	0.0000	0.0000	0.0000	0.0000	0.0000
TOTAL	10.5923	12.5000	89.1816	112.2739	0.0000	0.0000	0.0000	0.0000

UK/SRD MONK 6.3 PROD/ABS= 1.13441 NU= 2.46523

CAPTURES

	REGION 1				REGION 2			
	FAST	EPI	THERMAL	TOTAL	FAST	EPI	THERMAL	TOTAL
CAP 92235	0.1597	2.6358	6.2401	9.0356	0.0000	0.0000	0.0000	0.0000
CAP 92238	2.9353	16.8432	6.9989	26.7773	0.0000	0.0000	0.0000	0.0000
CAP 160	0.1797	0.0000	0.0000	0.1797	0.0000	0.0000	0.0000	0.0000
CAP H20	0.0000	0.0000	0.0000	0.0000	0.1697	0.4293	4.1733	4.7724
CAP B(NAT)	0.0000	0.0000	0.0000	0.0000	0.0300	1.3379	11.8511	13.2190
TOTAL	3.2748	19.4790	13.2389	35.9927	0.1997	1.7672	16.0245	17.9914

FISSIONS

	REGION 1				REGION 2			
	FAST	EPI	THERMAL	TOTAL	FAST	EPI	THERMAL	TOTAL
FIS 92235	0.6889	5.3116	36.9704	42.9708	0.0000	0.0000	0.0000	0.0000
FIS 92238	3.0451	0.0000	0.0000	3.0451	0.0000	0.0000	0.0000	0.0000
FIS 160	0.0000	0.0000	0.0000	0.0000	0.0000	0.0000	0.0000	0.0000
FIS H20	0.0000	0.0000	0.0000	0.0000	0.0000	0.0000	0.0000	0.0000
FIS B(NAT)	0.0000	0.0000	0.0000	0.0000	0.0000	0.0000	0.0000	0.0000
TOTAL	3.7340	5.3116	36.9704	46.0159	0.0000	0.0000	0.0000	0.0000

PRODUCTIONS

	REGION 1				REGION 2			
	FAST	EPI	THERMAL	TOTAL	FAST	EPI	THERMAL	TOTAL
PRD 92235	1.7440	12.9701	90.1799	104.8940	0.0000	0.0000	0.0000	0.0000
PRD 92238	8.5497	0.0000	0.0000	8.5497	0.0000	0.0000	0.0000	0.0000
PRD 160	0.0000	0.0000	0.0000	0.0000	0.0000	0.0000	0.0000	0.0000
PRD H20	0.0000	0.0000	0.0000	0.0000	0.0000	0.0000	0.0000	0.0000
PRD B(NAT)	0.0000	0.0000	0.0000	0.0000	0.0000	0.0000	0.0000	0.0000
TOTAL	10.2937	12.9701	90.1799	113.4437	0.0000	0.0000	0.0000	0.0000

UK/BNFL WIMSE PROD/ABS= 1.12691 NU= 2.45964

CAPTURES

	REGION 1				REGION 2			
	FAST	EPI	THERMAL	TOTAL	FAST	EPI	THERMAL	TOTAL
CAP 92235	0.1296	2.7188	6.1361	8.9845	0.0000	0.0000	0.0000	0.0000
CAP 92238	3.2369	17.5576	6.9869	27.7814	0.0000	0.0000	0.0000	0.0000
CAP 160	0.2157	0.0000	0.0005	0.2161	0.0000	0.0000	0.0000	0.0000
CAP H20	0.0000	0.0000	0.0000	0.0000	0.0071	0.4517	3.9815	4.4403
CAP B(NAT)	0.0000	0.0000	0.0000	0.0000	0.0247	1.3028	11.4345	12.7620
TOTAL	3.5822	20.2764	13.1235	36.9821	0.0318	1.7545	15.4160	17.2022

FISSIONS

	REGION 1				REGION 2			
	FAST	EPI	THERMAL	TOTAL	FAST	EPI	THERMAL	TOTAL
FIS 92235	0.7494	5.1250	36.6685	42.5428	0.0000	0.0000	0.0000	0.0000
FIS 92238	3.2730	0.0000	0.0000	3.2730	0.0000	0.0000	0.0000	0.0000
FIS 160	0.0000	0.0000	0.0000	0.0000	0.0000	0.0000	0.0000	0.0000
FIS H20	0.0000	0.0000	0.0000	0.0000	0.0000	0.0000	0.0000	0.0000
FIS B(NAT)	0.0000	0.0000	0.0000	0.0000	0.0000	0.0000	0.0000	0.0000
TOTAL	4.0224	5.1250	36.6685	45.8158	0.0000	0.0000	0.0000	0.0000

PRODUCTIONS

	REGION 1				REGION 2			
	FAST	EPI	THERMAL	TOTAL	FAST	EPI	THERMAL	TOTAL
PRD 92235	1.9091	12.4767	89.1207	103.5065	0.0000	0.0000	0.0000	0.0000
PRD 92238	9.1857	0.0000	0.0000	9.1857	0.0000	0.0000	0.0000	0.0000
PRD 160	0.0000	0.0000	0.0000	0.0000	0.0000	0.0000	0.0000	0.0000
PRD H20	0.0000	0.0000	0.0000	0.0000	0.0000	0.0000	0.0000	0.0000
PRD B(NAT)	0.0000	0.0000	0.0000	0.0000	0.0000	0.0000	0.0000	0.0000
TOTAL	11.0947	12.4767	89.1207	112.6921	0.0000	0.0000	0.0000	0.0000

ITALY/ENEA C XSDRNPM PROD/ABS= 1.10606 NU= 2.44762

CAPTURES

		REGION 1				REGION 2			
		FAST	EPI	THERMAL	TOTAL	FAST	EPI	THERMAL	TOTAL
CAP	CELL	4.0257	20.3751	13.3742	37.7751	0.1051	1.4971	15.4345	17.0366
	TOTAL	4.0257	20.3751	13.3742	37.7751	0.1051	1.4971	15.4345	17.0366

FISSIONS

		REGION 1				REGION 2			
		FAST	EPI	THERMAL	TOTAL	FAST	EPI	THERMAL	TOTAL
FIS	CELL	3.7957	4.8565	36.5369	45.1891	0.0000	0.0000	0.0000	0.0000
	TOTAL	3.7957	4.8565	36.5369	45.1891	0.0000	0.0000	0.0000	0.0000

PRODUCTIONS

		REGION 1				REGION 2			
		FAST	EPI	THERMAL	TOTAL	FAST	EPI	THERMAL	TOTAL
PRD	CELL	10.4959	11.7470	88.3607	110.6036	0.0000	0.0000	0.0000	0.0000
	TOTAL	10.4959	11.7470	88.3607	110.6036	0.0000	0.0000	0.0000	0.0000

JAPAN/PNC XSDRNPM PROD/ABS= 1.10470 NU= 2.44765

CAPTURES

		REGION 1				REGION 2			
		FAST	EPI	THERMAL	TOTAL	FAST	EPI	THERMAL	TOTAL
CAP	92235	0.1612	2.7064	6.2026	9.0701	0.0000	0.0000	0.0000	0.0000
CAP	92238	3.6840	18.1427	6.6550	28.4816	0.0000	0.0000	0.0000	0.0000
CAP	160	0.1800	0.0002	0.0028	0.1830	0.0000	0.0000	0.0000	0.0000
CAP	H2O	0.0000	0.0000	0.0000	0.0000	0.2239	2.1634	14.7487	17.1359
CAP	B(NAT)	0.0000	0.0000	0.0000	0.0000	0.0000	0.0000	0.0000	0.0000
	TOTAL	4.0252	20.8492	12.8604	37.7348	0.2239	2.1634	14.7487	17.1359

FISSIONS

		REGION 1				REGION 2			
		FAST	EPI	THERMAL	TOTAL	FAST	EPI	THERMAL	TOTAL
FIS	92235	0.7569	5.9831	35.3522	42.0922	0.0000	0.0000	0.0000	0.0000
FIS	92238	3.0403	0.0005	0.0000	3.0408	0.0000	0.0000	0.0000	0.0000
FIS	160	0.0000	0.0000	0.0000	0.0000	0.0000	0.0000	0.0000	0.0000
FIS	H2O	0.0000	0.0000	0.0000	0.0000	0.0000	0.0000	0.0000	0.0000
FIS	B(NAT)	0.0000	0.0000	0.0000	0.0000	0.0000	0.0000	0.0000	0.0000
	TOTAL	3.7972	5.9836	35.3522	45.1329	0.0000	0.0000	0.0000	0.0000

PRODUCTIONS

		REGION 1				REGION 2			
		FAST	EPI	THERMAL	TOTAL	FAST	EPI	THERMAL	TOTAL
PRD	92235	1.9239	14.4720	85.4950	101.8908	0.0000	0.0000	0.0000	0.0000
PRD	92238	8.5757	0.0012	0.0000	8.5769	0.0000	0.0000	0.0000	0.0000
PRD	160	0.0000	0.0000	0.0000	0.0000	0.0000	0.0000	0.0000	0.0000
PRD	H2O	0.0000	0.0000	0.0000	0.0000	0.0000	0.0000	0.0000	0.0000
PRD	B(NAT)	0.0000	0.0000	0.0000	0.0000	0.0000	0.0000	0.0000	0.0000
	TOTAL	10.4995	14.4731	85.4950	110.4677	0.0000	0.0000	0.0000	0.0000

JAPAN/JAERI ANISN PROD/ABS= 1.15469 NU= 2.44765

CAPTURES

		REGION 1				REGION 2			
		FAST	EPI	THERMAL	TOTAL	FAST	EPI	THERMAL	TOTAL
CAP	CELL	7.6946	23.3924	51.0651	82.1521	0.3106	1.8117	15.7277	17.8499
	TOTAL	7.6946	23.3924	51.0651	82.1521	0.3106	1.8117	15.7277	17.8499

FISSIONS

		REGION 1				REGION 2			
		FAST	EPI	THERMAL	TOTAL	FAST	EPI	THERMAL	TOTAL
FIS	CELL	0.0000	0.0000	0.0000	0.0000	0.0000	0.0000	0.0000	0.0000
	TOTAL	0.0000	0.0000	0.0000	0.0000	0.0000	0.0000	0.0000	0.0000

PRODUCTIONS

		REGION 1				REGION 2			
		FAST	EPI	THERMAL	TOTAL	FAST	EPI	THERMAL	TOTAL
PRD	CELL	12.0446	13.0400	90.3842	115.4689	0.0000	0.0000	0.0000	0.0000
	TOTAL	12.0446	13.0400	90.3842	115.4689	0.0000	0.0000	0.0000	0.0000

ITALY/ENEA CB4 MCNP PROD/ABS= 1.10274 NU= 2.44737

CAPTURES

		REGION 1				REGION 2			
		FAST	EPI	THERMAL	TOTAL	FAST	EPI	THERMAL	TOTAL
CAP	CELL	3.4806	21.0943	13.2110	37.7858	0.2120	1.7575	15.1830	17.1526
	TOTAL	3.4806	21.0943	13.2110	37.7858	0.2120	1.7575	15.1830	17.1526

FISSIONS

		REGION 1				REGION 2			
		FAST	EPI	THERMAL	TOTAL	FAST	EPI	THERMAL	TOTAL
FIS	CELL	3.7419	5.2628	36.0539	45.0587	0.0000	0.0000	0.0000	0.0000
	TOTAL	3.7419	5.2628	36.0539	45.0587	0.0000	0.0000	0.0000	0.0000

PRODUCTIONS

		REGION 1				REGION 2			
		FAST	EPI	THERMAL	TOTAL	FAST	EPI	THERMAL	TOTAL
PRD	CELL	10.3421	12.7302	87.2070	110.2793	0.0000	0.0000	0.0000	0.0000
	TOTAL	10.3421	12.7302	87.2070	110.2793	0.0000	0.0000	0.0000	0.0000

ITALY/ENEA T MCNP PROD/ABS= 1.12234 NU= 2.46395

CAPTURES

	REGION 1				REGION 2			
	FAST	EPI	THERMAL	TOTAL	FAST	EPI	THERMAL	TOTAL
CAP 92235	0.1317	2.5166	6.3780	9.0262	0.0000	0.0000	0.0000	0.0000
CAP 92238	2.9064	17.8382	7.0616	27.8061	0.0000	0.0000	0.0000	0.0000
CAP 160	0.0000	0.0000	0.0000	0.0000	0.0000	0.0000	0.0000	0.0000
CAP H2O	0.0000	0.0000	0.0000	0.0000	0.0073	0.4479	4.1105	4.5657
CAP B(NAT)	0.0000	0.0000	0.0000	0.0000	0.0241	1.2767	11.7506	13.0514
TOTAL	3.0381	20.3547	13.4395	36.8323	0.0314	1.7246	15.8611	17.6171

FISSIONS

	REGION 1				REGION 2			
	FAST	EPI	THERMAL	TOTAL	FAST	EPI	THERMAL	TOTAL
FIS 92235	0.6704	5.0934	36.6258	42.3896	0.0000	0.0000	0.0000	0.0000
FIS 92238	3.1611	0.0000	0.0000	3.1611	0.0000	0.0000	0.0000	0.0000
FIS 160	0.0000	0.0000	0.0000	0.0000	0.0000	0.0000	0.0000	0.0000
FIS H2O	0.0000	0.0000	0.0000	0.0000	0.0000	0.0000	0.0000	0.0000
FIS B(NAT)	0.0000	0.0000	0.0000	0.0000	0.0000	0.0000	0.0000	0.0000
TOTAL	3.8315	5.0934	36.6258	45.5507	0.0000	0.0000	0.0000	0.0000

PRODUCTIONS

	REGION 1				REGION 2			
	FAST	EPI	THERMAL	TOTAL	FAST	EPI	THERMAL	TOTAL
PRD 92235	1.7101	12.3985	89.2468	103.3554	0.0000	0.0000	0.0000	0.0000
PRD 92238	8.8755	0.0000	0.0000	8.8755	0.0000	0.0000	0.0000	0.0000
PRD 160	0.0000	0.0000	0.0000	0.0000	0.0000	0.0000	0.0000	0.0000
PRD H2O	0.0000	0.0000	0.0000	0.0000	0.0000	0.0000	0.0000	0.0000
PRD B(NAT)	0.0000	0.0000	0.0000	0.0000	0.0000	0.0000	0.0000	0.0000
TOTAL	10.5856	12.3985	89.2468	112.2309	0.0000	0.0000	0.0000	0.0000

TABLE I .3

A SUMMARY OF PARTICIPANTS REACTION RATES
NORMALIZED TO ONE ABSORPTION IN THE CELL AND
EXPRESSED AS A PERCENTAGE OF THE ABSORPTION RATE

CASE 1F (PF=0.6, 50% UO2 IN PELLET - 50% UO2 IN SOLUTION)

FRANCE/CEAREF APOLLO PROD/ABS= 1.07043 NU= 2.46417

CAPTURES

	REGION 1				REGION 2			
	FAST	EPI	THERMAL	TOTAL	FAST	EPI	THERMAL	TOTAL
CAP 92235	0.1398	2.1127	2.4162	4.6687	0.1391	2.1977	2.6217	4.9585
CAP 92238	3.0475	11.4126	2.6592	17.1193	3.1067	17.1777	2.8832	23.1677
CAP 160	0.1112	0.0002	0.0012	0.1125	0.1097	0.0002	0.0013	0.1111
CAP H2O	0.0000	0.0000	0.0000	0.0000	0.0997	0.3065	1.3050	1.7112
CAP B(NAT)	0.0000	0.0000	0.0000	0.0000	0.0238	0.9057	3.7782	4.7077
TOTAL	3.2984	13.5255	5.0766	21.9005	3.4790	20.5878	10.5893	34.6562

FISSIONS

	REGION 1				REGION 2			
	FAST	EPI	THERMAL	TOTAL	FAST	EPI	THERMAL	TOTAL
FIS 92235	0.6540	4.3079	13.7699	18.7318	0.6476	4.4298	14.9341	20.0115
FIS 92238	2.3653	0.0000	0.0000	2.3653	2.3309	0.0000	0.0000	2.3309
FIS 160	0.0000	0.0000	0.0000	0.0000	0.0000	0.0000	0.0000	0.0000
FIS H2O	0.0000	0.0000	0.0000	0.0000	0.0000	0.0000	0.0000	0.0000
FIS B(NAT)	0.0000	0.0000	0.0000	0.0000	0.0000	0.0000	0.0000	0.0000
TOTAL	3.0193	4.3079	13.7699	21.0971	2.9785	4.4298	14.9341	22.3424

PRODUCTIONS

	REGION 1				REGION 2			
	FAST	EPI	THERMAL	TOTAL	FAST	EPI	THERMAL	TOTAL
PRD 92235	1.6494	10.4250	33.3230	45.3974	1.6329	10.7203	36.1402	48.4934
PRD 92238	6.6215	0.0000	0.0000	6.6215	6.5259	0.0000	0.0000	6.5259
PRD 160	0.0000	0.0000	0.0000	0.0000	0.0000	0.0000	0.0000	0.0000
PRD H2O	0.0000	0.0000	0.0000	0.0000	0.0000	0.0000	0.0000	0.0000
PRD B(NAT)	0.0000	0.0000	0.0000	0.0000	0.0000	0.0000	0.0000	0.0000
TOTAL	8.2709	10.4250	33.3230	52.0189	8.1588	10.7203	36.1402	55.0193

USA/ORNL R-XSDRNPM PROD/ABS= 1.04307 NU= 2.46559

CAPTURES

	REGION 1				REGION 2			
	FAST	EPI	THERMAL	TOTAL	FAST	EPI	THERMAL	TOTAL
CAP 92235	0.1600	2.1604	2.2644	4.5849	0.1595	2.2456	2.4519	4.8570
CAP 92238	3.7279	11.3621	2.4106	17.5005	3.7295	17.9848	2.6092	24.3235
CAP 160	0.1380	0.0001	0.0003	0.1384	0.2602	0.0002	0.0007	0.2611
CAP H2O	0.0000	0.0000	0.0000	0.0000	0.0086	0.3764	1.1799	1.5648
CAP B(NAT)	0.0000	0.0000	0.0000	0.0000	0.0274	1.0600	3.3725	4.4599
TOTAL	4.0259	13.5226	4.6754	22.2238	4.1852	21.6670	9.6142	35.4663

FISSIONS

	REGION 1				REGION 2			
	FAST	EPI	THERMAL	TOTAL	FAST	EPI	THERMAL	TOTAL
FIS 92235	0.7268	4.8522	12.6094	18.1885	0.7209	4.9756	13.6953	19.3917
FIS 92238	2.3802	0.0000	0.0000	2.3802	2.3452	0.0000	0.0000	2.3452
FIS 160	0.0000	0.0000	0.0000	0.0000	0.0000	0.0000	0.0000	0.0000
FIS H2O	0.0000	0.0000	0.0000	0.0000	0.0000	0.0000	0.0000	0.0000
FIS B(NAT)	0.0000	0.0000	0.0000	0.0000	0.0000	0.0000	0.0000	0.0000
TOTAL	3.1070	4.8522	12.6094	20.5687	3.0661	4.9756	13.6953	21.7369

PRODUCTIONS

	REGION 1				REGION 2			
	FAST	EPI	THERMAL	TOTAL	FAST	EPI	THERMAL	TOTAL
PRD 92235	1.8338	11.7370	30.4946	44.0653	1.8183	12.0351	33.1209	46.9743
PRD 92238	6.6835	0.0000	0.0000	6.6835	6.5864	0.0000	0.0000	6.5864
PRD 160	0.0000	0.0000	0.0000	0.0000	0.0000	0.0000	0.0000	0.0000
PRD H2O	0.0000	0.0000	0.0000	0.0000	0.0000	0.0000	0.0000	0.0000
PRD B(NAT)	0.0000	0.0000	0.0000	0.0000	0.0000	0.0000	0.0000	0.0000
TOTAL	8.5173	11.7370	30.4946	50.7488	8.4047	12.0351	33.1209	53.5607

FRANCE/CEA APOLLO PROD/ABS= 1.02232 NU= 2.47439

CAPTURES

	REGION 1				REGION 2			
	FAST	EPI	THERMAL	TOTAL	FAST	EPI	THERMAL	TOTAL
CAP 92235	0.1367	2.1647	2.2532	4.5546	0.1362	2.2523	2.4444	4.8328
CAP 92238	3.0696	13.6316	2.5565	19.2577	3.1026	17.9079	2.7634	23.7740
CAP 160	0.1087	0.0001	0.0011	0.1099	0.1073	0.0001	0.0012	0.1087
CAP H2O	0.0000	0.0000	0.0000	0.0000	0.0975	0.2903	1.2265	1.6143
CAP B(NAT)	0.0000	0.0000	0.0000	0.0000	0.0239	0.8585	3.5505	4.4329
TOTAL	3.3150	15.7964	4.8108	23.9221	3.4676	21.3091	9.9860	34.7626

FISSIONS

	REGION 1				REGION 2			
	FAST	EPI	THERMAL	TOTAL	FAST	EPI	THERMAL	TOTAL
FIS 92235	0.6877	4.1302	12.9047	17.7226	0.6813	4.2540	14.0252	18.9604
FIS 92238	2.3329	0.0000	0.0000	2.3329	2.2996	0.0000	0.0000	2.2996
FIS 160	0.0000	0.0000	0.0000	0.0000	0.0000	0.0000	0.0000	0.0000
FIS H2O	0.0000	0.0000	0.0000	0.0000	0.0000	0.0000	0.0000	0.0000
FIS B(NAT)	0.0000	0.0000	0.0000	0.0000	0.0000	0.0000	0.0000	0.0000
TOTAL	3.0206	4.1302	12.9047	20.0555	2.9809	4.2540	14.0252	21.2600

PRODUCTIONS

	REGION 1				REGION 2			
	FAST	EPI	THERMAL	TOTAL	FAST	EPI	THERMAL	TOTAL
PRD 92235	1.7351	10.0363	31.3586	43.1299	1.7185	10.3377	34.0820	46.1382
PRD 92238	6.5286	0.0000	0.0000	6.5286	6.4362	0.0000	0.0000	6.4362
PRD 160	0.0000	0.0000	0.0000	0.0000	0.0000	0.0000	0.0000	0.0000
PRD H2O	0.0000	0.0000	0.0000	0.0000	0.0000	0.0000	0.0000	0.0000
PRD B(NAT)	0.0000	0.0000	0.0000	0.0000	0.0000	0.0000	0.0000	0.0000
TOTAL	8.2637	10.0363	31.3586	49.6585	8.1547	10.3377	34.0820	52.5744

UK/SRD MONK 6.3 PROD/ABS= 1.08530 NU= 2.46570

CAPTURES

	REGION 1				REGION 2			
	FAST	EPI	THERMAL	TOTAL	FAST	EPI	THERMAL	TOTAL
CAP 92235	0.1397	2.2158	2.3356	4.6911	0.1597	2.2857	2.5951	5.0405
CAP 92238	3.0043	11.2190	2.6849	16.9082	2.9145	16.9080	2.9344	22.7569
CAP 160	0.0998	0.0000	0.0000	0.0998	0.1797	0.0000	0.0000	0.1797
CAP H2O	0.0000	0.0000	0.0000	0.0000	0.0200	0.3094	1.3275	1.6569
CAP B(NAT)	0.0000	0.0000	0.0000	0.0000	0.0100	0.8983	3.7429	4.6512
TOTAL	3.2438	13.4348	5.0205	21.6991	3.2838	20.4014	10.5999	34.2850

FISSIONS

	REGION 1				REGION 2			
	FAST	EPI	THERMAL	TOTAL	FAST	EPI	THERMAL	TOTAL
FIS 92235	0.6687	4.5713	13.6740	18.9140	0.6787	4.6811	14.9210	20.2808
FIS 92238	2.4553	0.0000	0.0000	2.4553	2.3655	0.0000	0.0000	2.3655
FIS 160	0.0000	0.0000	0.0000	0.0000	0.0000	0.0000	0.0000	0.0000
FIS H2O	0.0000	0.0000	0.0000	0.0000	0.0000	0.0000	0.0000	0.0000
FIS B(NAT)	0.0000	0.0000	0.0000	0.0000	0.0000	0.0000	0.0000	0.0000
TOTAL	3.1240	4.5713	13.6740	21.3693	3.0442	4.6811	14.9210	22.6463

PRODUCTIONS

	REGION 1				REGION 2			
	FAST	EPI	THERMAL	TOTAL	FAST	EPI	THERMAL	TOTAL
PRD 92235	1.6924	11.0900	33.1410	45.9234	1.7123	11.3490	36.1580	49.2193
PRD 92238	6.8194	0.0000	0.0000	6.8194	6.5705	0.0000	0.0000	6.5705
PRD 160	0.0000	0.0000	0.0000	0.0000	0.0000	0.0000	0.0000	0.0000
PRD H2O	0.0000	0.0000	0.0000	0.0000	0.0000	0.0000	0.0000	0.0000
PRD B(NAT)	0.0000	0.0000	0.0000	0.0000	0.0000	0.0000	0.0000	0.0000
TOTAL	8.5118	11.0900	33.1410	52.7428	8.2828	11.3490	36.1580	55.7898

UK/BNFL WIMSE PROD/ABS= 1.07272 NU= 2.47834

CAPTURES

	REGION 1				REGION 2			
	FAST	EPI	THERMAL	TOTAL	FAST	EPI	THERMAL	TOTAL
CAP 92235	0.1340	2.2242	2.2943	4.6525	0.1335	2.3143	2.4893	4.9370
CAP 92238	3.2984	10.9812	2.6493	16.9288	3.2994	17.3719	2.8603	23.5316
CAP 160	0.1578	0.0000	0.0002	0.1580	0.2976	0.0000	0.0004	0.2980
CAP H2O	0.0000	0.0000	0.0000	0.0000	0.0063	0.3107	1.2841	1.6012
CAP B(NAT)	0.0000	0.0000	0.0000	0.0000	0.0222	0.8970	3.6894	4.6086
TOTAL	3.5902	13.2055	4.9437	21.7393	3.7590	20.8939	10.3235	34.9764

FISSIONS

	REGION 1				REGION 2			
	FAST	EPI	THERMAL	TOTAL	FAST	EPI	THERMAL	TOTAL
FIS 92235	0.7145	4.1935	13.5615	18.4694	0.7080	4.3245	14.7116	19.7441
FIS 92238	2.5533	0.0000	0.0000	2.5533	2.5173	0.0000	0.0000	2.5173
FIS 160	0.0000	0.0000	0.0000	0.0000	0.0000	0.0000	0.0000	0.0000
FIS H2O	0.0000	0.0000	0.0000	0.0000	0.0000	0.0000	0.0000	0.0000
FIS B(NAT)	0.0000	0.0000	0.0000	0.0000	0.0000	0.0000	0.0000	0.0000
TOTAL	3.2678	4.1935	13.5615	21.0227	3.2253	4.3245	14.7116	22.2613

PRODUCTIONS

	REGION 1				REGION 2			
	FAST	EPI	THERMAL	TOTAL	FAST	EPI	THERMAL	TOTAL
PRD 92235	1.8092	10.2111	32.9736	44.9939	1.7922	10.5312	35.7639	48.0873
PRD 92238	7.1428	0.0000	0.0000	7.1428	7.0438	0.0000	0.0000	7.0438
PRD 160	0.0000	0.0000	0.0000	0.0000	0.0000	0.0000	0.0000	0.0000
PRD H2O	0.0000	0.0000	0.0000	0.0000	0.0000	0.0000	0.0000	0.0000
PRD B(NAT)	0.0000	0.0000	0.0000	0.0000	0.0000	0.0000	0.0000	0.0000
TOTAL	8.9520	10.2111	32.9736	52.1367	8.8360	10.5312	35.7639	55.1310

ITALY/ENEA C XSDRNPM PROD/ABS= 0.97832 NU= 2.46873

CAPTURES

		REGION 1				REGION 2			
		FAST	EPI	THERMAL	TOTAL	FAST	EPI	THERMAL	TOTAL
CAP	CELL	4.0166	17.4141	4.6237	26.0544	4.1651	20.6024	9.5521	34.3196
	TOTAL	4.0166	17.4141	4.6237	26.0544	4.1651	20.6024	9.5521	34.3196

FISSIONS

		REGION 1				REGION 2			
		FAST	EPI	THERMAL	TOTAL	FAST	EPI	THERMAL	TOTAL
FIS	CELL	3.1023	3.8391	12.3399	19.2813	3.0614	3.9363	13.3496	20.3473
	TOTAL	3.1023	3.8391	12.3399	19.2813	3.0614	3.9363	13.3496	20.3473

PRODUCTIONS

		REGION 1				REGION 2			
		FAST	EPI	THERMAL	TOTAL	FAST	EPI	THERMAL	TOTAL
PRD	CELL	8.5047	9.2860	29.8427	47.6333	8.3924	9.5211	32.2852	50.1986
	TOTAL	8.5047	9.2860	29.8427	47.6333	8.3924	9.5211	32.2852	50.1986

JAPAN/PNC XSDRNPM PROD/ABS= 0.83603 NU= 2.47766

CAPTURES

		REGION 1				REGION 2			
		FAST	EPI	THERMAL	TOTAL	FAST	EPI	THERMAL	TOTAL
CAP	92235	0.1688	0.7751	1.6989	2.6428	0.1597	2.2233	1.7526	4.1356
CAP	92238	3.7153	14.7168	1.7681	20.2001	3.7747	27.8209	1.9557	33.5514
CAP	160	0.1355	0.0002	0.0008	0.1366	0.1330	0.0003	0.0009	0.1342
CAP	H2O	0.0000	0.0000	0.0000	0.0000	0.1497	1.8797	3.4243	5.4537
CAP	B(NAT)	0.0000	0.0000	0.0000	0.0000	0.0000	0.0000	0.0000	0.0000
	TOTAL	4.0196	15.4921	3.4678	22.9794	4.2171	31.9242	7.1335	43.2749

FISSIONS

		REGION 1				REGION 2			
		FAST	EPI	THERMAL	TOTAL	FAST	EPI	THERMAL	TOTAL
FIS	92235	0.7019	3.9408	9.3530	13.9956	0.7432	4.1115	10.1609	15.0156
FIS	92238	2.4065	0.0005	0.0000	2.4071	2.3242	0.0005	0.0000	2.3247
FIS	160	0.0000	0.0000	0.0000	0.0000	0.0000	0.0000	0.0000	0.0000
FIS	H2O	0.0000	0.0000	0.0000	0.0000	0.0000	0.0000	0.0000	0.0000
FIS	B(NAT)	0.0000	0.0000	0.0000	0.0000	0.0000	0.0000	0.0000	0.0000
	TOTAL	3.1084	3.9413	9.3530	16.4026	3.0674	4.1120	10.1609	17.3403

PRODUCTIONS

		REGION 1				REGION 2			
		FAST	EPI	THERMAL	TOTAL	FAST	EPI	THERMAL	TOTAL
PRD	92235	1.7638	9.5319	22.6196	33.9153	1.8820	9.9448	24.5729	36.3997
PRD	92238	6.7581	0.0012	0.0000	6.7593	6.5269	0.0012	0.0000	6.5281
PRD	160	0.0000	0.0000	0.0000	0.0000	0.0000	0.0000	0.0000	0.0000
PRD	H2O	0.0000	0.0000	0.0000	0.0000	0.0000	0.0000	0.0000	0.0000
PRD	B(NAT)	0.0000	0.0000	0.0000	0.0000	0.0000	0.0000	0.0000	0.0000
	TOTAL	8.5219	9.5331	22.6196	40.6747	8.4089	9.9460	24.5729	42.9278

JAPAN/JAERI ANISN PROD/ABS= 1.06038 NU= 2.47766

CAPTURES

		REGION 1				REGION 2			
		FAST	EPI	THERMAL	TOTAL	FAST	EPI	THERMAL	TOTAL
CAP	CELL	6.8039	18.8004	17.8056	43.4099	6.9531	25.4650	24.1719	56.5900
	TOTAL	6.8039	18.8004	17.8056	43.4099	6.9531	25.4650	24.1719	56.5900

FISSIONS

		REGION 1				REGION 2			
		FAST	EPI	THERMAL	TOTAL	FAST	EPI	THERMAL	TOTAL
FIS	CELL	0.0000	0.0000	0.0000	0.0000	0.0000	0.0000	0.0000	0.0000
	TOTAL	0.0000	0.0000	0.0000	0.0000	0.0000	0.0000	0.0000	0.0000

PRODUCTIONS

		REGION 1				REGION 2			
		FAST	EPI	THERMAL	TOTAL	FAST	EPI	THERMAL	TOTAL
PRD	CELL	9.5593	10.5441	31.4334	51.5368	9.4400	10.9420	34.1192	54.5011
	TOTAL	9.5593	10.5441	31.4334	51.5368	9.4400	10.9420	34.1192	54.5011

ITALY/ENEA CB4 MCNP PROD/ABS= 1.03890 NU= 2.46503

CAPTURES

		REGION 1				REGION 2			
		FAST	EPI	THERMAL	TOTAL	FAST	EPI	THERMAL	TOTAL
CAP	CELL	3.4725	13.8384	4.9059	22.2168	3.6020	21.8913	10.1446	35.6379
	TOTAL	3.4725	13.8384	4.9059	22.2168	3.6020	21.8913	10.1446	35.6379

FISSIONS

		REGION 1				REGION 2			
		FAST	EPI	THERMAL	TOTAL	FAST	EPI	THERMAL	TOTAL
FIS	CELL	3.0375	4.3605	13.0683	20.4663	2.9916	4.4829	14.2045	21.6790
	TOTAL	3.0375	4.3605	13.0683	20.4663	2.9916	4.4829	14.2045	21.6790

PRODUCTIONS

		REGION 1				REGION 2			
		FAST	EPI	THERMAL	TOTAL	FAST	EPI	THERMAL	TOTAL
PRD	CELL	8.3283	10.5476	31.6110	50.4869	8.2017	10.8429	34.3571	53.4017
	TOTAL	8.3283	10.5476	31.6110	50.4869	8.2017	10.8429	34.3571	53.4017

ITALY/ENEA T MCNP PROD/ABS= 1.05288 NU= 2.47563

CAPTURES

		REGION 1				REGION 2			
		FAST	EPI	THERMAL	TOTAL	FAST	EPI	THERMAL	TOTAL
CAP	92235	0.1385	2.1246	2.3500	4.6130	0.1372	2.2140	2.5269	4.8781
CAP	92238	3.0252	11.8688	2.6277	17.5216	2.9967	18.4118	2.8131	24.2215
CAP	160	0.0000	0.0000	0.0000	0.0000	0.0000	0.0000	0.0000	0.0000
CAP	H2O	0.0000	0.0000	0.0000	0.0000	0.0050	0.3309	1.3818	1.7177
CAP	B(NAT)	0.0000	0.0000	0.0000	0.0000	0.0225	0.8769	3.6196	4.5191
	TOTAL	3.1637	13.9933	4.9776	22.1346	3.1615	21.8335	10.3414	35.3364

FISSIONS

		REGION 1				REGION 2			
		FAST	EPI	THERMAL	TOTAL	FAST	EPI	THERMAL	TOTAL
FIS	92235	0.6500	4.3214	13.2382	18.2097	0.6416	4.4184	14.2463	19.3063
FIS	92238	2.5204	0.0000	0.0000	2.5204	2.4932	0.0000	0.0000	2.4932
FIS	160	0.0000	0.0000	0.0000	0.0000	0.0000	0.0000	0.0000	0.0000
FIS	H2O	0.0000	0.0000	0.0000	0.0000	0.0000	0.0000	0.0000	0.0000
FIS	B(NAT)	0.0000	0.0000	0.0000	0.0000	0.0000	0.0000	0.0000	0.0000
	TOTAL	3.1704	4.3214	13.2382	20.7301	3.1348	4.4184	14.2463	21.7995

PRODUCTIONS

		REGION 1				REGION 2			
		FAST	EPI	THERMAL	TOTAL	FAST	EPI	THERMAL	TOTAL
PRD	92235	1.6472	10.2140	32.2682	44.1293	1.6253	10.7656	34.7123	47.1031
PRD	92238	7.0696	0.0000	0.0000	7.0696	6.9844	0.0000	0.0000	6.9844
PRD	160	0.0000	0.0000	0.0000	0.0000	0.0000	0.0000	0.0000	0.0000
PRD	H2O	0.0000	0.0000	0.0000	0.0000	0.0000	0.0000	0.0000	0.0000
PRD	B(NAT)	0.0000	0.0000	0.0000	0.0000	0.0000	0.0000	0.0000	0.0000
	TOTAL	8.7168	10.2140	32.2682	51.1989	8.6097	10.7656	34.7123	54.0876

TABLE I .4

A SUMMARY OF PARTICIPANTS REACTION RATES
NORMALIZED TO ONE ABSORPTION IN THE CELL AND
EXPRESSED AS A PERCENTAGE OF THE ABSORPTION RATE

CASE 3F (PF=0.4, 50% UO2 IN PELLET - 50% UO2 IN SOLUTION)

FRANCE/CEAREF APOLLO PROD/ABS= 1.08756 NU= 2.45637

CAPTURES

		REGION 1				REGION 2			
	FAST	EPI	THERMAL	TOTAL	FAST	EPI	THERMAL	TOTAL
CAP 92235	0.0683	1.2510	2.9173	4.2366	0.0675	1.3131	3.2278	4.6084
CAP 92238	1.5251	7.2825	3.2127	12.0203	1.5495	13.7670	3.5536	18.8701
CAP 160	0.0753	0.0001	0.0014	0.0768	0.0730	0.0001	0.0015	0.0746
CAP H20	0.0000	0.0000	0.0000	0.0000	0.1494	0.4223	3.5956	4.1674
CAP B(NAT)	0.0000	0.0000	0.0000	0.0000	0.0264	1.2431	10.4014	11.6708
TOTAL	1.6687	8.5336	6.1313	16.3337	1.8658	16.7456	20.7800	39.3913

FISSIONS

		REGION 1				REGION 2			
	FAST	EPI	THERMAL	TOTAL	FAST	EPI	THERMAL	TOTAL
FIS 92235	0.3443	2.5244	16.8440	19.7127	0.3365	2.6081	18.6072	21.5518
FIS 92238	1.5314	0.0000	0.0000	1.5314	1.4790	0.0000	0.0000	1.4790
FIS 160	0.0000	0.0000	0.0000	0.0000	0.0000	0.0000	0.0000	0.0000
FIS H20	0.0000	0.0000	0.0000	0.0000	0.0000	0.0000	0.0000	0.0000
FIS B(NAT)	0.0000	0.0000	0.0000	0.0000	0.0000	0.0000	0.0000	0.0000
TOTAL	1.8758	2.5244	16.8440	21.2442	1.8155	2.6081	18.6072	23.0308

PRODUCTIONS

		REGION 1				REGION 2			
	FAST	EPI	THERMAL	TOTAL	FAST	EPI	THERMAL	TOTAL
PRD 92235	0.8751	6.1089	40.7618	47.7458	0.8547	6.3117	45.0299	52.1963
PRD 92238	4.2986	0.0000	0.0000	4.2986	4.5118	0.0000	0.0000	4.5118
PRD 160	0.0000	0.0000	0.0000	0.0000	0.0000	0.0000	0.0000	0.0000
PRD H20	0.0000	0.0000	0.0000	0.0000	0.0000	0.0000	0.0000	0.0000
PRD B(NAT)	0.0000	0.0000	0.0000	0.0000	0.0000	0.0000	0.0000	0.0000
TOTAL	5.1738	6.1089	40.7618	52.0444	5.3665	6.3117	45.0299	56.7081

USA/ORNL R-XSDRNPM PROD/ABS= 1.06437 NU= 2.44812

CAPTURES

		REGION 1				REGION 2			
	FAST	EPI	THERMAL	TOTAL	FAST	EPI	THERMAL	TOTAL
CAP 92235	0.0782	1.2928	2.8194	4.1904	0.0776	1.3572	3.1068	4.5415
CAP 92238	1.8471	7.4470	3.0240	12.3181	1.8416	14.6627	3.3379	19.8422
CAP 160	0.0936	0.0001	0.0004	0.0941	0.2772	0.0002	0.0014	0.2788
CAP H20	0.0000	0.0000	0.0000	0.0000	0.0095	0.5366	3.4128	3.9589
CAP B(NAT)	0.0000	0.0000	0.0000	0.0000	0.0301	1.5115	9.7617	11.3033
TOTAL	2.0190	8.7399	5.8437	16.6026	2.2360	18.0681	19.6205	39.9246

FISSIONS

		REGION 1				REGION 2			
	FAST	EPI	THERMAL	TOTAL	FAST	EPI	THERMAL	TOTAL
FIS 92235	0.3776	2.9176	16.0459	19.3411	0.3703	3.0028	17.7764	21.1495
FIS 92238	1.5181	0.0000	0.0000	1.5181	1.4679	0.0000	0.0000	1.4679
FIS 160	0.0000	0.0000	0.0000	0.0000	0.0000	0.0000	0.0000	0.0000
FIS H20	0.0000	0.0000	0.0000	0.0000	0.0000	0.0000	0.0000	0.0000
FIS B(NAT)	0.0000	0.0000	0.0000	0.0000	0.0000	0.0000	0.0000	0.0000
TOTAL	1.8957	2.9176	16.0459	20.8591	1.8382	3.0028	17.7764	22.6174

PRODUCTIONS

		REGION 1				REGION 2			
	FAST	EPI	THERMAL	TOTAL	FAST	EPI	THERMAL	TOTAL
PRD 92235	0.9601	7.0570	38.8054	46.8224	0.9408	7.2632	42.9900	51.1940
PRD 92238	4.2825	0.0000	0.0000	4.2825	4.1424	0.0000	0.0000	4.1424
PRD 160	0.0000	0.0000	0.0000	0.0000	0.0000	0.0000	0.0000	0.0000
PRD H20	0.0000	0.0000	0.0000	0.0000	0.0000	0.0000	0.0000	0.0000
PRD B(NAT)	0.0000	0.0000	0.0000	0.0000	0.0000	0.0000	0.0000	0.0000
TOTAL	5.2426	7.0570	38.8054	51.1050	5.0832	7.2632	42.9900	55.3364

FRANCE/CEA APOLLO PROD/ABS= 1.05650 NU= 2.45791

CAPTURES

		REGION 1				REGION 2			
	FAST	EPI	THERMAL	TOTAL	FAST	EPI	THERMAL	TOTAL
CAP 92235	0.0668	1.2882	2.7881	4.1431	0.0661	1.3589	3.0903	4.5152
CAP 92238	1.5481	8.8166	3.1343	13.4990	1.5650	14.3240	3.4617	19.3508
CAP 160	0.0739	0.0001	0.0013	0.0753	0.0716	0.0001	0.0015	0.0732
CAP H20	0.0000	0.0000	0.0000	0.0000	0.1467	0.4115	3.4840	4.0422
CAP B(NAT)	0.0000	0.0000	0.0000	0.0000	0.0267	1.2120	10.0783	11.3170
TOTAL	1.6888	10.1049	5.9237	17.7174	1.8761	17.3065	20.1158	39.2984

FISSIONS

		REGION 1				REGION 2			
	FAST	EPI	THERMAL	TOTAL	FAST	EPI	THERMAL	TOTAL
FIS 92235	0.3633	2.4431	16.2490	19.0553	0.3553	2.5388	18.0461	20.9401
FIS 92238	1.5201	0.0000	0.0000	1.5201	1.4684	0.0000	0.0000	1.4684
FIS 160	0.0000	0.0000	0.0000	0.0000	0.0000	0.0000	0.0000	0.0000
FIS H20	0.0000	0.0000	0.0000	0.0000	0.0000	0.0000	0.0000	0.0000
FIS B(NAT)	0.0000	0.0000	0.0000	0.0000	0.0000	0.0000	0.0000	0.0000
TOTAL	1.8834	2.4431	16.2490	20.5754	1.8237	2.5388	18.0461	22.4086

PRODUCTIONS

		REGION 1				REGION 2			
	FAST	EPI	THERMAL	TOTAL	FAST	EPI	THERMAL	TOTAL
PRD 92235	0.9231	5.9366	39.4857	46.3453	0.9022	6.1693	43.8512	50.9227
PRD 92238	4.2645	0.0000	0.0000	4.2645	4.1206	0.0000	0.0000	4.1206
PRD 160	0.0000	0.0000	0.0000	0.0000	0.0000	0.0000	0.0000	0.0000
PRD H20	0.0000	0.0000	0.0000	0.0000	0.0000	0.0000	0.0000	0.0000
PRD B(NAT)	0.0000	0.0000	0.0000	0.0000	0.0000	0.0000	0.0000	0.0000
TOTAL	5.1875	5.9366	39.4857	50.6098	5.0228	6.1693	43.8512	55.0433

UK/SRD MONK 6.3 PROD/ABS= 1.10201 NU= 2.47529

CAPTURES

		REGION 1				REGION 2			
	FAST	EPI	THERMAL	TOTAL	FAST	EPI	THERMAL	TOTAL
CAP 92235	0.0799	1.3576	2.9746	4.4121	0.0599	1.3176	3.1843	4.5618
CAP 92238	1.4773	7.0873	3.1443	11.7089	1.3975	13.7851	3.6734	18.8561
CAP 160	0.0599	0.0000	0.0100	0.0699	0.2196	0.0000	0.0000	0.2196
CAP H20	0.0000	0.0000	0.0000	0.0000	0.0000	0.4492	3.5636	4.0128
CAP B(NAT)	0.0000	0.0000	0.0000	0.0000	0.0299	1.2278	10.3811	11.6389
TOTAL	1.6171	8.4449	6.1289	16.1909	1.7070	16.7797	20.8025	39.2892

FISSIONS

		REGION 1				REGION 2			
	FAST	EPI	THERMAL	TOTAL	FAST	EPI	THERMAL	TOTAL
FIS 92235	0.3693	2.5354	17.0792	19.9839	0.3294	2.7151	18.4372	21.4817
FIS 92238	1.5572	0.0000	0.0000	1.5572	1.4973	0.0000	0.0000	1.4973
FIS 160	0.0000	0.0000	0.0000	0.0000	0.0000	0.0000	0.0000	0.0000
FIS H20	0.0000	0.0000	0.0000	0.0000	0.0000	0.0000	0.0000	0.0000
FIS B(NAT)	0.0000	0.0000	0.0000	0.0000	0.0000	0.0000	0.0000	0.0000
TOTAL	1.9266	2.5354	17.0792	21.5411	1.8267	2.7151	18.4372	22.9790

PRODUCTIONS

		REGION 1				REGION 2			
	FAST	EPI	THERMAL	TOTAL	FAST	EPI	THERMAL	TOTAL
PRD 92235	0.9353	6.2151	41.8154	48.9657	0.8548	6.6576	45.1244	52.6368
PRD 92238	4.3545	0.0000	0.0000	4.3545	4.2439	0.0000	0.0000	4.2439
PRD 160	0.0000	0.0000	0.0000	0.0000	0.0000	0.0000	0.0000	0.0000
PRD H20	0.0000	0.0000	0.0000	0.0000	0.0000	0.0000	0.0000	0.0000
PRD B(NAT)	0.0000	0.0000	0.0000	0.0000	0.0000	0.0000	0.0000	0.0000
TOTAL	5.2898	6.2151	41.8154	53.3203	5.0988	6.6576	45.1244	56.8808

UK/BNFL WIMSE PROD/ABS= 1.08645 NU= 2.46081

CAPTURES

		REGION 1				REGION 2			
	FAST	EPI	THERMAL	TOTAL	FAST	EPI	THERMAL	TOTAL
CAP 92235	0.0646	1.3191	2.7961	4.1798	0.0639	1.3831	3.0922	4.5391
CAP 92238	1.6111	7.0994	3.1872	11.8976	1.6051	14.1907	3.5072	19.3029
CAP 160	0.1077	0.0000	0.0002	0.1079	0.3186	0.0000	0.0007	0.3193
CAP H20	0.0000	0.0000	0.0000	0.0000	0.0071	0.4287	3.5652	4.0010
CAP B(NAT)	0.0000	0.0000	0.0000	0.0000	0.0247	1.2371	10.2405	11.5023
TOTAL	1.7834	8.4184	5.9835	16.1853	2.0194	17.2396	20.4057	39.6647

FISSIONS

		REGION 1				REGION 2			
	FAST	EPI	THERMAL	TOTAL	FAST	EPI	THERMAL	TOTAL
FIS 92235	0.3731	2.4791	16.7008	19.5531	0.3649	2.5711	18.4509	21.3869
FIS 92238	1.6321	0.0000	0.0000	1.6321	1.5781	0.0000	0.0000	1.5781
FIS 160	0.0000	0.0000	0.0000	0.0000	0.0000	0.0000	0.0000	0.0000
FIS H20	0.0000	0.0000	0.0000	0.0000	0.0000	0.0000	0.0000	0.0000
FIS B(NAT)	0.0000	0.0000	0.0000	0.0000	0.0000	0.0000	0.0000	0.0000
TOTAL	2.0052	2.4791	16.7008	21.1851	1.9430	2.5711	18.4509	22.9650

PRODUCTIONS

		REGION 1				REGION 2			
	FAST	EPI	THERMAL	TOTAL	FAST	EPI	THERMAL	TOTAL
PRD 92235	0.9507	6.0363	40.6020	47.5891	0.9295	6.2603	44.8522	52.0421
PRD 92238	4.5802	0.0000	0.0000	4.5802	4.4312	0.0000	0.0000	4.4312
PRD 160	0.0000	0.0000	0.0000	0.0000	0.0000	0.0000	0.0000	0.0000
PRD H20	0.0000	0.0000	0.0000	0.0000	0.0000	0.0000	0.0000	0.0000
PRD B(NAT)	0.0000	0.0000	0.0000	0.0000	0.0000	0.0000	0.0000	0.0000
TOTAL	5.5310	6.0363	40.6020	52.1693	5.3608	6.2603	44.8522	56.4733

ITALY/ENEA C XSDRNPM PROD/ABS= 1.02781 NU= 2.44911

CAPTURES

		REGION 1				REGION 2			
		FAST	EPI	THERMAL	TOTAL	FAST	EPI	THERMAL	TOTAL
CAP	CELL	1.9892	10.8792	5.7967	18.6651	2.2365	17.2598	19.8684	39.3647
	TOTAL	1.9892	10.8792	5.7967	18.6651	2.2365	17.2598	19.8684	39.3647

FISSIONS

		REGION 1				REGION 2			
		FAST	EPI	THERMAL	TOTAL	FAST	EPI	THERMAL	TOTAL
FIS	CELL	1.8698	2.2752	15.8174	19.9624	1.8405	2.4003	17.7632	22.0040
	TOTAL	1.8698	2.2752	15.8174	19.9624	1.8405	2.4003	17.7632	22.0040

PRODUCTIONS

		REGION 1				REGION 2			
		FAST	EPI	THERMAL	TOTAL	FAST	EPI	THERMAL	TOTAL
PRD	CELL	5.1713	5.5032	38.2526	48.9270	5.0899	5.8060	42.9585	53.8545
	TOTAL	5.1713	5.5032	38.2526	48.9270	5.0899	5.8060	42.9585	53.8545

JAPAN/PNC XSDRNPM PROD/ABS= 0.93936 NU= 2.45229

CAPTURES

		REGION 1				REGION 2			
		FAST	EPI	THERMAL	TOTAL	FAST	EPI	THERMAL	TOTAL
CAP	92235	0.0906	1.5395	2.4363	4.0664	0.0817	1.7889	2.6510	4.5216
CAP	92238	1.8384	8.9629	2.6099	13.4113	1.8679	20.6414	2.8868	25.3961
CAP	160	0.0912	0.0001	0.0012	0.0924	0.0880	0.0001	0.0012	0.0894
CAP	H2O	0.0000	0.0000	0.0000	0.0000	0.2120	2.4772	11.4307	14.1198
CAP	B(NAT)	0.0000	0.0000	0.0000	0.0000	0.0000	0.0000	0.0000	0.0000
	TOTAL	2.0202	10.5026	5.0474	17.5701	2.2496	24.9076	16.9697	44.1269

FISSIONS

		REGION 1				REGION 2			
		FAST	EPI	THERMAL	TOTAL	FAST	EPI	THERMAL	TOTAL
FIS	92235	0.3773	2.6166	13.8585	16.8524	0.3711	2.7297	15.3642	18.4650
FIS	92238	1.5195	0.0003	0.0000	1.5198	1.4676	0.0003	0.0000	1.4678
FIS	160	0.0000	0.0000	0.0000	0.0000	0.0000	0.0000	0.0000	0.0000
FIS	H2O	0.0000	0.0000	0.0000	0.0000	0.0000	0.0000	0.0000	0.0000
FIS	B(NAT)	0.0000	0.0000	0.0000	0.0000	0.0000	0.0000	0.0000	0.0000
	TOTAL	1.8968	2.6169	13.8585	18.3722	1.8386	2.7300	15.3642	19.9328

PRODUCTIONS

		REGION 1				REGION 2			
		FAST	EPI	THERMAL	TOTAL	FAST	EPI	THERMAL	TOTAL
PRD	92235	0.9581	6.3292	33.5158	40.8031	0.9437	6.6028	37.1575	44.7039
PRD	92238	4.2874	0.0006	0.0000	4.2881	4.1408	0.0006	0.0000	4.1414
PRD	160	0.0000	0.0000	0.0000	0.0000	0.0000	0.0000	0.0000	0.0000
PRD	H2O	0.0000	0.0000	0.0000	0.0000	0.0000	0.0000	0.0000	0.0000
PRD	B(NAT)	0.0000	0.0000	0.0000	0.0000	0.0000	0.0000	0.0000	0.0000
	TOTAL	5.2456	6.3298	33.5158	45.0912	5.0844	6.6034	37.1575	48.8453

JAPAN/JAERI ANISN PROD/ABS= 1.07904 NU= 2.45229

CAPTURES

		REGION 1				REGION 2			
		FAST	EPI	THERMAL	TOTAL	FAST	EPI	THERMAL	TOTAL
CAP	CELL	3.8427	11.7471	22.2996	37.8895	4.0717	19.7113	38.3275	62.1104
	TOTAL	3.8427	11.7471	22.2996	37.8895	4.0717	19.7113	38.3275	62.1104

FISSIONS

		REGION 1				REGION 2			
		FAST	EPI	THERMAL	TOTAL	FAST	EPI	THERMAL	TOTAL
FIS	CELL	0.0000	0.0000	0.0000	0.0000	0.0000	0.0000	0.0000	0.0000
	TOTAL	0.0000	0.0000	0.0000	0.0000	0.0000	0.0000	0.0000	0.0000

PRODUCTIONS

		REGION 1				REGION 2			
		FAST	EPI	THERMAL	TOTAL	FAST	EPI	THERMAL	TOTAL
PRD	CELL	6.0229	6.2120	39.5221	51.7570	5.8537	6.4908	43.8028	56.1473
	TOTAL	6.0229	6.2120	39.5221	51.7570	5.8537	6.4908	43.8028	56.1473

ITALY/ENEA CB4 MCNP PROD/ABS= 1.05958 NU= 2.44786

CAPTURES

		REGION 1				REGION 2			
		FAST	EPI	THERMAL	TOTAL	FAST	EPI	THERMAL	TOTAL
CAP	CELL	1.7441	8.9725	5.9922	16.7088	1.9293	17.9216	20.1519	40.0029
	TOTAL	1.7441	8.9725	5.9922	16.7088	1.9293	17.9216	20.1519	40.0029

FISSIONS

		REGION 1				REGION 2			
		FAST	EPI	THERMAL	TOTAL	FAST	EPI	THERMAL	TOTAL
FIS	CELL	1.8652	2.5666	16.3351	20.7669	1.8053	2.6567	18.0566	22.5185
	TOTAL	1.8652	2.5666	16.3351	20.7669	1.8053	2.6567	18.0566	22.5185

PRODUCTIONS

		REGION 1				REGION 2			
		FAST	EPI	THERMAL	TOTAL	FAST	EPI	THERMAL	TOTAL
PRD	CELL	5.1540	6.2082	39.5111	50.8733	4.9869	6.4261	43.6739	55.0868
	TOTAL	5.1540	6.2082	39.5111	50.8733	4.9869	6.4261	43.6739	55.0868

ITALY/ENEA T MCNP PROD/ABS= 1.07323 NU= 2.46462

CAPTURES

	REGION 1				REGION 2			
	FAST	EPI	THERMAL	TOTAL	FAST	EPI	THERMAL	TOTAL
CAP 92235	0.0678	1.2490	2.8684	4.1852	0.0667	1.3380	3.2065	4.6112
CAP 92238	1.4948	7.7732	3.1787	12.4468	1.4815	14.8591	3.4790	19.8196
CAP 160	0.0000	0.0000	0.0000	0.0000	0.0000	0.0000	0.0000	0.0000
CAP H20	0.0000	0.0000	0.0000	0.0000	0.0085	0.4560	3.5546	4.0191
CAP B(NAT)	0.0000	0.0000	0.0000	0.0000	0.0250	1.2234	10.1245	11.3728
TOTAL	1.5626	9.0223	6.0471	16.6319	1.5816	17.8765	20.3646	39.8227

FISSIONS

	REGION 1				REGION 2			
	FAST	EPI	THERMAL	TOTAL	FAST	EPI	THERMAL	TOTAL
FIS 92235	0.3430	2.5292	16.4496	19.3217	0.3359	2.6348	18.0957	21.0664
FIS 92238	1.6038	0.0000	0.0000	1.6038	1.5536	0.0000	0.0000	1.5536
FIS 160	0.0000	0.0000	0.0000	0.0000	0.0000	0.0000	0.0000	0.0000
FIS H20	0.0000	0.0000	0.0000	0.0000	0.0000	0.0000	0.0000	0.0000
FIS B(NAT)	0.0000	0.0000	0.0000	0.0000	0.0000	0.0000	0.0000	0.0000
TOTAL	1.9468	2.5292	16.4496	20.9256	1.8895	2.6348	18.0957	22.6200

PRODUCTIONS

	REGION 1				REGION 2			
	FAST	EPI	THERMAL	TOTAL	FAST	EPI	THERMAL	TOTAL
PRD 92235	0.8746	6.1639	40.0618	47.1003	0.8564	6.4186	44.0880	51.3630
PRD 92238	4.5004	0.0000	0.0000	4.5004	4.3590	0.0000	0.0000	4.3590
PRD 160	0.0000	0.0000	0.0000	0.0000	0.0000	0.0000	0.0000	0.0000
PRD H20	0.0000	0.0000	0.0000	0.0000	0.0000	0.0000	0.0000	0.0000
PRD B(NAT)	0.0000	0.0000	0.0000	0.0000	0.0000	0.0000	0.0000	0.0000
TOTAL	5.3751	6.1639	40.0618	51.6008	5.2154	6.4186	44.0880	55.7220

FRANCE/CEA APOLLO PROD/ABS= 1.10205 NU= 2.47243

CAPTURES

	REGION 1				REGION 2			
	FAST	EPI	THERMAL	TOTAL	FAST	EPI	THERMAL	TOTAL
CAP 92235	0.2790	4.6048	5.1604	10.0442	0.0000	0.0000	0.0000	0.0000
CAP 92238	6.1457	26.2030	5.8493	38.1981	0.0000	0.0000	0.0000	0.0000
CAP 160	0.2225	0.0003	0.0025	0.2253	0.0000	0.0000	0.0000	0.0000
CAP H2O	0.0000	0.0000	0.0000	0.0000	0.0993	0.3207	1.4295	1.8495
CAP B(NAT)	0.0000	0.0000	0.0000	0.0000	0.0244	0.9471	4.1382	5.1097
TOTAL	6.6472	30.8081	11.0122	48.4675	0.1237	1.2678	5.5678	6.9593

FISSIONS

	REGION 1				REGION 2			
	FAST	EPI	THERMAL	TOTAL	FAST	EPI	THERMAL	TOTAL
FIS 92235	1.4094	8.7617	29.6025	39.7736	0.0000	0.0000	0.0000	0.0000
FIS 92238	4.7996	0.0000	0.0000	4.7996	0.0000	0.0000	0.0000	0.0000
FIS 160	0.0000	0.0000	0.0000	0.0000	0.0000	0.0000	0.0000	0.0000
FIS H2O	0.0000	0.0000	0.0000	0.0000	0.0000	0.0000	0.0000	0.0000
FIS B(NAT)	0.0000	0.0000	0.0000	0.0000	0.0000	0.0000	0.0000	0.0000
TOTAL	6.2090	8.7617	29.6025	44.5732	0.0000	0.0000	0.0000	0.0000

PRODUCTIONS

	REGION 1				REGION 2			
	FAST	EPI	THERMAL	TOTAL	FAST	EPI	THERMAL	TOTAL
PRD 92235	3.5563	21.2917	71.9347	96.7826	0.0000	0.0000	0.0000	0.0000
PRD 92238	13.4271	0.0000	0.0000	13.4271	0.0000	0.0000	0.0000	0.0000
PRD 160	0.0000	0.0000	0.0000	0.0000	0.0000	0.0000	0.0000	0.0000
PRD H2O	0.0000	0.0000	0.0000	0.0000	0.0000	0.0000	0.0000	0.0000
PRD B(NAT)	0.0000	0.0000	0.0000	0.0000	0.0000	0.0000	0.0000	0.0000
TOTAL	16.9834	21.2917	71.9347	110.2098	0.0000	0.0000	0.0000	0.0000

UK/SRD MONK 6.3 PROD/ABS= 1.12340 NU= 2.48024

CAPTURES

	REGION 1				REGION 2			
	FAST	EPI	THERMAL	TOTAL	FAST	EPI	THERMAL	TOTAL
CAP 92235	0.2707	4.5814	5.4236	10.2757	0.0000	0.0000	0.0000	0.0000
CAP 92238	6.0451	25.4640	5.4035	36.9126	0.0000	0.0000	0.0000	0.0000
CAP 160	0.2406	0.0000	0.0000	0.2406	0.0000	0.0000	0.0000	0.0000
CAP H2O	0.0000	0.0000	0.0000	0.0000	0.0902	0.4010	1.4837	1.9749
CAP B(NAT)	0.0000	0.0000	0.0000	0.0000	0.0301	1.0125	4.2607	5.3033
TOTAL	6.5564	30.0454	10.8271	47.4288	0.1203	1.4135	5.7444	7.2782

FISSIONS

	REGION 1				REGION 2			
	FAST	EPI	THERMAL	TOTAL	FAST	EPI	THERMAL	TOTAL
FIS 92235	1.2832	9.1429	29.8350	40.2611	0.0000	0.0000	0.0000	0.0000
FIS 92238	5.0326	0.0000	0.0000	5.0326	0.0000	0.0000	0.0000	0.0000
FIS 160	0.0000	0.0000	0.0000	0.0000	0.0000	0.0000	0.0000	0.0000
FIS H2O	0.0000	0.0000	0.0000	0.0000	0.0000	0.0000	0.0000	0.0000
FIS B(NAT)	0.0000	0.0000	0.0000	0.0000	0.0000	0.0000	0.0000	0.0000
TOTAL	6.3158	9.1429	29.8350	45.2937	0.0000	0.0000	0.0000	0.0000

PRODUCTIONS

	REGION 1				REGION 2			
	FAST	EPI	THERMAL	TOTAL	FAST	EPI	THERMAL	TOTAL
PRD 92235	3.2683	22.2850	72.7080	98.2613	0.0000	0.0000	0.0000	0.0000
PRD 92238	14.0790	0.0000	0.0000	14.0790	0.0000	0.0000	0.0000	0.0000
PRD 160	0.0000	0.0000	0.0000	0.0000	0.0000	0.0000	0.0000	0.0000
PRD H2O	0.0000	0.0000	0.0000	0.0000	0.0000	0.0000	0.0000	0.0000
PRD B(NAT)	0.0000	0.0000	0.0000	0.0000	0.0000	0.0000	0.0000	0.0000
TOTAL	17.3473	22.2850	72.7080	112.3403	0.0000	0.0000	0.0000	0.0000

UK/BNFL WIMSE PROD/ABS= 1.10313 NU= 2.47656

CAPTURES

	REGION 1				REGION 2			
	FAST	EPI	THERMAL	TOTAL	FAST	EPI	THERMAL	TOTAL
CAP 92235	0.2683	4.5543	4.9709	9.7935	0.0000	0.0000	0.0000	0.0000
CAP 92238	6.6132	26.2365	5.7300	38.5796	0.0000	0.0000	0.0000	0.0000
CAP 160	0.3153	0.0000	0.0004	0.3157	0.0000	0.0000	0.0000	0.0000
CAP H2O	0.0000	0.0000	0.0000	0.0000	0.0063	0.3236	1.4150	1.7449
CAP B(NAT)	0.0000	0.0000	0.0000	0.0000	0.0222	0.9343	4.0667	5.0232
TOTAL	7.1968	30.7908	10.7012	48.6888	0.0285	1.2579	5.4816	6.7681

FISSIONS

	REGION 1				REGION 2			
	FAST	EPI	THERMAL	TOTAL	FAST	EPI	THERMAL	TOTAL
FIS 92235	1.4310	8.5959	29.4109	39.4378	0.0000	0.0000	0.0000	0.0000
FIS 92238	5.1051	0.0000	0.0000	5.1051	0.0000	0.0000	0.0000	0.0000
FIS 160	0.0000	0.0000	0.0000	0.0000	0.0000	0.0000	0.0000	0.0000
FIS H2O	0.0000	0.0000	0.0000	0.0000	0.0000	0.0000	0.0000	0.0000
FIS B(NAT)	0.0000	0.0000	0.0000	0.0000	0.0000	0.0000	0.0000	0.0000
TOTAL	6.5361	8.5959	29.4109	44.5429	0.0000	0.0000	0.0000	0.0000

PRODUCTIONS

	REGION 1				REGION 2			
	FAST	EPI	THERMAL	TOTAL	FAST	EPI	THERMAL	TOTAL
PRD 92235	3.6170	20.9291	71.4894	96.0355	0.0000	0.0000	0.0000	0.0000
PRD 92238	14.2798	0.0000	0.0000	14.2798	0.0000	0.0000	0.0000	0.0000
PRD 160	0.0000	0.0000	0.0000	0.0000	0.0000	0.0000	0.0000	0.0000
PRD H2O	0.0000	0.0000	0.0000	0.0000	0.0000	0.0000	0.0000	0.0000
PRD B(NAT)	0.0000	0.0000	0.0000	0.0000	0.0000	0.0000	0.0000	0.0000
TOTAL	17.8969	20.9291	71.4894	110.3153	0.0000	0.0000	0.0000	0.0000

ITALY/ENEA C XSDRNPM PROD/ABS= 1.07417 NU= 2.46437

CAPTURES

		REGION 1				REGION 2			
		FAST	EPI	THERMAL	TOTAL	FAST	EPI	THERMAL	TOTAL
CAP	CELL	7.9746	30.8004	10.9258	49.7008	0.1584	1.0691	5.4861	6.7136
	TOTAL	7.9746	30.8004	10.9258	49.7008	0.1584	1.0691	5.4861	6.7136

FISSIONS

		REGION 1				REGION 2			
		FAST	EPI	THERMAL	TOTAL	FAST	EPI	THERMAL	TOTAL
FIS	CELL	6.1959	8.1681	29.2235	43.5875	0.0000	0.0000	0.0000	0.0000
	TOTAL	6.1959	8.1681	29.2235	43.5875	0.0000	0.0000	0.0000	0.0000

PRODUCTIONS

		REGION 1				REGION 2			
		FAST	EPI	THERMAL	TOTAL	FAST	EPI	THERMAL	TOTAL
PRD	CELL	16.9845	19.7571	70.6759	107.4175	0.0000	0.0000	0.0000	0.0000
	TOTAL	16.9845	19.7571	70.6759	107.4175	0.0000	0.0000	0.0000	0.0000

JAPAN/PNC XSDRNPM PROD/ABS= 1.07414 NU= 2.46447

CAPTURES

		REGION 1				REGION 2			
		FAST	EPI	THERMAL	TOTAL	FAST	EPI	THERMAL	TOTAL
CAP	92235	0.3171	4.4781	4.9355	9.7307	0.0000	0.0000	0.0000	0.0000
CAP	92238	7.3949	27.0453	5.2581	39.6983	0.0000	0.0000	0.0000	0.0000
CAP	160	0.2718	0.0003	0.0023	0.2744	0.0000	0.0000	0.0000	0.0000
CAP	H20	0.0000	0.0000	0.0000	0.0000	0.1585	1.5049	5.0514	6.7147
CAP	B(NAT)	0.0000	0.0000	0.0000	0.0000	0.0000	0.0000	0.0000	0.0000
	TOTAL	7.9838	31.5237	10.1958	49.7034	0.1585	1.5049	5.0514	6.7147

FISSIONS

		REGION 1				REGION 2			
		FAST	EPI	THERMAL	TOTAL	FAST	EPI	THERMAL	TOTAL
FIS	92235	1.4511	9.8269	27.5479	38.8260	0.0000	0.0000	0.0000	0.0000
FIS	92238	4.7581	0.0010	0.0000	4.7591	0.0000	0.0000	0.0000	0.0000
FIS	160	0.0000	0.0000	0.0000	0.0000	0.0000	0.0000	0.0000	0.0000
FIS	H20	0.0000	0.0000	0.0000	0.0000	0.0000	0.0000	0.0000	0.0000
FIS	B(NAT)	0.0000	0.0000	0.0000	0.0000	0.0000	0.0000	0.0000	0.0000
	TOTAL	6.2092	9.8279	27.5479	43.5851	0.0000	0.0000	0.0000	0.0000

PRODUCTIONS

		REGION 1				REGION 2			
		FAST	EPI	THERMAL	TOTAL	FAST	EPI	THERMAL	TOTAL
PRD	92235	3.6611	23.7700	66.6207	94.0517	0.0000	0.0000	0.0000	0.0000
PRD	92238	13.3603	0.0023	0.0000	13.3626	0.0000	0.0000	0.0000	0.0000
PRD	160	0.0000	0.0000	0.0000	0.0000	0.0000	0.0000	0.0000	0.0000
PRD	H20	0.0000	0.0000	0.0000	0.0000	0.0000	0.0000	0.0000	0.0000
PRD	B(NAT)	0.0000	0.0000	0.0000	0.0000	0.0000	0.0000	0.0000	0.0000
	TOTAL	17.0214	23.7722	66.6207	107.4143	0.0000	0.0000	0.0000	0.0000

JAPAN/JAERI ANISN PROD/ABS= 1.12946 NU= 2.46447

CAPTURES

		REGION 1				REGION 2			
		FAST	EPI	THERMAL	TOTAL	FAST	EPI	THERMAL	TOTAL
CAP	CELL	13.4636	36.9321	40.9379	91.3336	0.2257	2.8627	5.5759	8.6643
	TOTAL	13.4636	36.9321	40.9379	91.3336	0.2257	2.8627	5.5759	8.6643

FISSIONS

		REGION 1				REGION 2			
		FAST	EPI	THERMAL	TOTAL	FAST	EPI	THERMAL	TOTAL
FIS	CELL	0.0000	0.0000	0.0000	0.0000	0.0000	0.0000	0.0000	0.0000
	TOTAL	0.0000	0.0000	0.0000	0.0000	0.0000	0.0000	0.0000	0.0000

PRODUCTIONS

		REGION 1				REGION 2			
		FAST	EPI	THERMAL	TOTAL	FAST	EPI	THERMAL	TOTAL
PRD	CELL	18.7591	22.0811	72.1055	112.9457	0.0000	0.0000	0.0000	0.0000
	TOTAL	18.7591	22.0811	72.1055	112.9457	0.0000	0.0000	0.0000	0.0000

ITALY/ENEA CB4 MCNP PROD/ABS= 1.07495 NU= 2.46406

CAPTURES

		REGION 1				REGION 2			
		FAST	EPI	THERMAL	TOTAL	FAST	EPI	THERMAL	TOTAL
CAP	CELL	6.9427	31.9421	10.7366	49.6213	0.1483	1.2481	5.3591	6.7555
	TOTAL	6.9427	31.9421	10.7366	49.6213	0.1483	1.2481	5.3591	6.7555

FISSIONS

		REGION 1				REGION 2			
		FAST	EPI	THERMAL	TOTAL	FAST	EPI	THERMAL	TOTAL
FIS	CELL	6.0547	8.9084	28.6622	43.6253	0.0000	0.0000	0.0000	0.0000
	TOTAL	6.0547	8.9084	28.6622	43.6253	0.0000	0.0000	0.0000	0.0000

PRODUCTIONS

		REGION 1				REGION 2			
		FAST	EPI	THERMAL	TOTAL	FAST	EPI	THERMAL	TOTAL
PRD	CELL	16.6175	21.5479	69.3281	107.4935	0.0000	0.0000	0.0000	0.0000
	TOTAL	16.6175	21.5479	69.3281	107.4935	0.0000	0.0000	0.0000	0.0000

APPENDIX II.

PROBLEM SPECIFICATION

Problem Set Title: $U(2.5)O_2$ in Borated H_2O

General Description: Square and triangular pitch lattices, Figures 1 & 2, of $U(2.5)O_2$ spherical pellets suspended in borated water and borated water-UO_2 slurries. Lattice materials in one-dimensional cylindrical geometry, Figure 3, reflected by 30 cm of water.

Pellet Diameters: 0.960 cm (full); 0.872 cm (3/4); 0.762 cm (1/2)

Boron Levels: 3500, 1500 WPPM

UO_2 Volume Fractions: Square Pitch - 0.5, 0.4
Triangular Pitch - 0.6, 0.5, 0.4

Temperature: 293 K, all materials

Atom Densities: Attached

Lattice Descriptions: Attached

Desired Results: k_∞ for 30 lattice cells;
k_{eff} for 30 water-reflected systems.

Set 1: All UO_2 in 0.96 cm dia. Pellet

Case	Lattice Type	UO_2 Cell Fraction	Lattice Pitch (cm)	Boron (WPPM)	k_∞	k_{eff}
1a	Triangular	0.6	1.0297	3500		
1b	"	0.6	1.0297	1500		
2a	"	0.5	1.0943	3500		
2b	"	0.5	1.0943	1500		
3a	"	0.4	1.1788	3500		
3b	"	0.4	1.1788	1500		
4a	Square	0.5	0.9749	3500		
4b	"	0.5	0.9749	1500		
5a	"	0.4	1.0501	3500		
5b	"	0.4	1.0501	1500		

Set 2: 75% UO_2 in 0.872 cm dia. Pellets
25% UO_2 in Borated Water

Case	Lattice Pitch (cm)	Boron (WPPM)	UO_2 Fraction in Water	Water & Boron Fractions	k_∞	k_{eff}
1c	1.0297(T)	3500	0.273	0.727		
1d	"	1500	"	"		
2c	1.0943(T)	3500	0.2	0.8		
2d	"	1500	"	"		
3c	1.1788(T)	3500	0.143	0.857		
3d	"	1500	"	"		
4c	0.9749(S)	3500	0.2	0.8		
4d	"	1500	"	"		
5c	1.0501(S)	3500	0.143	0.857		
5d	"	1500	"	"		

Set 3: 50% UO_2 in 0.762 cm dia. Pellet
50% UO_2 in Borated Water

Case	Lattice Pitch (cm)	Boron (WPPM)	UO_2 Fraction in Water	Water & Boron Fractions	k_∞	k_{eff}
1e	1.0297(T)	3500	0.429	0.571		
1f	"	1500	"	"		
2e	1.0943(T)	3500	0.333	0.667		
2f	"	1500	"	"		
3e	1.1788(T)	3500	0.25	0.75		
3f	"	1500	"	"		
4e	0.9749(S)	3500	0.333	0.667		
4f	"	1500	"	"		
5e	1.0501(S)	3500	0.25	0.75		
5f	"	1500	"	"		

Atom Densities $\left(\frac{\text{atoms}}{\text{bn-cm}}\right)$

Pellet (All Cases)

$N(^{235}U) = 6.189\text{-}4$; $N(^{238}U) = 2.383\text{-}2$; $N(O) = 4.890\text{-}2$.

Moderator, $H_2O + B + UO_2$

Case	N(H)	N(O)	$N(^{10}B)$	$N(^{11}B)$	$N(^{235}U)$	$N(^{238}U)$
1a through 5a	6.676-2	3.338-2	3.854-5	1.565-4	-	-
1b through 5b	6.676-2	3.338-2	1.652-5	6.706-5	-	-
1c	4.853-2	3.762-2	2.802-5	1.137-4	1.690-4	6.506-3
1d	4.853-2	3.762-2	1.201-5	4.875-5	1.690-4	6.506-3
2c and 4c	5.341-2	3.648-2	3.083-5	1.252-4	1.238-4	4.766-3
2d and 4d	5.341-2	3.648-2	1.321-5	5.364-5	1.238-4	4.766-3
3c and 5c	5.721-2	3.560-2	3.303-5	1.341-4	8.850-5	3.408-3
3d and 5d	5.721-2	3.560-2	1.416-5	5.747-5	8.850-5	3.408-3
1e	3.812-2	4.004-2	2.201-5	8.934-5	2.655-4	1.022-2
1f	3.812-2	4.004-2	9.431-6	3.829-5	2.655-4	1.022-2
2e and 4e	4.453-2	3.855-2	2.571-5	1.044-4	2.061-4	7.936-3
2f and 4f	4.453-2	3.855-2	1.102-5	4.473-5	2.061-4	7.936-3
3e and 5e	5.007-2	3.726-2	2.891-5	1.173-4	1.547-4	5.958-3
3f and 5f	5.007-2	3.726-2	1.239-5	5.029-5	1.547-4	5.958-3

Water Reflector

$N(H) = 6.676\text{-}2$; $N(O) = 3.338\text{-}2$.

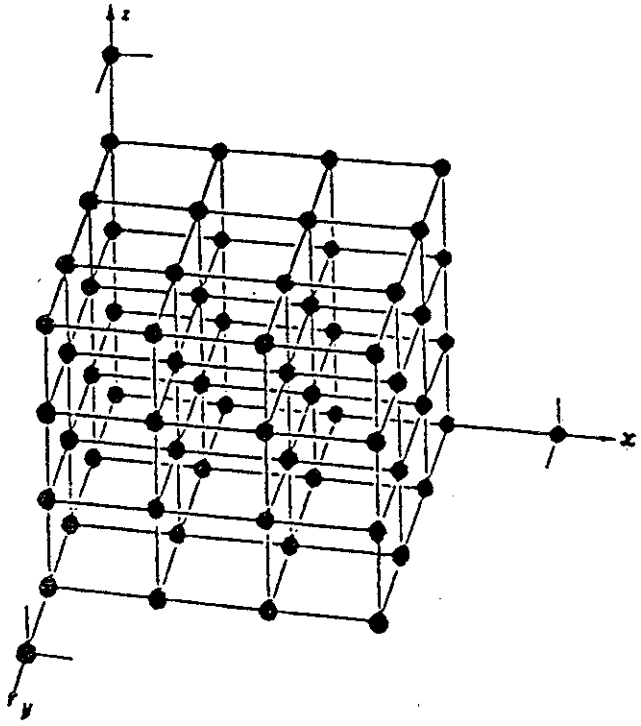

Fig. 1. Square Pitch, Cubic Cell, Infinite Lattice

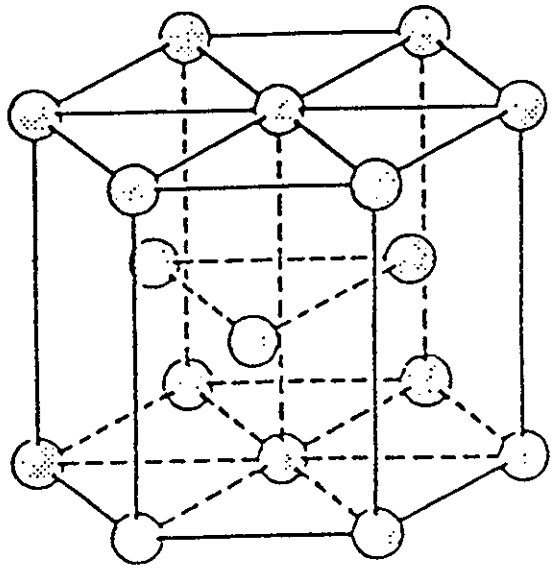

Fig. 2. Triangular Pitch, Dodecahedral Cell, Infinite Lattice

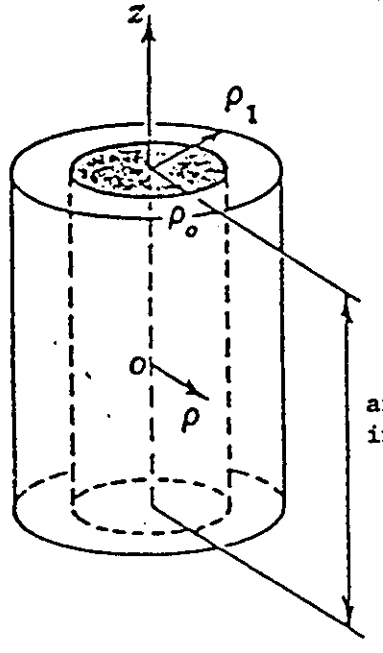

ρ_o = 20 cm

ρ_1 = 50 cm

Fig. 3. Water-Reflected Cylinder of Lattice Material